TECHNISCHE
UNIVERSITÄT
WIEN
Vienna University of Technology

Diplomarbeit

Experimental and Numerical Studies on Autoignition and Extinction, properties of DME/ Ethanol fuel mixtures

ausgeführt zum Zwecke der Erlangung des akademischen Grades eines
Diplom-Ingenieurs unter der Leitung von

Ao.Univ.Prof. Dipl.-Ing. Dr.techn. Ernst Pucher
E 315 - Institut für Fahrzeugantriebe und Automobiltechnik
Technische Universität Wien

Prof. Dr. Kalyanasundaram Seshadri
Department of Mechanical and Aerospace Engineering
University of California, San Diego, USA

eingereicht an der Technischen Universität Wien
Fakultät für Maschinenwesen und Betriebswissenschaften

von

Johannes Reiter
Matrikel Nr.: 0925161
Franckstraße 6
A-4910 Ried

Wien, Jänner 2015

Experimental and Numerical Studies on Autoignition and Extinction, properties of DME/ Ethanol fuel mixtures

Diploma Thesis

Johannes Reiter

Institute of Internal Combustion Engines and Automotive Engineering

Vienna University of Technology

Advisor:

Ao. Univ-Prof. Dipl.-Ing. Dr.techn. Ernst Pucher
Institute for Powertrains and Automotive Technology
Vienna University of Technology, Austria

Prof. Dr. Kalyanasundaram Seshadri
Department of Mechanical and Aerospace Engineering
University of California, San Diego, USA

San Diego, January 2015

Abstract

Isomers are characterized by the same molecular formula yet different chemical structures. This study is concerned with the non-premixed combustion of the isomers of C_2H_6O; dimethyl ether (DME) and ethanol. They have the same number of atoms of each element yet completely different properties due to the different molecular structures. Experimental and numerical studies are carried out employing the counterflow configuration.

In the counterflow configuration, two axisymmetric reactant streams flow from opposite directions toward a stagnation plane. One stream, called the oxidizer stream, is a mixture of oxygen and nitrogen and the other stream, called the fuel stream, is a mixture of fuel and nitrogen. The fuels considered are DME, ethanol and mixtures of DME and ethanol. The Reynolds numbers of the flow are considered to be large. A thin viscous boundary layer establishes in the vicinity of the stagnation plane, at a position where the flux of the reactants that enter the reaction zone, are in stoichiometric proportions.

Critical conditions of autoignition and extinction are measured. These conditions depend on the characteristic flow time and the characteristic chemical time. The characteristic flow time is given by the strain rate. The chemical time depends on the adiabatic flame temperature and the stoichiometric mixture fraction. Critical conditions of autoignition are measured under ambient pressure at fixed values of the mass fractions of fuel equal to 0,4. At fixed values of strain rate the temperature at autoignition of mixtures of DME and ethanol is higher than that of pure ethanol and pure dimethylether, which is approximately equal at low strain rates. At higher values of strain rate, the temperature at autoignition of DME is higher than both that of ethanol as well as mixtures of them. Critical conditions of extinction are measured for mixtures of DME and ethanol. The mass fractions of the reactants are chosen so that the adiabatic flame temperature and stoichiometric mixture fraction are the same. The strain rate at extinction is found to be positively correlated to an increase of DME in the combustible mixture.

Kurzfassung

Die vorliegende Arbeit beschäftigt sich mit der nicht vorgemischten Verbrennung vom Isomer C_2H_6O: Dimethylether (DME) und Ethanol. Isomere sind charakterisiert durch die gleiche allgemeine Summenformel aber ungleiche chemische Struktur. Dadurch weisen DME und Ethanol sehr unterschiedliche chemische und physikalische Eigenschaften auf. Um die Eigenschaften und Unterschiede während der Verbrennung zu quantifizieren, werden kritische Zustände der Selbstentzündung und Erlöschung in einem Gegenstrombrenner sowohl auf experimentellem Wege, als auch mit Hilfe von numerischen Simulationen untersucht. Für die numerischen Simulationen wird ein reduzierter detaillierter chemischer Reaktions-Mechanismus entwickelt.

In einem Gegenstrombrenner werden zwei Ströme, nämlich der Oxidationsstrom und der Brennstoffstrom entgegengesetzt axial symmetrisch ausgerichtet, sodass eine Stauebene zwischen ihnen entsteht. Der Oxidationsstrom besteht aus einer Mischung aus Sauerstoff und Stickstoff, der Brennstoffstrom besteht aus einer Mischung aus DME, Ethanol bzw. einer Mischung aus den beiden Brennstoffen und Stickstoff. In der Nähe der Stauebene entsteht eine dünne viskose Grenzschicht, in der die Ströme in stöchiometrischem Verhältnis stehen.

Die kritischen Bedingungen der Selbstentzündung und Erlöschung hängen vorwiegend von der Verweilzeit der Reaktionspartner (abhängig von der Strömungsgeschwindigkeit des Gases) und der chemischen Reaktionszeit (abhängig von der adiabaten Flammentemperatur und vom Mischungsbruch) in der Grenzschicht ab. Das Selbstentzündungs-Experiment wird bei konstant gehaltenem Brennstoffmassenanteil durchgeführt. Bei niedrigen Strain-Rates werden bei Mischungen von DME und Ethanol höhere Selbstentzündungs-Temperaturen gemessen als bei purem DME und purem Ethanol, die in etwa gleiche Selbstentzündungs-Temperaturen aufweisen. Bei höheren Strain-Rates ist die Selbstentzündungs-Temperatur von DME höher als die von Ethanol und Mischungen von DME und Ethanol. Die kritische Bedingung der Erlöschung der Flamme wurde bei konstant gehaltener adiabaten Flammentemperatur und konstant gehaltenem stöchiometrischen Mischungsbruch eruiert. Mit steigendem Ethanol-Anteil im Brennstoff sinkt die Erlöschungs-Strain-Rate.

Acknowledgements

Contents

List of Symbols

A	pre-exponential Factor for Arrhenius Equation
A_1	fuel duct area [m^3]
A_2	oxidizer duct area [m^3]
$A_{curt,1}$	fuel curtain area [m^3]
$A_{curt,1}$	oxidizer curtain area [m^3]
A_{rad}	surface of the thermocouple wire and bead [m^2]
A_w	surface of the thermocouple wire [m^2]
a_1	fuel duct strain rate [1/s]
a_2	oxidizer duct strain rate [1/s]
c_p	Specific heat capacity (isobaric) [J/kgK]
d_{sc}	diameter of the oxidizer screen [m]
d_w	diameter of the thermocouple wire [m]
Da	Damköhler number [-]
E_A	activation energy [cal/mol]
E_b	activation energy for a backward reaction [cal/mol]
E_f	activation energy for a forward reaction [cal/mol]
F_{sc}	view factor of the oxidizer screen [-]
$F_{sur,lower}$	view factor of the upper surroundings [-]
$F_{sur,upper}$	view factor of the lower surroundings [-]
ΔH	heat of reaction [cal/mol]
k	reaction rate constant
k_f	thermal conductivity of air [W/mK]
L	distance between the fuel duct and the oxidizer duct [mm]
L_2	distance between the thermocouple bead and the lowest oxidizer screen [m]
Le_{DME}	Lewis number dimethylether [-]
Le_{Eth}	Lewis number ethanol [-]
M_{air}	molecular weight air [g/mol]
M_{DME}	molecular weight dimethyl ether [g/mol]
M_{Eth}	molecular weight ethanol [g/mol]
M_{N_2}	molecular weight nitrogen [g/mol]

M_{O_2}	molecular weight oxygen [g/mol]
$\dot{m}_1$	mass flux of the fuel stream [kg/s]
$\dot{m}_2$	mass flux of the oxidizer stream [kg/s]
Nu_{cyl}	Nusselt number [-]
p	ambient pressure [Pa]
Q_{Eth}	heat release of ethanol [J/mol]
Q_{DME}	heat release of dimethyl ether [J/mol]
$\dot{Q}_{cat}$	heat flow loss due to surface-induced catalytic reactions [W]
$\dot{Q}_{cond}$	heat flow loss due to conduction [W]
$\dot{Q}_{conv}$	heat flow loss due to convection [W]
$\dot{Q}_{rad}$	heat flow loss due to radiation [W]
R	gas constant [J/molK]
Re	Reynolds number of air [-]
T	absolute temperature (Arrhenius equation) [K]
T_1	temperature of the stream at the fuel duct exit [K]
T_2	temperature of the stream at the oxidizer duct exit [K]
T_f	film temperature [K]
T_{sur}	surrounding temperature [K]
T_{tc}	temperature measured by the thermocouple [K]
t_c	chemical time (reactive time) [s]
t_m	time of transport and mixing of reactants (convective and diffusive time) [s]
V	volume (energy balance thermocouple) [m^3]
V_1	normalcomponent of the velocity of the fuel stream at the duct exit [m/s]
V_2	normalcomponent of the velocity of the oxidizer stream at the duct exit [m/s]
$\dot{V}_{air,2}$	volume stream of air (oxidizer stream) [m^3/s]
$\dot{V}_{CURT,1}$	volume stream of the fuel curtain [m^3/s]
$\dot{V}_{CURT,2}$	volume stream of the oxidizer curtain [m^3/s]
$\dot{V}_{DME,1}$	volume stream of dimethyl ether (fuel stream) [m^3/s]
$\dot{V}_{Eth,1}$	volume stream of ethanol (fuel stream) [m^3/s]
$\dot{V}_{N,,1}$	volume stream of nitrogen (fuel stream) [m^3/s]
$\dot{V}_{N,,2}$	volume stream of nitrogen (oxidizer stream) [m^3/s]
$\dot{V}_{SLM,i,j}$	volume stream scaled to the normal temperature [m^3/s]
$v_{rel,curt}$	relative velocity of the curtain to the inner duct [-]
$X_{air,2}$	air mass fraction of oxidizer stream [-]
$X_{DME,1}$	dimethyl ether mass fraction of fuel stream [-]

$X_{eth,1}$	ethanol mass fraction of fuel stream [-]
$X_{N_2,1}$	nitrogen mole fraction fuel stream [-]
$X_{N_2,2}$	nitrogen mole fraction oxidizer stream [-]
$X_{O_2,2}$	oxygen mole fraction oxidizer stream [-]
$Y_{air,2}$	air mass fraction of oxidizer stream[-]
$Y_{DME,1}$	dimethyl ether mass fraction fuel stream [-]
$Y_{Eth,1}$	ethanol mass fraction fuel stream[-]
$Y_{N_2,1}$	nitrogen mass fraction fuel stream [-]
$Y_{N_2,2}$	nitrogen mass fraction oxidizer stream [-]
$Y_{O_2,2}$	oxygen mass fraction oxidizer stream [-]
Z	mixture fraction [-]
Z_{st}	stoichiometric mixture fraction [-]
β	temperature exponent [-]
ε_{th}	emissivity of the thermocouple [-]
ρ	density [kg/m^3]
ρ_1	density at the fuel duct exit [kg/m^3]
ρ_2	density at the oxidizer duct exit [kg/m^3]
σ	Stefan-Boltzmann constant 5,67e-8 [W/m^{2}K^4]

Subscripts

1	fuel duct side
2	oxidizer duct side
b	burned
u	unburned

Nomenclature

CIDI	Compression-Ignition Direct-Injection
CO	Carbon Monoxide
CO_2	Carbon Dioxide
DME	Dimethyl ether
LHV	Lower Heating Value
LLNL	Lawrence Livermore National Laboratory
LPG	Liquefied Petroleum Gas
MFC	Mass Flow Controller
MM	Merged mechanism
NO_x	Nitrogen Oxides
PID	Proportional Integral Derivative

Chapter 1

Introduction

The use of fossil fuels dates back over 500000 years, mainly as a source for heat and light. The first use of combustion to produce energy on an industrial scale emerged with the development of the steam engine in the 18th century. In the last centuries, fossil fuels have had a tremendous impact on the economic progress. The use of combusting fossil fuels in transportation, manufacturing and the production of electric power has led to the economic vitality of the modern world. Fossil fuels are not only used as an energy source, but also as the basis for a variety of chemical products making them one of the most important resources in modern times.

From a chemical perspective, combustion can be simplified as the transformation of chemical bond energy into thermal energy. The reactants, in this case fuels, are converted into the products. This simplification shows two of the biggest challenges of the modern world: to ensure the supply of fuels and to deal with the products. Fossil fuels are a limited resource that will eventually deplete. Hence, it is very important to search for alternatives and develop infrastructure that can gradually replace fossil fuels. Dealing with the products and the resulting change in climate has grown to become one of the biggest problems of the modern world. Particularly the last few decades have had a huge impact on the environment due to the increasing consumption of fossil fuels. In effect, several governments have restricted emissions in various sectors including transportation. California was one of the first states to restrict the emissions from vehicles and factories. This forced the industry not only to make the conversion of energy more efficient; but to also use renewable energy sources and search for alternatives.

Combustion is a very complex process in which only limited knowledge exists. In a flame thousands of reactions take place in a small lengths scale and in a very short amount of time. The autoignition of most fuels involves a one-stage process of high temperature chemistry. However, some fuels autoignite in a two-step process in which a transient cool flame (650-950K) appears before a hot flame (>2000K) is established. The existence of cool flames strongly depends on the structure of the fuel molecule. For example, a cool flame occurs readily for dimethyl ether (DME) CH_3OCH_3, but not for its isomer for ethanol C_2H_5OH. With a better knowledge of cool flames the efficiency of spark ignition internal combustion engines (pre-ignition, knocking) and diesel engines can be improved, thus eventually leading to lower emissions. A better knowledge of cool flame reaction rates would especially help HCCI research. [1–3]
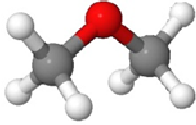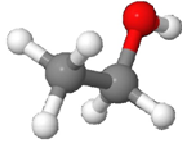
This thesis deals with the isomers of C_2H_6O: dimethyl ether (DME; CH_3OCH_3) and ethanol (C_2H_5OH). These are potential alternative fuels for applications in internal combustion engines. DME and ethanol are not only used as alternative fuels, they are also used as additive fuels for gasoline and diesel. [4, 5] To better understand the combustion of DME, ethanol and the mixtures of these fuels, critical conditions of extinction and autoignition are studied under ambient pressure.

Fundamental experimental data is very important as a reference for simulations and therefore for improving, calibrating and testing mechanisms.

1.1 Tested fuels

Ethanol is predicted to be an alternative for fossil fuels in spark-ignited internal combustion engines. Due to its high octane number (~110) it is also used as anti knock addition to gasoline. DME is predicted to be an alternative for diesel engines due its high cetane number (55-60). As mentioned previously DME and ethanol are isomers of C_2H_6O. This means they have the same amount of atoms of each element: carbon, hydrogen and oxygen. The fact that DME and ethanol are isomers makes the combustion comparison very interesting. The properties of DME and ethanol can be found in Table 1.1.

Table 1.1: Properties of dimethyl ether (gaseous) and ethanol (liquid) [6–8]

	Dimethyl ether	Ethanol
Chemical structure		
Chemical structure	CH_3OCH_3	CH_3CH_2OH
Molecular weight [*g/mol*]	46.07	46.07
Carbon content [*wt.%*]	52.2	52.2
Cetane number	55-60	---
Octane number [RON]	---	110
Density [k*g/m³*] @298*K*	1,86	785
Normal boiling point [*°C*]	-24.9	78
LHV [*MJ/kg*]	28,62	26,87
Heat of vaporization [*KJ/kg*]	467	900
Vapor pressure [*kPa*] @298,1K	596,21	--

1.1.1 Dimethyl Ether

Dimethyl ether (DME) has the chemical formula CH_3OCH_3 and is the simplest ether. Due to its low normal boiling point (-24,9°C) DME is gaseous at 1atm and liquid above 6,1atm at 20°C. During combustion DME displays a visible blue flame and has an ether-like scent. These are important safety indicators for its use in stoves and similar applications. Furthermore, its similar properties to LPG enable handling in LPG infrastructures with small modifications.

Its high cetane number (55-60) that is comparable to that of diesel (55) makes it an attractive alternative. Compared to diesel the use of DME in CIDI engines leads to less emissions of nitrogen oxides NO_x, hydrocarbons and carbon monoxide CO. Moreover, the combustion of DME produces less particulate matter and enables soot free operation. However, the energy by mass of DME (28,62 KJ/kg) is lower than the energy by mass of diesel (41,66 KJ/kg), resulting in higher fuel consumption during combustion. Thus, a larger fuel storage tank is required and a larger volume must be injected into the engine cylinder to obtain the same combustion performance as diesel. [9]

Compared to other fuels DME is non-mutagenic, non-toxic and non-carcinogenic. It does not corrode any metals and it does not cause ozone layer depletion as a result

of its quick decomposition in the troposphere. Another big advantage of DME is the fact that it does not contain sulfur or nitrogen. [6]

Two different methods are used to produce DME, the conventional indirect synthesis and the recently developed direct synthesis. The primary feedstock used for both methods is synthesis gas (syngas). Since methane is crucial for the production of syngas, the primary source of the production of DME is natural gas obtained through steam reforming. Methane can also be generated through the gasification of waste material, various bio sources and coal. The variety of suitable renewable raw material makes DME very interesting as alternative fuel.

The indirect synthesis takes place in two steps: first synthesis gas (syngas) is converted to methanol and then the methanol is dehydrated to DME.
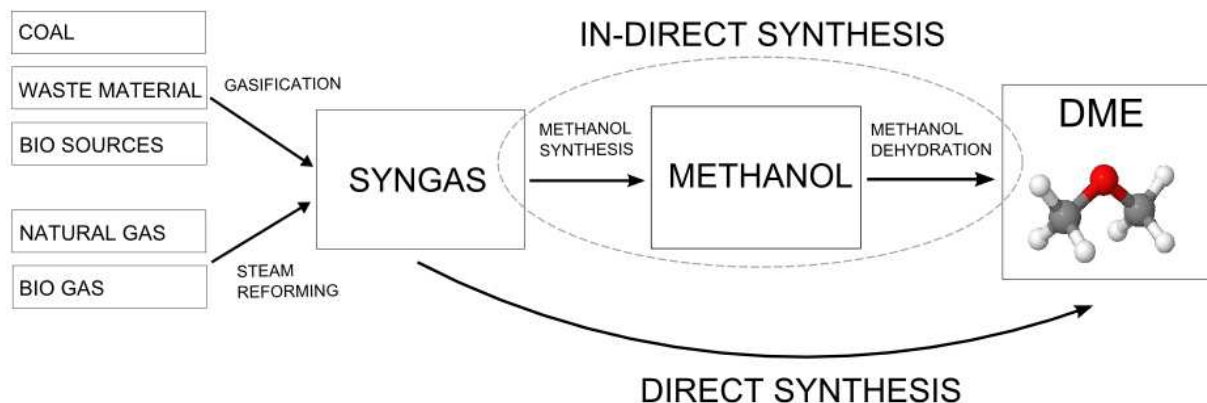
Figure 1.1: In-direct Synthesis and Direct Synthesis of syngas to DME

During direct synthesis, both the methanol synthesis and the dehydration process take place in the same reactor. Methanol preparation is avoided, making this method more economically efficient since the thermodynamic limitations of methanol synthesis can be obviated. [6, 8, 9]

1.1.1 Ethanol

Ethanol has the chemical formula C_2H_5OH. It has a long history of production for humankind, initially produced through fermentation for alcoholic beverages, later used as lamp oil in the 1800's and then used as fuel for internal combustion engines by the 19th century. Today ethanol is considered to be one of the most common

alternative fuels of the future and serves as the most widely used bio fuel. It is used as a substitute for petrol or as blend for gasoline. During combustion, ethanol shows a visible blue flame.

The hydroxyl moiety has a big influence on ethanol's physical properties. Thus, it is liquid at room temperature making it very suitable for the use as a fuel for transportation. Ethanol is miscible with water because the hydroxyl moiety introduces a dipole moment to the non-polar hydrocarbon backbone. Ethanol has a higher octane number than gasoline. The octane number is very important for spark ignited internal combustion engines. A high octane number is a measure of gasoline quality, which is important for preventing early ignition and thus cylinder knocking. Combustion engines that run with high octane number fuels can operate at higher compression ratios, which increases efficiency. Using ethanol as fuel in internal combustion engines can decrease thermal losses and increase power output due to higher latent heat of vaporization and lower flame temperatures than petroleum based fuels. However, the high latent heat of vaporization of ethanol can cause problems when starting a combustion engine under cold conditions. Another disadvantage of ethanol compared to gasoline is the fact that the energy by mass of ethanol (26,87 KJ/kg) is lower than that of gasoline (43,47 KJ/kg), resulting in higher fuel consumption during combustion.[6] Thus, a larger fuel storage tank is required to ensure the same range of driving. Furthermore, some parts have to be adapted due to ethanol's corrosiveness.

Currently the most common way to produce ethanol is by fermentating grain and sugar. Using grain and sugar as feedstock for the production of ethanol causes ethical and physical problems. The production of these raw materials conflicts with the production of food for animals and humans and its availability can vary from season to season. To avoid these problem lignocelluloses is seen as a promising alternative feedstock for the future due to its high availability and lower costs. However, the implementation in large-scale industrial production has not been possible yet due to conversion problems. [10–12]

1.2   Counter flow combustion

A flame can be characterized either as premixed or non-premixed. In gasoline powered engines the fuel and oxidizer are provided premixed. In diesel engines the fuel and oxidizer are non-premixed; mixing occurs simultaneously with the combustion process. A candle flame is an easy example of a non-premixed laminar diffusion flame, were the fuel and the oxidizer mix simultaneously with the combustion process. Surrounding air diffuses into the flame due to buoyancy. By blowing air into the candle, the flame temperature increases due to an increase of oxygen delivered into the diffusion zone. If the velocity of oxygen reaches a certain level, the flame extinguishes; the candle goes out. A candle is an example how variations of flow and velocity can influence combustion. In internal combustion engines this phenomena is called quenching, which can occur through high turbulences. Even though it is very turbulent in a combustion chamber during combustion, it is locally laminar on a micro scale. [2]

To investigate combustion behavior premixed and diffusion flames are used. In order to obtain a premixed flame, the reactants (fuel and the oxidizer) are premixed before they enter the reaction zone. A premixed flame has a finite velocity. If the reactants are not pre-mixed the reactants mix in the same region the combustion takes place. Compared to the premixed flame, the diffusion flame does not propagate. To simulate laminar diffusion flames counter flow configurations are commonly used.

The most important parts are the oxidizer duct and the fuel duct. The ducts are opposite from each other and the distance between them can be varied. In the configuration set up for this experiment, the distance is L=14,5mm for the autoignition experiment and L=12,5mm for the extinction experiment.
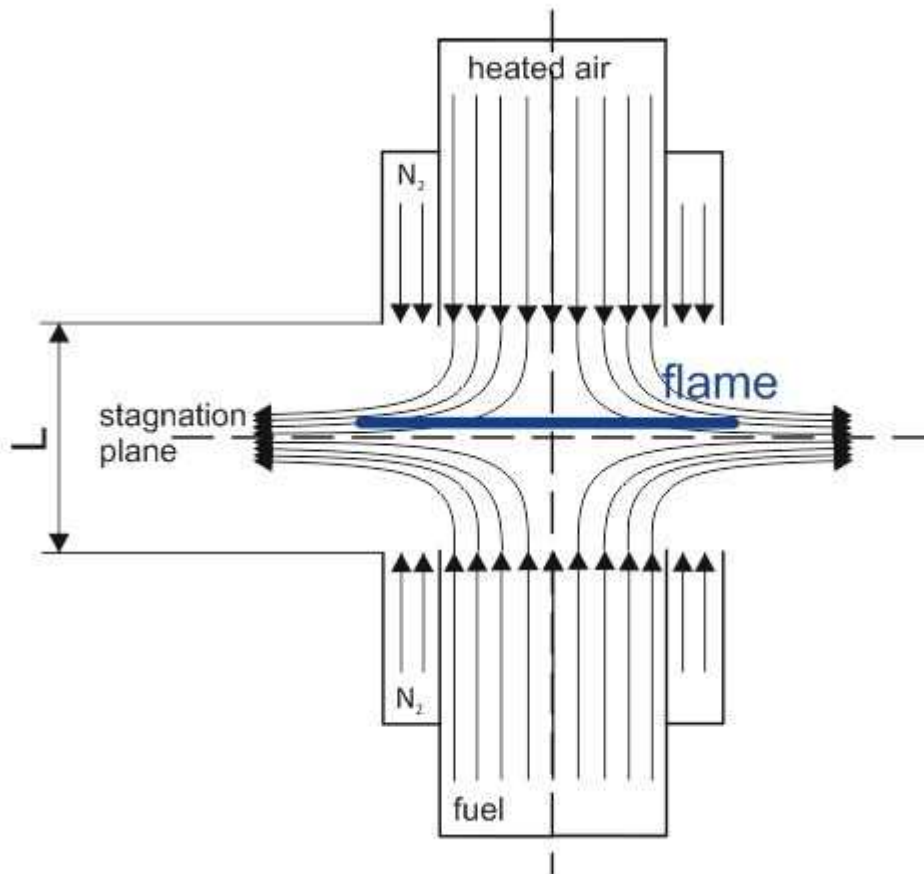
Figure 1.2: Section few of the counter flow setup showing an established diffusion flame

The exit of the fuel duct is called the fuel boundary and the exit of the oxidizer duct is called oxidizer boundary. In the counterflow configuration two axisymmetric reactant streams flow from opposite directions towards a stagnation plane. The stream coming from the oxidizer duct, called oxidizer stream, is a mixture of oxygen and nitrogen. The stream coming from the fuel duct, called fuel stream, is a mixture of fuel and nitrogen. The flows are considered steady, axisymmetric and laminar. The Reynolds numbers of the flows are large. A thin viscous boundary layer establishes near the stagnation plane in a narrow zone between the oxidizer duct and the fuel duct. A flame stabilizes in the viscous boundary, which is the region with the maximum energy output. Hence, this is the position where the fluxes of the reactants that enter the reaction zone are in stoichiometric proportions. Since diffusion only occurs in a very thin layer, the combustion zone becomes a flame sheet. Nitrogen curtains surround the ducts. The combustion in a counter flow burner is mainly dependant on the chemical reaction time and the velocity of the flow of the fuel and the flow of the oxidizer. If the fuel and oxidizer velocity exceed a certain value, the

reaction of the fuel and the oxidizer ends abruptly. This is called the extinction of the flame. [2, 12, 13]

1.3   The Arrhenius Law

It is essential to understand the molecular basis of the temperature dependence of the rates of most reactions in order to develop a chemical kinetic mechanism. Arrhenius describes the temperature dependence of the rate constant of a reaction as:

$$k = AT^{\beta} e^{-\frac{E_A}{RT}} \tag{1.1}$$

Where k is the reaction rate constant, A is the pre-exponential factor [1/K$^{\beta}$s], β is the temperature exponent [-], T is the absolute temperature [K], R is the gas constant [J/molK] and E_A is the activation energy [J/mol].

To start a chemical reaction a minimum amount of energy, called the activation energy, is needed. In Figure 1.3 the chemical bond energy over the reaction coordinate for the reaction A+B $\rightleftharpoons$ C+D is shown. Starting with the reactants A and B a transition term AB is formed, which has a higher activation energy than the reactants. By decomposing the transition term to the products, not only is the activation energy rereleased, the heat of reaction ΔH is also released (exothermic reaction). The heat of reaction is the maximum theoretical energy that can be generated by an exothermic reaction. [14, 15]
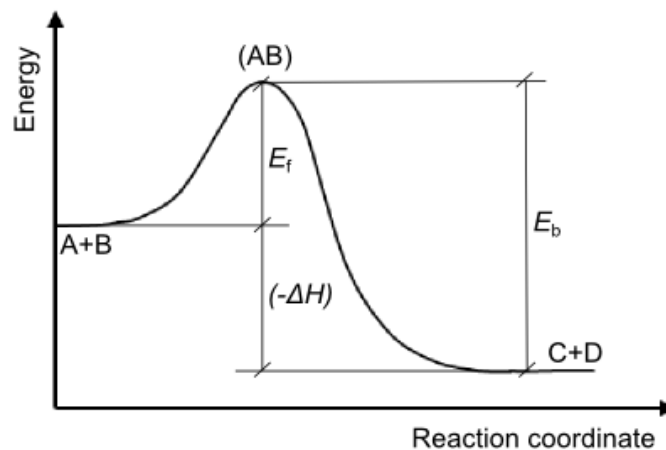
Figure 1.3: Schematic figure of the chemical bond energy as function of the reaction coordinate [14]

1.4 S-shaped curve

The Damköhler number Da is the ratio of the characteristic time of convection and diffusion t_m (residence time) to the characteristic chemical reaction time t_c of combustion. The chemical time t_c depends on the fuel and is an indicator for the reactivity of a fuel. The time of transport and mixing of reactants depends on the properties of the flow field.

$$Da = \frac{t_m}{t_c} \qquad (1.2)$$

High Damköhler numbers indicate fast chemical reactions, whereas low Damköhler numbers indicate slow chemical reactions. Since the time of transport and mixing of reactants t_m is large in a diffusion flame the Damköhler number is very high.

To describe a flame the S-shaped curve is a very useful tool. It can be determined by calculating the maximum temperature in a flow field. The S-shaped curve is characterized by two stable branches; the upper branch and the lower branch, and by one unstable branch in the middle. The upper branch represents the temperature of the burning flame at different strain rates; the lower branch represents the temperature of the non-burning mixture at different strain rates.
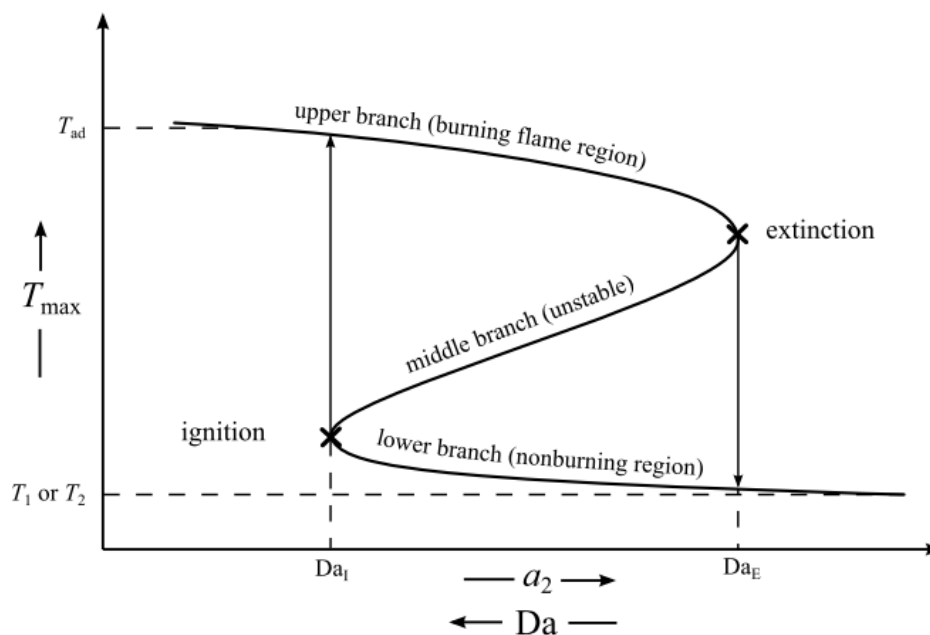
Figure 1.4: S-shaped curve: Da$_I$ represents the Damköhler number at ignition, Da$_E$ represents the Damköhler number at extinction, T_1 or T_2 are the temperatures of the fuel and oxidizer stream depending on which one is higher, T_{ad} is the adiabatic flame temperature and a_2 is the oxidizer strain rate [2]

At high strain rates, two opposite streams can mix as frozen flow where the temperature is equal to the higher temperature of the two streams (lower branch). By decreasing the strain rate the Damköhler number increases because of a rise in residence time of the reactants. Due to exothermic reactions, the temperature rises to a critical point where no steady state solution in the non-burning region can be provided. The mixture autoignites. The maximum temperature of the flame is shown by the upper branch of the S-shaped curve.

An increase of the strain rate in the upper regime is accompanied by a decrease in the residential time of the reactants in the mixing layer. At a certain strain rate the flame extinguishes. The lower branch now represents the maximum temperature of the flows. By replacing the temperature axis through the concentration of certain radicals like O, H, or OH similar S-shaped curves can be obtained. [2]

1.5   Strain rate

The strain rate is defined as the normal gradient of the normal component of the flow velocity. The strain rate at the oxidizer stream is different to the strain rate at the fuel stream. The strain rate a_2 at the oxidizer stream is given by

$$a_2 = \frac{2|V_2|}{L}\left(1 + \frac{|V_1|\sqrt{\rho_1}}{|V_2|\sqrt{\rho_2}}\right)$$

(1.3)

with ρ_1 as the density of the fuel stream at the boundary [kg/m^3] and respectively ρ_2 as the density of the oxidizer stream at the boundary [kg/m^3]. L stands for the distance [m] between the fuel duct and the oxidizer duct. V_1 and V_2 denote the normal components of the flow velocities [m/s] for the fuel duct and for the oxidizer duct, respectively. The equation is developed from an asymptotic theory where the Reynolds numbers of the laminar flows at the duct exits are assumed to be large.[16] Equation (1.3) is reduced to the following simplification.

$$V_2 = \frac{a_2 L}{4}$$

(1.4)

According to this equation the velocity of the oxidizer stream can be calculated with a given oxidizer strain rate.

Chapter 2

Experimental Setup

As shown in Figure 3.1 the experimental setup contains the oxidizer duct, the fuel duct, the piping, the vaporizer for vaporizing the liquid fuel, the mass flow controllers and the air, nitrogen and fuel supply. Both the oxidizer duct and the fuel duct are interchangeable in order to run different types of experiments.
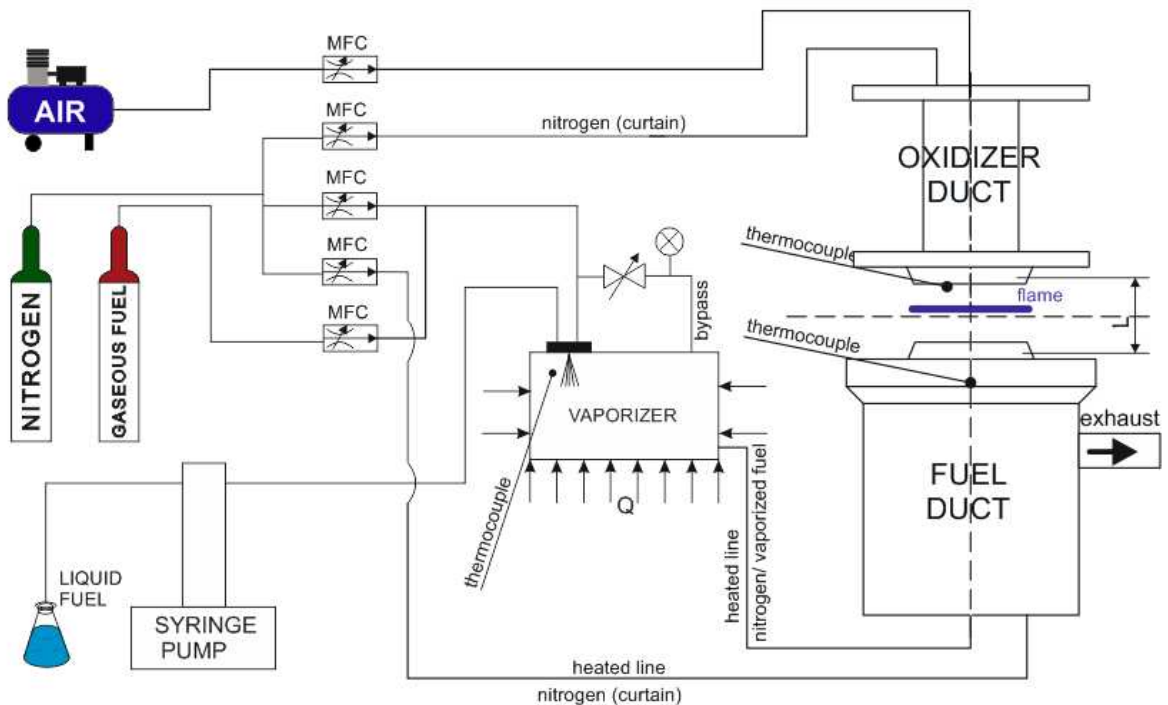
Figure 2.1: Schematic illustration of the experimental setup. The figure shows the counterflow burner, the vaporizer and the nitrogen, fuel and air feed system

All lines between the vaporizer and the fuel duct are heated by heating tape to make sure that there is no condensation of fuel inside the piping. A process controller controls the heating tape.

2.1   Lower Part of the Burner

The burner (lower duct) mainly consists of two pipes, one for the fuel supply and one for the curtain that are arranged concentrically with the pipe of the fuel supply. To ensure a uniform velocity profile (plug flow profile) three screens are arranged at the exit of the fuel duct, which are held in place by 4 steel rings. The screens are made out of stainless steel with a mesh of 200 lines per inch. The exhaust is an annular section arranged concentrically around the curtain pipe, which draws the hot combustion products from the area where the combustion takes place.
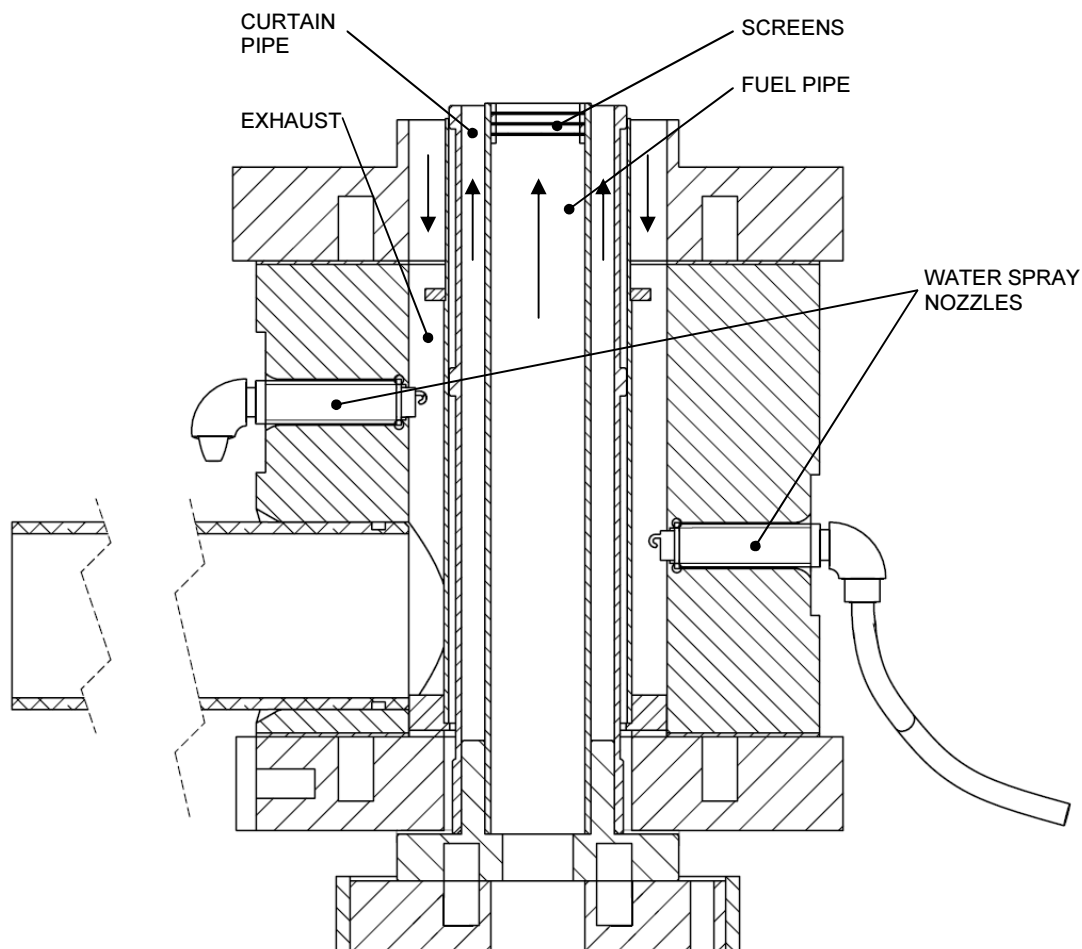
Figure 2.2: Section view of the fuel duct

The exhaust is connected to the internal building extraction system, guaranteeing that the exhaust gases are properly removed from the area where combustion takes place. The exhaust gases are cooled on their way through six water sprays inside the cylinder that surrounds the ducts as shown in figure 3.2.

2.2 Upper Part of the Burner

Different types of upper parts (oxidizer ducts) are used for the autoignition and for the extinction experiments. The tops are interchangeable and connected to the lower part of the burner through three adjustable pins.

2.2.1 Autoignition

To measure the critical conditions of autoignition the oxidizer stream is heated up
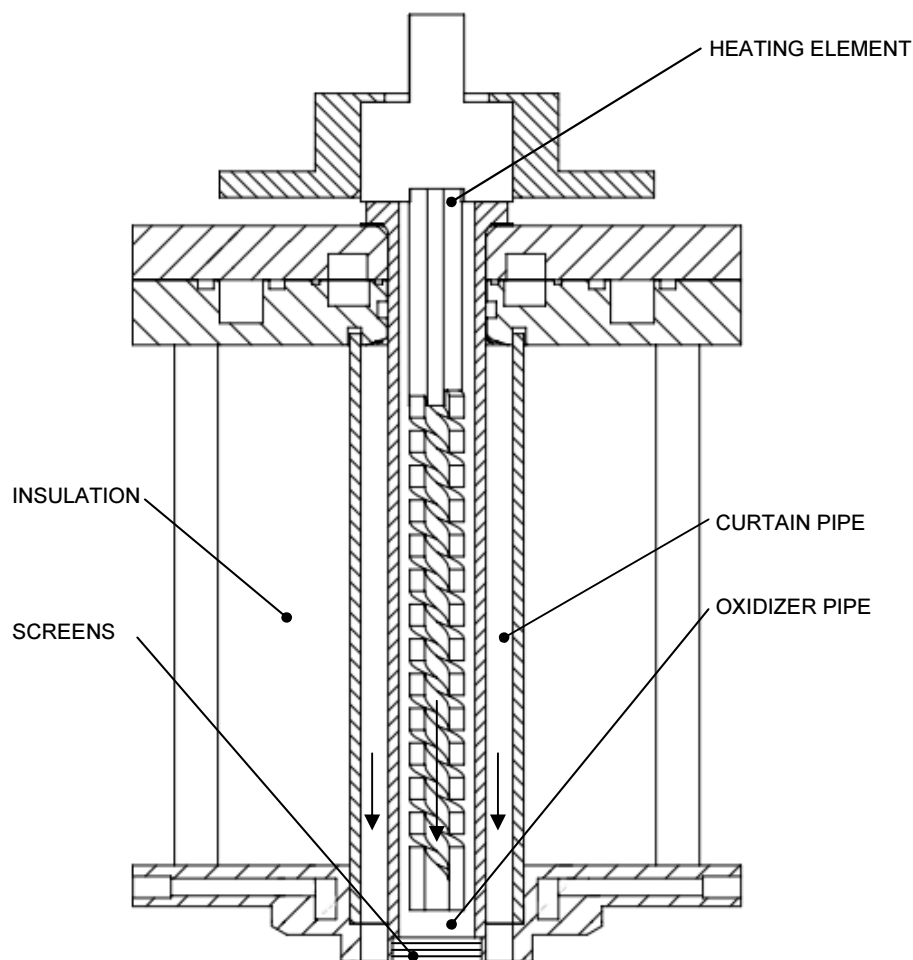
Figure 2.3: Section view of the autoignition top

until it reaches the autoignition temperature of the air and fuel mixture. Due to this, a powerful heating element is the key part of the autoignition top. The oxidizer duct (quartz tube) surrounds the heating element. To ensure circular symmetric heating and autoignition in the middle of the flame zone the heating element and the quartz tube are aligned precisely. Since the heating element is very powerful (>2000K) the curtain duct, which is axisymmetric with the oxidizer duct, is also made out of quartz. All metal parts surrounding the quartz tube are cooled by water. To minimize heat losses the curtain duct is insulated. The screens used at the autoignition top are the same screens used at the fuel duct; the only difference is that the screens used at the autoignition top are made out of Inconel 600 in order to withstand high temperatures. Inconel rings prevent the screens from falling out and ensure the correct distance between the screens. Due to the fact that the screens are held in place by rings, the effective diameter of the oxidizer duct reduces to 23mm.

2.2.2 Extinction

The extinction top consists of two concentric tubes that separate the oxidizer gas from the curtain gas.
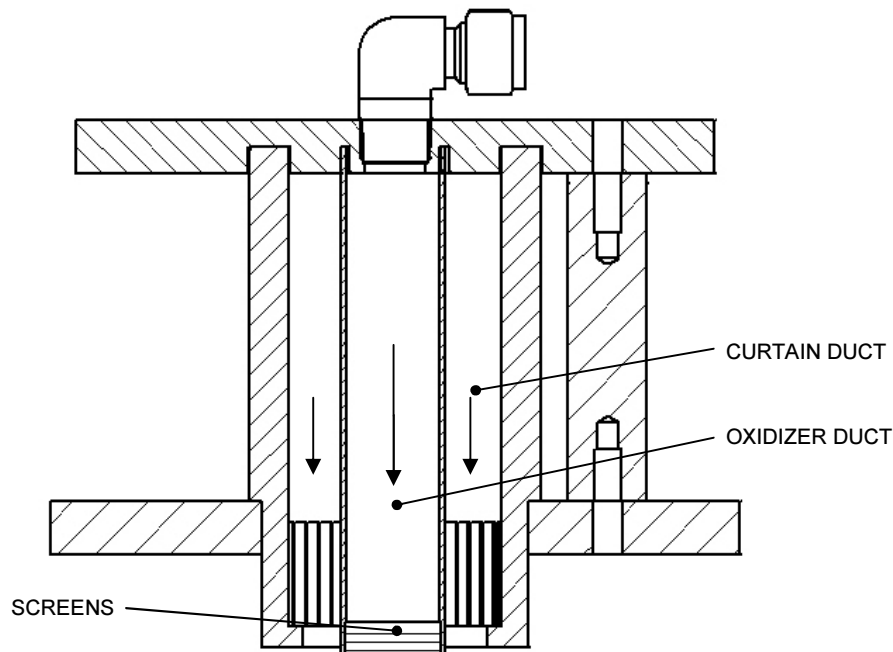
Figure 2.4: Section view of the extinction top

Steel screens with the same mesh as the fuel duct screens are used to assure plug flow conditions at the extinction top. Since the screens are held in place by rings the effective diameter of the oxidizer duct reduces to 23mm.

2.3   Gas and Fuel Supply

In the experiments carried out for this thesis, ethanol is supplied via a syringe pump, which is directly hooked up with the vaporizer. High-pressure bottles ensure the supply of nitrogen and DME. Air is supplied through the internal pressurized air supply system.

2.3.1 Vaporizer

The experiments are carried out with gaseous fuels. Hence, ethanol needs to be vaporized since it is liquid under normal conditions. Simplified, the vaporizer consists of a heated aluminum box where the liquid fuel is sprayed in. The case, nozzle, cooling plate and heating elements are the main parts of the vaporizer. The nozzle vaporizes the ethanol and the nitrogen/ dimethylether serves as carrier gas to pick up the vaporized ethanol. To ensure that there is no re-condensation of the fuel, the entire vaporizer is heated through a heating plate and heating tape. The nozzle is cooled by a cooling plate attached to the bottom to avoid vaporization which would influence the constant flow.

The nozzle is one of the most important parts of the vaporizer to ensure proper vaporization. The high thermal conductivity of aluminum makes it suitable as case material. Since ethanol is very corrosive to aluminum, high temperatures need to be avoided. Thus the design of the nozzle alone should guarantee proper atomization. The required flow rates of liquid fuel are between 0ml/min and 15ml/min. To get the highest possible degree of evaporation a Siphon Set-up is used. Siphon Set-ups provide the lowest flow rates compared to Internal and External Mix Set-ups.

Used nozzle Set-up:
  – BETE FOG NOOZLE XA SR 050

- FLUID CAP FC07

- AIR CAP AC1201/ ¼ XA 05

The technical details for the used Set-up are attached in the appendix D.
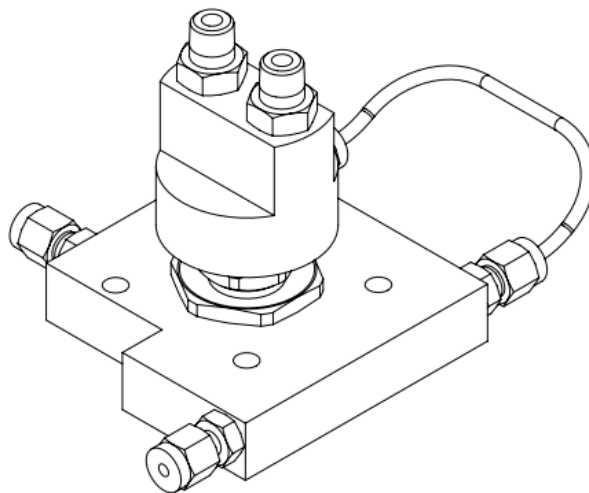
Figure 2.5: New nozzle and cooling plate

The cooling plate (detailed dimensions in appendix D) and the positions of the connections are designed to fit on the existing vaporizer. The cooling plate is attached to the vaporizer via four fasteners. It consists of an aluminum plate, the fittings and a stainless steel tube. The used coolant is deionized water with a temperature of 296K from the internal building extraction system.

2.4   Controlling Software

Since the experimental procedure requires a lot of data processing, it is not possible to handle the experiments without software. For this purpose, software was built in LabView that controls all inputs and outputs. The software was improved over the last years and adopted for high-pressure experiments. It shows all the important data in a graphical user interface.
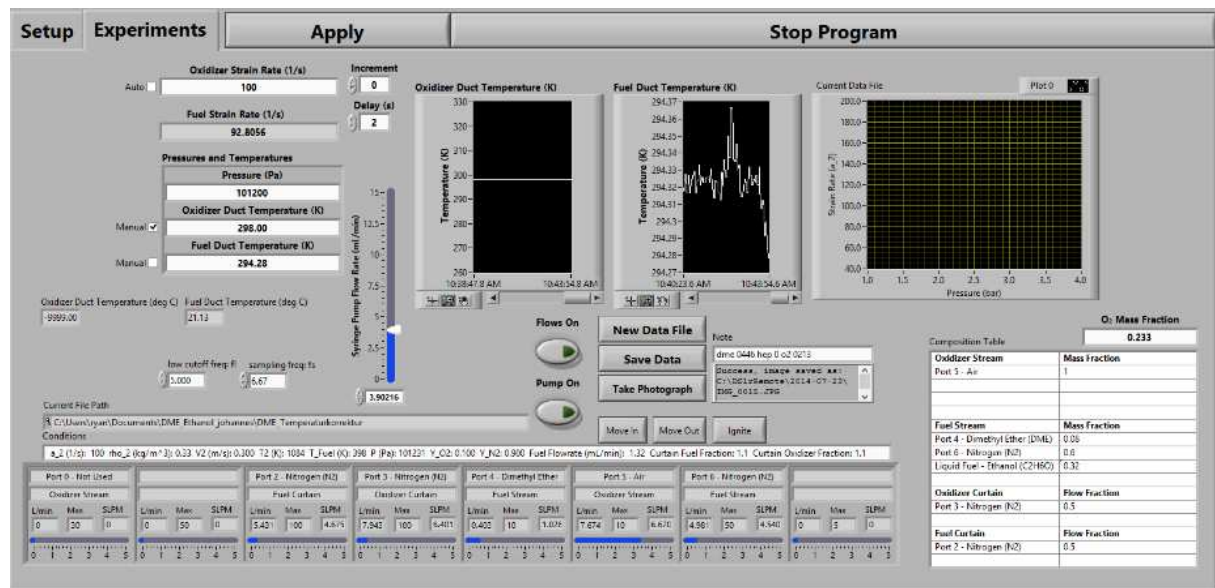
Figure 2.6: Graphical user interface of the LabView based software with typical settings for autoignition before starting heating up

To avoid manual failures the software is designed to emit different kinds of errors and show limits of feasibility such as too high strain rates. By hitting the save button all important data is saved as a text file including the flow rates, velocities, mass fractions, mol fractions, temperatures, densities and the pressure. Also the calibration of the mass flow controllers are included in the software. Since several parameters change during the experiment, the properties are recalculated and refreshed every two seconds.

2.4.1 Input parameters

To set up an experiment the software requires different types of parameters. In order to calculate the flow rate of the syringe pump the density of the liquid fuel is assumed to be constant. The values of the densities of the liquid fuels are the densities at 296°K.

By setting the software either to autoignition or to extinction, it automatically sets the distance L to the correct value.

The areas of the duct exits A_1 and A_2 and the areas of the curtains $A_{curt,1}$ and $A_{curt,2}$ are identical in order to obtain a concentric and steady state flame. Since the experiments in this setup take place under ambient pressure, the value of the pressure is set to 101200 Pa.

2.4.2 Calculated parameters

The mass fractions [-] of the fuel mixture are chosen to stay within the limitations of the experimental setup. The maximum flow rates of the mass flow controllers, the grade of vaporization of the liquid fuels and the temperatures restrict the range of data.

$$Y_{N_2,1} = 1 - Y_{Eth,1} - Y_{DME,1} \qquad (2.1)$$

By choosing the mass fractions for a composition of the fuel mixture the mol fractions can be calculated with

$$X_{i,1} = \frac{\dfrac{Y_{i,1}}{M_{i,1}}}{\displaystyle\sum_{Eth,DME,N_2} \dfrac{Y_{i,1}}{M_{i,1}}} \qquad (2.2)$$

where Eth stands for ethanol, DME for dimethyl ether and N_2 for the nitrogen added to the fuel stream. $M_{i,1}$ is the molecular weight of the relevant element.

By using the ideal gas equation, the density of the oxidizer stream ρ_1 and the density of the fuel stream [kg/m^3] ρ_2 can be calculated [kg/m^3].

$$\rho_1 = \frac{p\sum_{i=DME,ETH,N_2} X_{i,1} M_{i,1}}{RT_1} \qquad (2.3)$$

$$\rho_2 = \frac{p\sum_{i=air,N_2} X_{i,2} M_{i,2}}{RT_2} \qquad (2.4)$$

The temperature of the fuel stream T_1 is constantly measured by a thermocouple that sits in the end of the fuel duct directly under the screens. The temperature of the oxidizer stream T_2 of the extinction experiment is set to 296K; the ambient temperature of the laboratory. In the autoignition experiment the temperature T_2 is constantly measured via a thermocouple below the last screen of the oxidizer duct. R is the ideal gas constant 8,314[J/molK] and p is the ambient pressure [Pa].

By introducing the momentum balance, the velocity of the fuel stream can be calculated.

$$V_1 = \frac{V_2}{\sqrt{\dfrac{\rho_1}{\rho_2}}} \tag{2.5}$$

The needed volume fluxes of the different elements in the fuel stream then are

$$\begin{aligned}
\dot{V}_{N_2,1} &= X_{N_2,1} V_1 A_1 \\
\dot{V}_{DME,1} &= X_{DME,1} V_1 A_1 \\
\dot{V}_{Eth,1} &= X_{Eth,1} V_1 A_1
\end{aligned} \tag{2.6}$$

and in the oxidizer stream

$$\begin{aligned}
\dot{V}_{air,2} &= X_{air,2} V_2 A_2 \\
\dot{V}_{N_2,2} &= X_{N_2,2} V_2 A_2
\end{aligned} \tag{2.7}$$

Since the curtains should adjust to the velocities of the streams it is necessary to set a relative velocity to the duct velocities. Thereby the velocity of the curtain stream will increase when the velocity of the oxidizer and fuel streams increases. In these experiments the relative velocities $v_{relcurt,1}$ and $v_{relcurt,2}$ are set to 0,5[-].

$$\begin{aligned}
\dot{V}_{curt,1} &= v_{relcurt,1} V_1 A_1 \\
\dot{V}_{curt,2} &= v_{relcurt,2} V_2 A_2
\end{aligned} \tag{2.8}$$

To receive the volume fluxes in standard liters per minute they are scaled to standard temperature 273,15K by using the ideal gas equation.

$$\dot{V}_{SLM,i,j} = \dot{V}_{i,j} \frac{273,15\text{K}}{T_{i,j}} \tag{2.9}$$

Since either the strain rate or the temperature constantly change during the experiment, the software runs these calculations every two seconds. This can also be initiated by hitting the apply button. A re-run also resets the mass flow controllers and the syringe pump to the new values.

2.5   Controlling Units

2.5.1 Mass Flow Controllers

The mass flow controllers (MFC) are connected to the software via two Teledyne PowerPod 400. The PowerPod provides a voltage for the MFC's that is linear to the mass flow rate. The integrated sensor of the MFC constantly provides information for the integrated control valve so that the sensor's measurement matches the set-point input.

Based on mass flow controllers set up for nitrogen the MFC's are calibrated for the maximum flow rate for each individual gas needed. The needed volume in standard liter per minute is set in the program and piped through the wet test meter. The wet test meter used is a Ritter TG 5/5-ER- drum-type gas meter. The wet test meter measures the volumetric flows of the gas by measuring the positive displacement of a rotating rigid chamber with a measuring unit over the time. Out of the set-point volume and the measured volumetric flow, the maximum flow rate is calculated and compared to that of the previous calibration process. These steps are repeated until the derivation of the mass flow reaches a tolerance less than ±1%.

2.5.2 Temperature Measurement

Different types of thermoelectric effect sensors, in short called thermocouples, are used for the temperature measurement. Thermocouples consist of two dissimilar metals that are connected by a bead at one end. A voltage can be measured if the junction of the two metals is subjected to temperature change. The voltage change is linked to the temperature change through a function. There is a wide variety of metals that can be used for thermocouples, in this experiment a type R thermocouple is used for the temperature measurement at the oxidizer duct exit in the autoignition experiment (T_2). Type E thermocouples are used for the control of the temperature of the heated lines between the burner and the vaporizer and for the vaporizer itself. Each type E thermocouple is hooked up to a closed loop proportional integral derivative (PID) control. This ensures adequate temperature control of the heating tape due to constant measuring of the process temperature and application of an

appropriate duty cycle. To measure the temperature of the fuel stream another type E thermocouple sits inside the burner under the screens of the fuel duct (T_1).

2.5.3 Exhaust System

The exhaust of the burner is connected to the in house deduction system. Thus, the combustion gases are sucked out of the combustion zone by a small vacuum without influencing the flame. The combustion gases are cooled by six water sprays to avoid further reactions and to avoid heating up the burner. The water is separated from the exhaust gases in a vertical tube.

Chapter 3

Experiments

3.1 Autoignition

3.1.1 Preparation

The method used for autoignition is the following: By choosing a certain strain rate, a flow field is established in the non-burning regime. Due to the high operation temperature it is important to heat up the autoignition top very slowly to avoid thermal stress. When approaching the expected autoignition temperature of a certain strain rate and mixture fraction, the increase in temperature is slowed down. By further increasing the temperature of the oxidizer stream the mixture autoignites. A high-speed camera is set up to document proper autoignition at a location close to the centerline where the highest temperatures are measured. The temperature measured milliseconds before autoignition is reported as the autoignition temperature. The described procedure is repeated for different values of strain rates and mixture fractions.
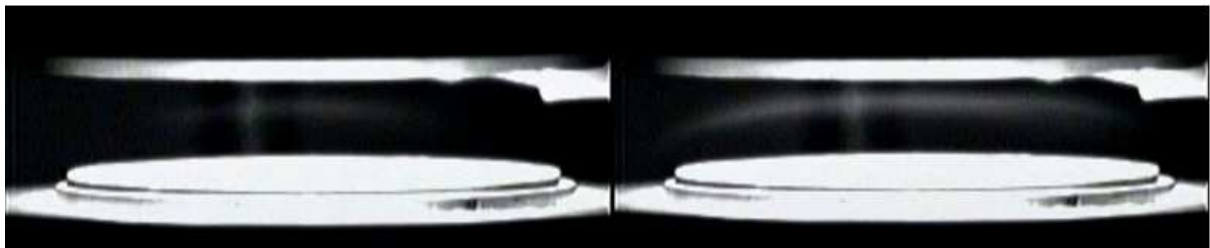
Figure 3.1: Snapshot of a mixture of DME and ethanol at autoignition. The left picture shows a blue flame shortly after the ignition process. The right picture shows a blue flame that already expanded horizontally along the surface of stoichiometry. The time interval between the left and the right picture is 4 milliseconds. The picture was taken at an oxidizer strain rate a_2=165,52 [1/s] and at a mass fraction of DME $Y_{DME,1}$=0,24 and ethanol $Y_{Eth,1}$=0,16 in the fuel stream.

Figure 3.1 shows snapshots milliseconds after ignition occurred. The horizontal reflection in the flame in both pictures close to the centerline is one of three adjustable pins of the extinction top. The white reflection on the right top side of the pictures is the isolation (ceramic tube) of the support wires of the thermocouple used for measuring the oxidizer stream temperature.

3.1.2 Temperature correction

The autoignition temperature is measured by a Pt/13%Rh-Pt type R thermocouple that is placed close to the last screen at the end of the oxidizer duct. To ensure a fast response of the thermocouple an unsheathed fine gage micro-temp thermocouple is used. Its quoted measuring range is 0 to 1450°C with the error limits of 1,5°C or 0,25%. [17]

The wiring diameter of the thermocouple is 0,076 mm and the bead diameter of the welding is 0,21 mm. The wires of the thermocouple are welded to two conductors for support. The conductors are routed separately through a ceramic tube to avoid short-circuiting. The thermocouple is installed on a two-dimensional moveable mounting to guarantee proper positioning. This also ensures the repeatability of the measurements. The thermocouple and respectively the sensor wires are positioned horizontally and orthogonally to the gas flow to prevent heat conduction. A measured temperature profile close to the duct exit shows that the highest temperature is measured at a third of the diameter. The bead is positioned at the point of highest temperature. At higher strain rates the thermocouple wires tend to bend down slightly, but the measured temperatures are still accurate. [2]

Since the wires and the bead are subjected to conduction along the thermocouple wires, convection between the thermocouple and the gases, heat transfer through surface-induced catalytic reactions and radiation losses, the initially measured temperatures have to be corrected. An energy balance on a thermocouple yields to

$$\dot{Q}_{cat} + \dot{Q}_{conv} + \dot{Q}_{rad} + \dot{Q}_{cond} = \rho c_p V \frac{dT_{tc}}{dt} \tag{3.1}$$

In practice, conduction along the thermocouple wires can be neglected if the length-to-diameter ratio of the thermocouple is large enough (>200). Heat losses due to surface-induced catalytic reactions can be neglected since the thermocouple sits in an air stream. [18]

Given that the dimensions of the thermocouple are a lot smaller than the dimensions of the oxidizer, all surroundings of the thermocouple are treated as hypothetical black surfaces. This simplification can be made because even if the surroundings reflect some of the radiation of the thermocouple surface, the probability is much higher that the reflected radiation will reach another point of the surroundings than a point on the small, thermocouple surface. Sooner or later the reflection is absorbed by the surroundings and thus none of the reflected radiation can reach the thermocouple surface.[19, 20]

The temperature of the screen is assumed to be the same temperature as the oxidizer gas flowing through it. The temperature of the surroundings is assumed to be 296K. This assumption denotes that there is a heat transfer caused by radiation from the screen of the oxidizer duct to the thermocouple as well as a heat transfer caused by radiation from the thermocouple to the surroundings. To address this problem correctly, view factors need to be calculated for the screen area and the surroundings. To approach this problem it is assumed that the thermocouple is a small plane surface relative to a large disk surface of the surroundings for the upper area of the thermocouple and the lower area of the thermocouple. By using the view factor integral

$$F_{ij} = \frac{1}{A_i} \int_{A_i} \int_{A_j} \frac{cos\Theta_i cos\Theta_j}{\pi R^2} dA_i dA_j \tag{3.2}$$

and the view factor summation rule

$$\sum_{j=1}^{N} F_{ij} = 1 \tag{3.3}$$

the view factors can be calculated.[19]

$$F_{sc} = \frac{d_{sc}^2}{d_{sc}^2 + 4L_2^2},$$

$$F_{sur.upper} = 1 - F_{sc},$$

$$F_{sur.lower} = 1,$$

(3.4)

F_{sc} is the view factor of the screen [-], $F_{sur,upper}$ is the view factor of the upper surroundings [-], $F_{sur,lower}$ is the view factor of the lower surroundings [-], d_{sc} is the diameter of the oxidizer screen [m] and L_2 is the distance between the thermocouple bead and the lowest screen [m].

These approximations as well as assuming a steady state measurement ($dT_{tc}/dt = 0$) equation (3.1) leads to

$$\frac{Nu_{cyl}k_f}{d_w} A_w(T_2 - T_{tc}) = \frac{A_{rad}}{2} \sigma \varepsilon_{th}[F_{sc}(T_{tc}^4 - T_2^4) + (2 - F_{sc})(T_{tc}^4 - T_{sur}^4)]$$

(3.5)

Where A_w is the thermocouple wire surface [m²], d_w is the thermocouple wire diameter [m], T_2 is the oxidizer gas temperature [K], T_{tc} is the temperature measured by the thermocouple [K], A_{rad} is the surface of the wire and the bead of the thermocouple [m²], σ is the Stefan-Boltzmann constant 5,67e-8 [W/m²K⁴], T_{sur} is the temperature of the facing surroundings [K], k_f is the thermal conductivity of air [W/mK] and ε_{th} is the emissivity of the thermocouple set to 0,2 according to [21].

The Nusselt number Nu_{cyl} [-] is calculated by

$$Nu_{cyl} = (0,24 + 0,56Re^{0,45})\left(\frac{T_f}{T_2}\right)^{0,17}$$

(3.6)

Where Re is the Reynolds number of air [-] and T_f the film temperature [K] which is the average of the thermocouple and the oxidizer gas temperature. Equation (3.6) is valid for $0.02 < Re < 40$. [18]

3.2   Extinction

At a strain rate close to and below the extinction strain rate a flame is established with a blowtorch. The strain rate is increased in small steps until the flame extinguishes. This procedure is repeated at least three times to obtain results as accurate as possible. The fuel stream is heated up to 400K to avoid fuel condensation. The uncertainties and fluctuations in the fuel stream temperature can measure up to ±20K.

Extinction in a diffusion flame occurs when the heat release out of the reaction zone towards the lean (oxidizer) and rich (fuel) side of the flame exceeds the heat produced by the chemical reaction. This indicates that at extinction the heat produced by the reaction balances the heat lost by conduction in the reaction zone. Therefore, increasing the strain rate of the oxidizer and the fuel stream causes the heat towards the lean and rich side of the reaction zone to exceed the heat generated by the chemical reaction, and so the flame extinguishes. [22]

3.2.1 Adiabatic flame temperature

The adiabatic flame temperature is the flame temperature that can theoretically be reached during a complete combustion without performing work, changing the kinetic or potential energy and without any heat transfer from or to the reaction zone. This implements that the resulting products are water and carbon monoxide and that the absolute enthalpy of the reactants before the combustion is the same as the absolute enthalpy of the products after the complete combustion. The adiabatic temperature is also the maximum temperature that can be reached for given reactants during combustion because any losses and incomplete combustion would result in lowering the flame temperature. The value of the adiabatic flame temperature depends mostly on the initial mixture and temperature of the reactants and the pressure. Conversely, by choosing the adiabatic flame temperature (1900K) and mixture fraction the mass fractions can be calculated. [2, 23]

3.2.2 Mixture fraction

The mixture fraction is a very useful tool to describe important properties of a diffusion flame without going into detail on chemical kinetics. For a known mixture of the fuel stream and of the oxidizer stream, the mixture fraction allows the quantification of the state of local composition before the combustion. The value of the mixture fraction Z can vary between zero and one. In the fuel stream, the mixture fraction Z is equal to one and in the oxidizer stream Z is equal to zero. For a homogenous two feed system the mixture fraction is given by

$$Z = \frac{\dot{m}_1}{\dot{m}_1 + \dot{m}_2} .$$

(3.7)

where $\dot{m}_1$ is the mass flux of the fuel stream and $\dot{m}_2$ the mass flux of the oxidizer stream. Both the mass flux of the fuel stream and the mass flux of the oxidizer stream can contain inert gases. For a stoichiometric mixture

$$Z_{st} = \left(1 + \frac{\nu Y_{F,1}}{Y_{O_2,2}}\right)^{-1}$$

(3.8)

can be calculated. ν is the stoichiometric oxygen-to-fuel mass ratio, $Y_{F,1}$ is the mass fraction of fuel in the fuel stream and $Y_{O_2,2}$ is the mass fraction of oxygen in the oxidizer stream, respectively. Equation (3.8) is valid for Lewis numbers equal to unity. The Lewis number is defined as the ratio of the thermal diffusivity to the mass diffusivity.

The flamelet model developed by Burke Schumann 1928 assumes that the combustion in a diffusion flame takes place in the area of stoichiometric mixture fraction. Fuel and oxygen diffuse from opposite sides into the flame area. They immediately vanish and the products of the reaction and the temperature have a maximum. Therefore, it is assumed that the characteristic chemical reaction time is significantly smaller than the characteristic time of convection and diffusion. The characteristic time of convection and diffusion are approximately equal. Mathematically it is assumed that the reactions take place under infinite residence time and under complete combustion for a one- step reaction. Under these conditions following figures can be obtained.[14, 22]
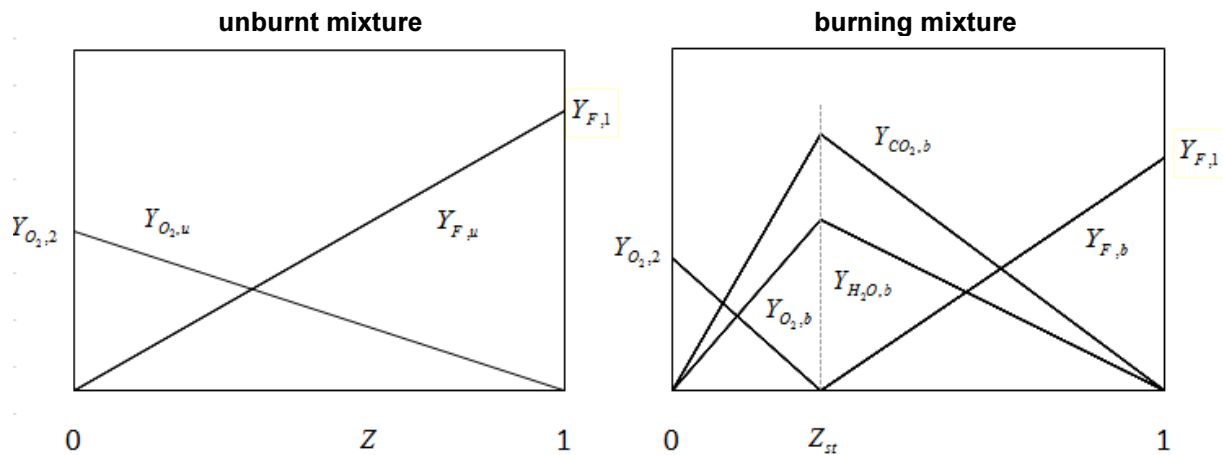
Figure 3.2: Left side: Profiles of $Y_{O_2,u}$ and $Y_{F,u}$ in the unburnt gas mixture

Right side: Profiles of $Y_{O_2,b}$, $Y_{F,b}$, $Y_{CO_2,b}$ and $Y_{H_2O,b}$ in the burning gas mixture [22]

The stoichiometric mixture fraction Z_{st} represents the point where fuel and oxidizer are mixed so that the mass fractions are in a stoichiometric ratio. This implicates that all oxygen and fuel is consumed and reacts to its products water and carbon monoxide.

The stoichiometric mixture fraction Z_{st} selected in this experiment is 0,328.

Since these experiments are carried out with mixtures of dimethylether and ethanol it is not trivial to calculate the mass fractions by given mixture fraction and adiabatic flame temperature. Professor Seshadri developed an asymptotic formulation of the problem where the stoichiometric mixture fraction Z_{st} and the adiabatic flame temperature T_{ad} are fixed and the according mass fractions of oxygen, nitrogen, DME and ethanol can be calculated. The equations shown in this chapter (3.9-3.15) are the result of the asymptotic model, which is attached in appendix B. In this formulation, it is assumed that the Damköhler numbers are high due to the assumption that the reaction takes place simultaneously with the mix of the fuel. The Lewis numbers are assumed to be1,5 [-].

By determining x_{st} from

$$Z_{st} = \frac{1}{2} erfc\left(x_{st} \sqrt{\frac{1}{2}} \right) \tag{3.9}$$

and with the Lewis number of ethanol $Le_{eth} = 1,5$ and the Lewis number of dimethylether $Le_{dme} = 1,5$ the stoichiometric mixture for ethanol $Z_{eth,st}$ and dimethylether $Z_{dme,st}$ can be calculated.

$$Z_{Eth,st} = \frac{1}{2} erfc\left(x_{st} \sqrt{\frac{Le_{Eth}}{2}} \right) \tag{3.10}$$

$$Z_{DME,st} = \frac{1}{2} erfc\left(x_{st} \sqrt{\frac{Le_{DME}}{2}} \right) \tag{3.11}$$

The mass fraction of ethanol $Y_{Eth,1}$ and the mass fraction of oxygen $Y_{O_2,2}$ can be obtained by choosing the mass fraction of dimethylether $Y_{DME,1}$ and by solving

$$3g + 3m = c \tag{3.12}$$

with

$$
\begin{aligned}
g &= \frac{1}{\sqrt{Le_{Eth}}} \frac{X_{Eth,1}}{1 - Z_{Eth,st}} \left(exp\left(\frac{x_{st}^2 \left(1 - Le_{Eth}\right)}{2} \right) \right) \\
m &= \frac{1}{\sqrt{Le_{DME}}} \frac{X_{DME,1}}{1 - Z_{DME,st}} \left(exp\left(\frac{x_{st}^2 \left(1 - Le_{DME}\right)}{2} \right) \right) \\
c &= \frac{X_{O_2,2}}{Z_{st}}
\end{aligned}
\tag{3.13}
$$

$$T_{st} = T_{sur} + \frac{1}{c_p W_{N_2}} \left(Q_{Eth} g + Q_{DME} m \right) Z_{st} \left(1 - Z_{st}\right) \tag{3.14}$$

$$X_{Eth,1} = \frac{Y_{eth,1} M_{N_2}}{M_{Eth}} ; \quad X_{DME,1} = \frac{Y_{dme,1} M_{N_2}}{M_{DME}} ; \quad X_{O_2,2} = \frac{Y_{O_2,2} M_{N_2}}{M_{O_2}} \tag{3.15}$$

where Q_{DME} is the heat release of dimethylether $1328 \cdot 10^3$ [J/mol], Q_{Eth} is the heat release of ethanol $1278 \cdot 10^3$ [J/mol], c_p is the heat capacity 1300 [J/kgK] and $M_{O_2,2}$

is the molecular weight of oxygen 0,032 [kg/mol]. Since dimethylether and ethanol have the same number of oxygen, carbon and hydrogen atoms the molecular weight (0,046 [kg/mol]) is equal.

By iteratively solving the equations (3,13) to (3,15) for $Y_{DME,1}$ from 0 to 1 following figures are obtained.
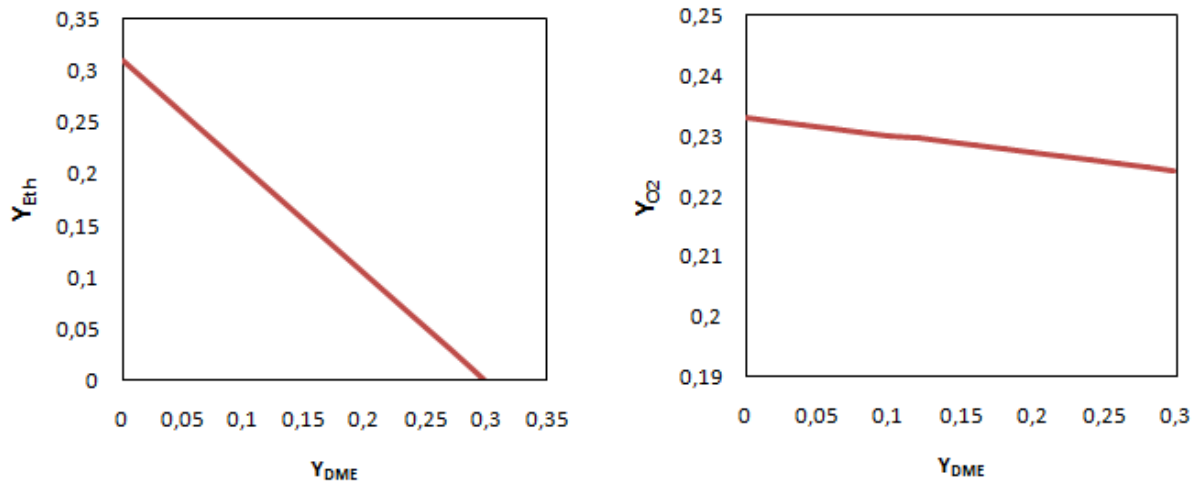
Figure 3.3: Results of solving equation (3,13) till equation (3,15) iteratively with $Y_{DME,1}$ from 0 to 0,298, with a fixed adiabatic flame temperature T_{ad}=1900K and a fixed stoichiometric mixture fraction Z_{st}=0,328

In accordance to the figures following mass fractions are picked for the extinction experiment.

Table 3.1: Mass fraction of DME, ethanol and oxygen
calculated at a fixed adiabatic flame temperature T_{ad}=1900K
and a fixed stoichiometric mixture fraction Z_{st}=0,328

	$Y_{2,O2}$	$Y_{1,DME}$	$Y_{1,ETH}$	$Y_{1,fuel}$	$Y_{1,N2}$
1	0,2330	0,000	0,3105	0,3105	0,6895
2	0,2325	0,020	0,2897	0,3097	0,6903
3	0,2319	0,040	0,2689	0,3089	0,6911
4	0,2313	0,060	0,2481	0,3081	0,6919
5	0,2307	0,080	0,2273	0,3073	0,6927
6	0,2301	0,100	0,2065	0,3065	0,6935
7	0,2296	0,120	0,1858	0,3058	0,6942
8	0,2290	0,140	0,1650	0,3050	0,6950
9	0,2284	0,160	0,1442	0,3042	0,6958
10	0,2278	0,180	0,1234	0,3034	0,6966
11	0,2272	0,200	0,1026	0,3026	0,6974
12	0,2266	0,220	0,0818	0,3018	0,6982
13	0,2260	0,240	0,0610	0,3010	0,6990
14	0,2255	0,260	0,0403	0,3003	0,6997
15	0,2249	0,280	0,0195	0,2995	0,7005
16	0,2243	0,298	0,0000	0,2980	0,7020

Chapter 4

Computational Simulations

Computational modeling and simulations have become very important tools for analyzing many different kinds of systems. Kinetic modeling is applied for solving a great variety of problems, due to the ever-increasing processing power of computers. Another advantage of computational simulations that has contributed to their rise in the last decades is that they are not restricted to physical limitations. Unfortunately, computing detailed kinetic mechanisms requires a lot of time and extremely powerful processors, making it time-consuming and expensive. To reduce the complexity and the dimensions of kinetic mechanisms, analogy rules are adopted and simplifying assumptions are made. Developing a reliable and robust reaction mechanism for the combustion of fuels is a complex problem. A large amount of experimental and computational research is required to improve already existing mechanisms and develop new mechanisms for various applications. Verifying a new kinetic mechanism entails comparing it to other kinetic mechanisms and more importantly to experimental data. [24]

4.1 CHEMKIN

The software CHEMKIN is used for the computation of the mechanism developed in this study. To simulate the kinetic behavior of reaction in different gas phases CHEMKIN needs four different types of inputs:

- the gas-phase kinetics input
- the thermodynamic input
- the gas transport input

– the input settings

The gas-phase kinetics includes information on the species and the reaction mechanism. It can also include the thermodynamic data. The reaction mechanism includes all reactions that take place as well as the Arrhenius rate coefficients A, β and E_A for each reaction. It also contains information on if a reaction is reversible or irreversible and if it is a three-body reaction with an enhanced third-body and/or an arbitrary third body. In addition, pressure dependence and auxiliary reaction data can be entered in lines immediately following the reaction data. The thermodynamic input file includes the species name, the elemental composition of the species and the temperature ranges over which the polynomial coefficient for the entropy, enthalpy and isobaric heat capacity are valid. All species listed in the gas phase kinetic file also have to be listed in the thermodynamic file with their thermodynamic data and in the transport data file. The complier uses these three files to create a gas-phase kinetics-linking file (chem.asc) that contains all relevant information about the mechanism. The gas-phase kinetics-linking file is accessed permanently during the reactor-model simulation.

The input settings mainly contain the boundary conditions; in further detail the reactor physical properties, the grid properties, the stream properties and the species-specific properties. The detailed input settings for autoignition and extinction are listed in section 4.3.

CHEMKIN provides several applications of idealized reactor models. The reactor used for the computations carried out in this thesis is the "Diffusion or Premixed Opposed-flow Flame" reactor.

The solver then calculates a solution for each point using the CHEMKIN application code, the input settings, the gas-phase kinetics linking file and the reactor.[25–27]

4.2 Development of a short DME and ethanol mechanism

When merging two well-tested and valid mechanisms, the first step is choosing which of the two should serve as the master mechanism and which should serve as the donor mechanism. The master mechanism is the base frame for the new merged

mechanism while the donor mechanism is used as a donor for reactions and species that are not originally listed in the master mechanism. The Lawrence Livermore National Laboratory Dimethyl Ether 2000 mechanism (LLNL) is used as the master mechanism for the mechanism developed in this thesis. Since the LLNL mechanism does not include ethanol the San Diego (SD) mechanism is used as the donor mechanism and is merged to the LLNL mechanism. The new merged mechanism is abbreviated as MM. In addition, the thermodynamic data and the gas transport data from the LLNL mechanism are used as the base frame and are merged with the thermodynamic data and the gas transport data from the SD mechanism. [28, 29]

Merging two well-tested mechanisms from different institutions to a new mechanism is not a simple task since a coherent model of species, thermodynamic properties and transport properties does not exist. Every institution defines their species differently. When merging the SD mechanism with the LLNL mechanism all similar reactions and species first must be found, compared and then checked for duplicates. The same method is applied to the gas transport data and the thermodynamic data.

4.2.1 Verification

To verify the new merged mechanism the ignition delay times in a closed homogenous 0-D reactor at different equivalence ratios of air and ethanol and air and DME respectively are compared to the initial mechanisms. The reactor has a volume of 400cm^3, an initial temperature of 900K and an initial pressure of 1atm.
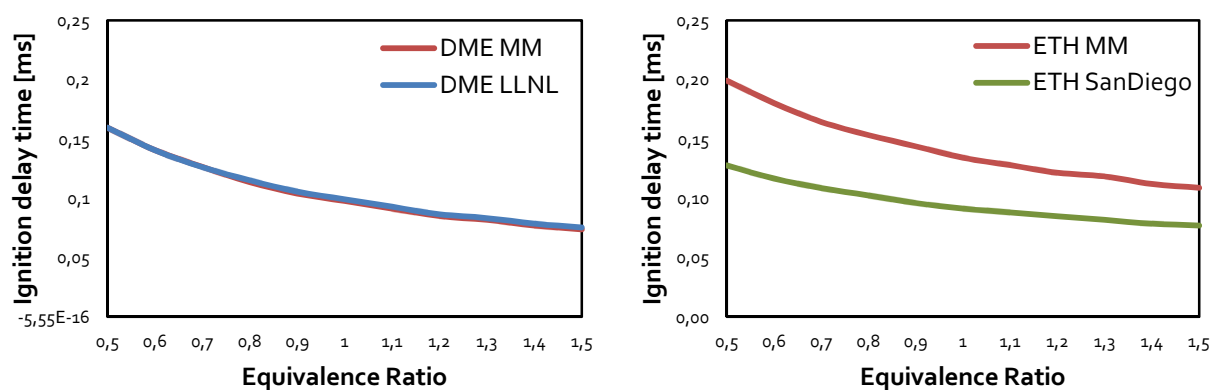
Figure 4.1: Ignition delay time over the equivalence ratio in a closed homogenous 0-D reactor;
Left side: numerical calculation of the ignition delay time in a closed homogenous 0-D reactor with a mixture of air and DME; comparison of the MM and the LLNL mechanism

Right side: numerical calculation of the ignition delay time in a closed homogenous 0-D reactor with a mixture of air and ethanol; comparison of the MM and the SD mechanism

Since the LLNL mechanism was used as the master mechanism for the new developed mechanism the ignition delay times only differ 2% at most at an equivalence ratio of 1,5.

The differences of the ignition delay times of the San Diego mechanism and the new developed mechanism are much more significant (between 29% at an equivalence ratio of 0,5 and 36% at an equivalence ratio of 1,5). This is an expected result since the SD mechanism is used as the donor mechanism. Only the equations and the species that are not originally in the LLNL mechanism are used in the MM mechanism; the entire base frame is replaced by the LLNL mechanism.

4.3 Computational setup
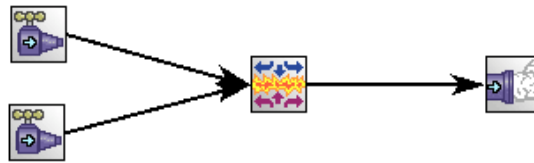
Figure 4.2: Reactor model by CHEMKIN (Diffusion or Premixed Opposed-flow flame)

Reactor physical properties are set up for solving the gas equation for both the autoignition computations as well as for the extinction computations. The pressure is set to 1atm and the ambient temperature is set to 296K. The maximum temperature for the initial profile is set to 400K for autoignition (starting from no initial flame) and to 2100K (starting from an initial flame) for extinction. For the computations in this thesis a manual approach is used to find the autoignition temperature and the extinction strain rate.

Pseudo Time Steps (Fixed Temperature)		
Number of Time Steps	100.0	
Initial Size of Time Step	1.0E-6	sec ▼
Pseudo Time Steps (Energy Equation)		
Number of Time Steps	100.0	
Initial Size of Time Step	1.0E-6	sec ▼
Minimum Pseudo Time Step	1.0E-10	sec ▼
Maximum Pseudo Time Step	0.01	sec ▼
Number Time Steps Before Increasing	25	
Time Step Decrement Factor	2.0	
Time Step Increment Factor	2.0	
Number of Transient Iterations before Updating Jacobian	20	
Maximum Number of Iterations per Pseudo Time Step	25	
Maximum Number of Pseudo Time Stepping Operations Allowed	100	
Number of Initial Pseudo Time Steps	0	
Number of Iterations before Updating Jacobian	20	
Maximum Number of Iterations per Steady State Search	100	
Pseudo Time Stepping Only		
Number of Time Steps		
Initial Size of Time Step		sec ▼
Output Frequency during Integration	100	
Minimum Bounds on Species Fractions	-0.0001	
Positive Value to Reset Species Fractions	0.0	

◉ Windward Differencing
○ Central Differencing

Figure 4.3: Mathematical boundary conditions for the computations (solving gas energy equation)

4.3.1 Autoignition

The number of uniform Grid Points is set to 100, with the further specifications of:

– Adaptive Grid Control Based on Solution Gradient: 0,1

– Adaptive Grid Control Based on Solution Curvature: 0,5

– Maximum Number of Grid Points Allowed: 500

– Number of Adaptive Grid Points: 10

The distance between the ducts is set to 1,45cm with an estimated flame center position of 0,5cm.

To calculate the autoignition computationally the same approach as by the experiments is used; the oxidizer stream temperature is increased until the mixture autoignites. By increasing the oxidizer stream temperature the fuel velocity has to be decreased to meet the momentum balance. To find the correct autoignition temperature a parameter study is used, where a pre-defined list of the oxidizer gas temperature and fuel velocity for every single data point is processed. The criterion for autoignition is the temperature over the distance. When the point of autoignition is reached a step change in temperature occurs between the two ducts; a flame establishes. In reverse, by comparing the solutions with the pre-defined list, the autoignition temperature can be calculated. For simplification the inlet fuel gas temperature measured during the experiments is averaged and set to 400K.

4.3.2 Extinction

The number of uniform Grid Points is set to 30, with the further specifications of:

- Adaptive Grid Control Based on Solution Gradient: 0,1
- Adaptive Grid Control Based on Solution Curvature: 0,5
- Maximum Number of Grid Points Allowed: 500
- Number of Adaptive Grid Points: 10

The distance between the ducts was set to 1,25cm with an estimated flame center position of 0,5cm.

Continuations are used to compute the extinction behavior. These defer from parameter studies based on the fact that the solutions from a previous run are used as starting conditions for a new run. Additionally, a pre-defined list of changing parameters is needed for every single data point. In this case the fuel gas temperature is set to 395K and the oxidizer gas temperature is set to 296K. To fulfill momentum balance the fuel gas velocity has to be increased by increasing the oxidizer gas temperature. The criterion for extinction is the temperature over the distance. When extinction is reached a step change in temperature occurs between the two ducts; the flame extinguishes. In reverse, by comparing the solutions with the pre-defined list, the autoignition velocity of extinction can be calculated. For

simplification, the inlet fuel gas temperature measured during the experiments is averaged and set to 385K.

Chapter 5

Experimental and Numerical Results

Chapter 5 summarizes the numerical and experimental results; the detailed experimental results are shown in appendix A, the approach for the computation is explained in Chapter 4.

5.1 Autoignition

The shown autoignition temperatures are corrected due to losses according to section 3.2.1. The displayed experimental data points are arithmetically averaged values and the displayed curves are best-fit lines based on polynomial equations.

Below the autoignition temperature of a given fuel autoignition will never occur, while above the autoignition temperature autoignition will always occur. Hence, the figures are divided into two regions.

Generally, the autoignition temperature of a certain fuel rises by increasing the strain rate. This rise in temperature of autoignition occurs because when increasing the strain rate, which accompanies an increase of the velocities, the time for chemical reactions decreases. For this reason, the mixture is harder to ignite and the required temperature for autoignition increases. Figure 5.1 displays the autoignition temperature of mixtures of DME and ethanol over the oxidizer strain rate.
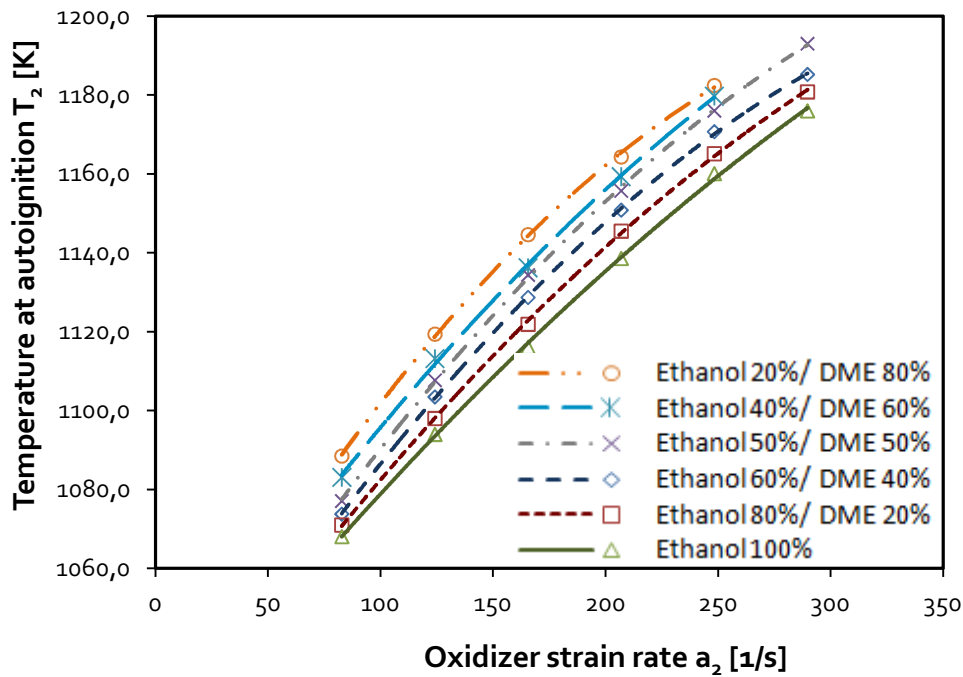
Figure 5.1: The temperature at autoignition of the oxidizer stream as a function of the oxidizer strain rate at a constant fuel mass fraction of $Y_{F,1}$=0,4. The figure shows data for blends of Ethanol and DME from 100% ethanol and 0% DME up to 20% ethanol and 80% DME. The symbols represent the experimental data and the lines are of best-fit curves based on polynomials second order.

Ethanol is found to have the lowest autoignition temperature at all strain rates of the tested fuel mixtures. By increasing the DME content in the mixture the temperature of autoignition rises. It seems that an increase in DME concentration has a uniform enhancing effect on the temperature of autoignition, independent of the strain rates and hence independent of the velocities. The gradient dT_2/da_2 is very steep for all tested strain rates.

Figure 5.2 compares the temperature at autoignition for pure DME, pure ethanol and the blend of 20% ethanol and 80% DME. Despite the expectation that a further increase of DME content up to 100% in the fuel will shift the autoignition temperature upwards, it shows a completely different behavior. Pure DME has higher autoignition temperatures than ethanol but the gradient dT_2/da_2 is a lot steeper than that of ethanol. Another very interesting observation is that the temperature at autoignition at an oxidizer strain rate $a_2 = 82,78$ [1/s] of DME is only 3,6K higher than that of ethanol compared to the blend of 20% ethanol and 80% DME where the autoignition temperature is 20,4K higher.
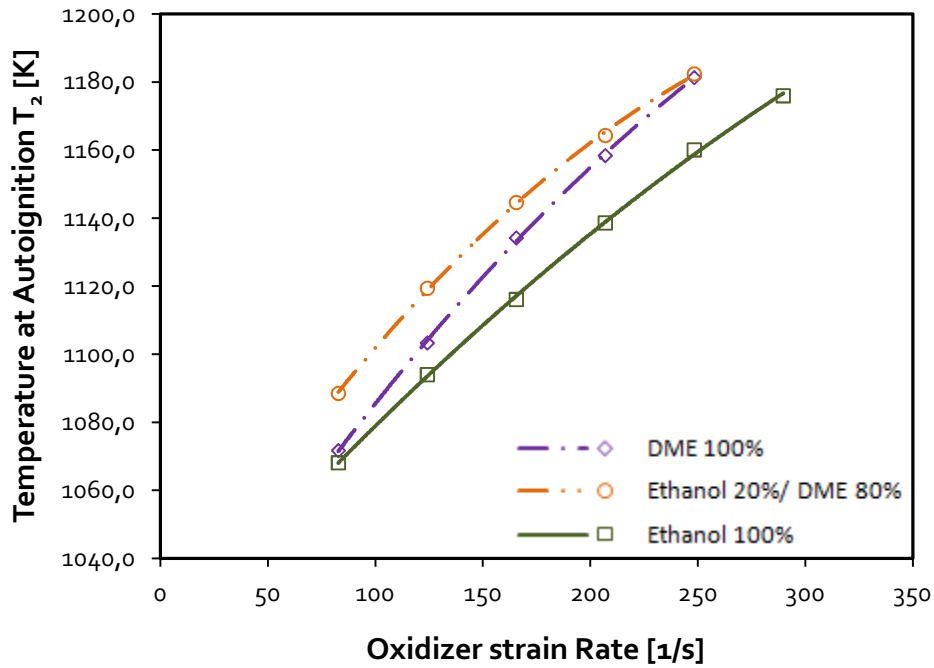
Figure 5.2: The temperature at autoignition of the oxidizer stream as a function of the oxidizer strain rate at a constant fuel mass fraction of $Y_{F,1}=0,4$. The figure shows data for pure DME, pure ethanol and mixtures of DME and ethanol. The symbols represent the experimental data and the lines are of best fit curves based on polynomials second order.

By plotting the oxidizer temperature at autoignition over the compositions of the blend ethanol/ DME the behavior of the tested fuels can be shown from a different point of view. As in Figure 5.1 and 5.2, Figure 5.3 shows that the blend of 20% ethanol and 80% DME has the highest temperature of autoignition of the measured fuels and fuel blends.

Figure 5.3: The temperature at autoignition of the oxidizer stream as a function of the composition of the DME and ethanol blend at a constant fuel mass fraction of $Y_{F,1}=0,4$. The figure shows data at different oxidizer strain rates. The symbols represent the experimental data and the lines are best-fit curves based on polynomials fourth order.

However, Figure 5.3 illustrates the differences in behavior of various blends at different strain rates more clearly. When comparing the blend of 20% ethanol and 80% DME to 100% DME, the difference in autoignition temperature is higher at low strain rates. In particular the autoignition temperature increases by $\Delta T_2 = 16,8\text{K}$ at an oxidizer strain rate of $a_2 = 82,78$ [1/s] by adding 20% ethanol to DME. At the oxidizer strain rate $a_2 = 248,28$ [1/s] the increase of the autoignition temperature is almost zero; $\Delta T_2 = 1,1\text{K}$. Thus, dimethylether inhibits ignition at higher strain rates.
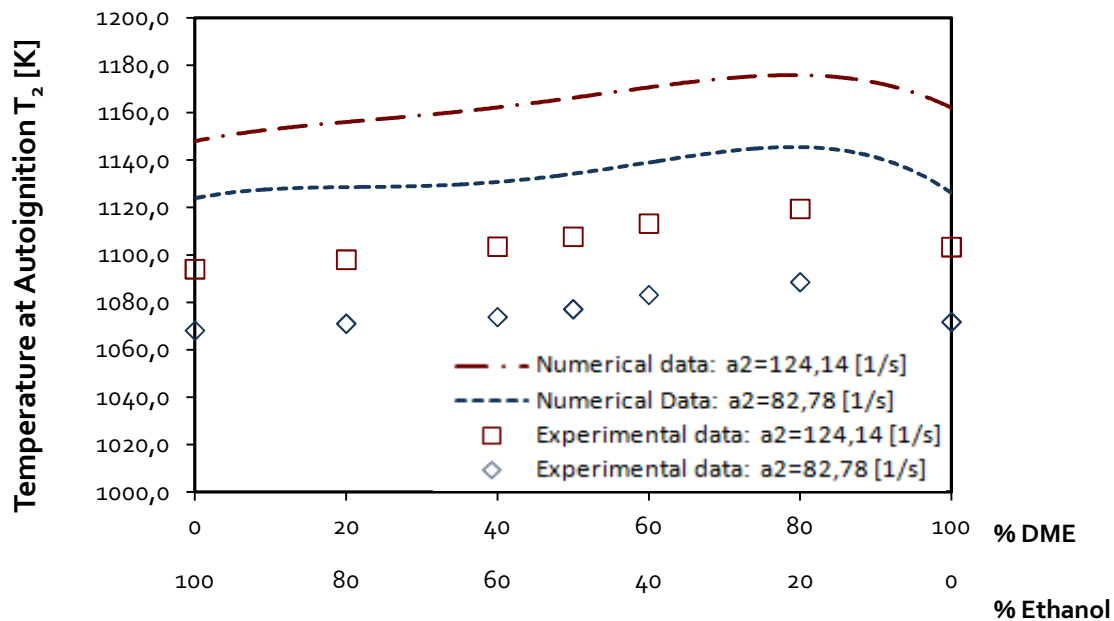
Figure 5.4: The temperature at autoignition of the oxidizer stream as a function of the composition of a DME/ethanol blend at a constant fuel mass fraction of $Y_{F,1}$=0,4. The figure shows data for blends of Ethanol and DME for an oxidizer strain rate a_2=82,78 [1/s] and a_2=124,14 [1/s]. The symbols represent the experimental and numerical data and the lines best-fit curves based on polynomials fourth order.

Figures 5.4 and 5.5 show the computational data compared to the data obtained from the autoignition experiments. The lines (best-fit curves based on polynomials fourth order) in these figures are the results of numerical calculations; the symbols represent the experimental data. In general, the chemical kinetic mechanism developed in this thesis comes very close to the obtained experimental data. The computational data processed by the MM shows the same behavior at autoignition as the data obtained from the autoignition experiment. However, as shown in Figures 5.3 and 5.4 the absolute values from the autoignition temperatures of the numerical data over predict the absolute values obtained by the experimental work at all strain rates. The absolute divergence at lower strain rates is more significant than at higher

strain rates with an absolute divergence up to $\Delta T_2 = 59,3\text{K}$ for a blend of 40% DME and 60% ethanol at the oxidizer strain rate $a_2 = 124,14$ [1/s].
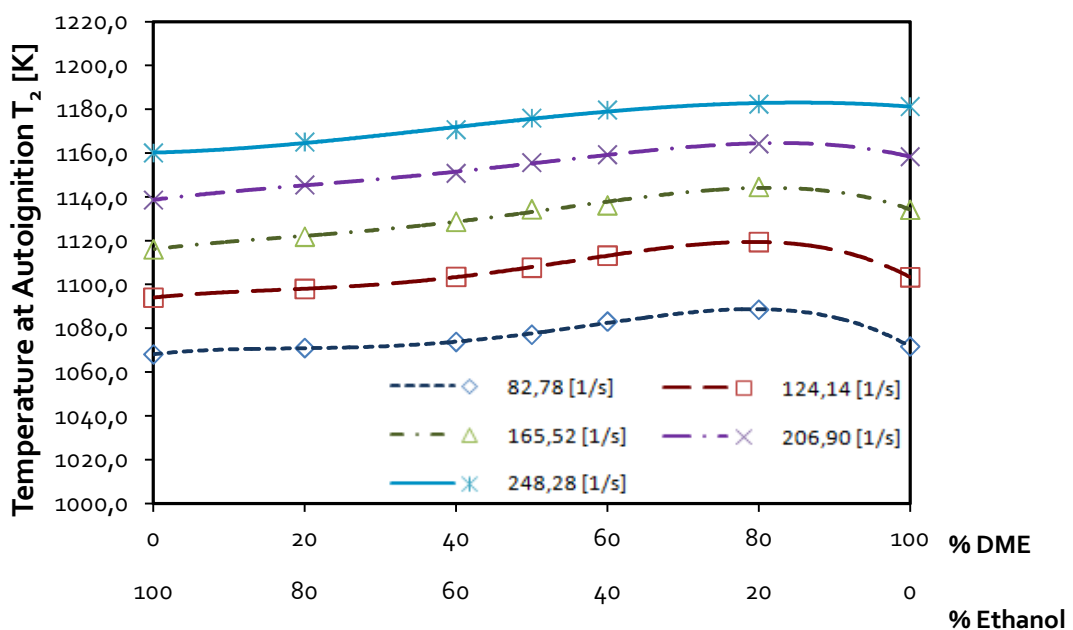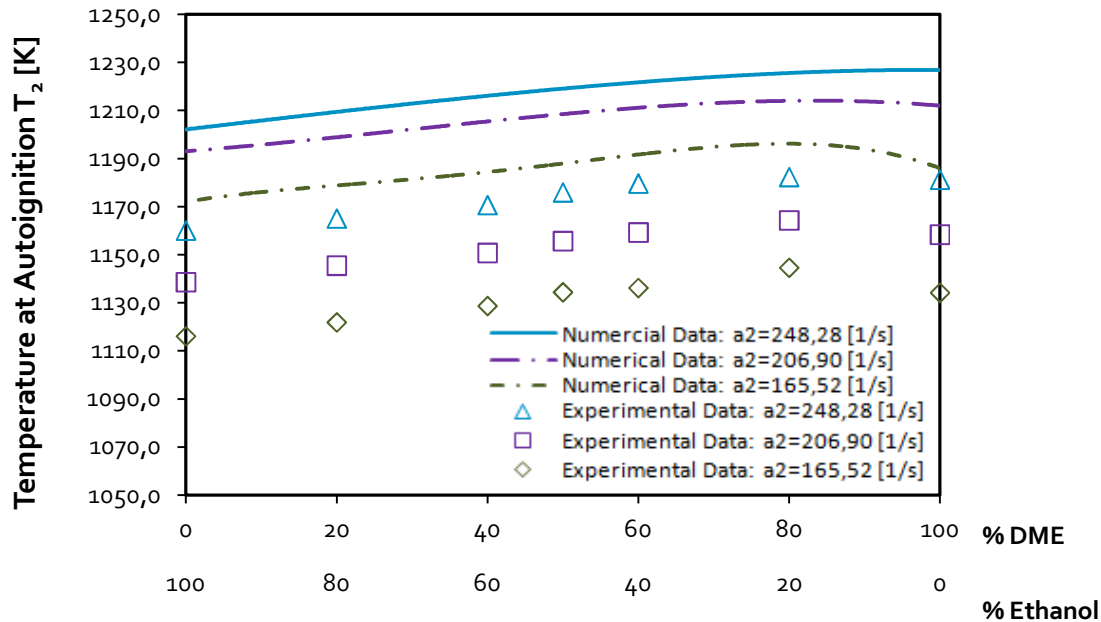

Figure 5.5: The temperature at autoignition of the oxidizer stream as a function of the composition of a DME/ethanol blend at a constant fuel mass fraction of $Y_{F,1}$=0,4. The figure shows data for blends of ethanol and DME for an oxidizer strain rate a_2=165,52 [1/s], a_2=206,90 [1/s] and a_2=248,28 [1/s]. The symbols represent the experimental and numerical data and the lines are best-fit curves based on polynomials fourth order.

5.2   Extinction

In the extinction experiment, the extinction behavior of different blends of DME and ethanol is demonstrated under a fixed adiabatic flame temperature and a fixed stoichiometric mixture fraction according to section 3.2. Since both DME and ethanol have a visible blue flame, their blends also have a visible blue flame.

Figure 5.6 shows the oxidizer strain rate at extinction as a function of the relative amount of DME and ethanol in the combustible mixture. This figure compares the extinction data obtained from the numerical calculations from the SD mechanism, the LLNL mechanism and the new developed mechanism. The symbols represent the data obtained from the numerical calculations; the lines represent best-fit curves based on polynomials second order.

Figure 5.6: Oxidizer extinction strain rates as a function of the composition of the DME/ ethanol blend. The measured mass fraction are according to table 3.1 for a constant stoichiometric mixture fraction Z_{st}=0,328 and constant adiabatic flame temperature T_{ad}=1900. The symbols represent the numerical data and the lines are best-fit curves based on polynomials second order.

The numerical calculations for pure DME of the LLNL mechanism and the new merged mechanism show the same result. This was expected because the LLNL mechanism was used as master mechanism. The numerical calculations for pure ethanol carried out with the San Diego mechanism and the new merged mechanism show an absolute divergence of $\Delta a_2 = 13$ [1/s]. This is an acceptable result considering the fact that two mechanisms are merged without customizing the chemical data.

Figure 5.7 shows the strain rate at extinction as a function of the relative amount of DME and ethanol in the combustible mixture. The dotted line is a result of numerical calculations; the symbols represent the experimental data. The detailed composition of the tested blends is shown in Table 3.1. The critical condition of extinction of the numerical calculations (dotted line) is compared with those obtained from the experimental trials.

The plotted data can be seen as a boundary between the flammable and non-flammable region. In the state above the boundary, the mixture cannot be ignited. Yet by decreasing the strain rate (downwards vertical shift) and by increasing the DME

content of the mixture (horizontal shift to the right) the flammable region can be reached and the mixture can be ignited by an external energy source.

The computational data over predicts the data obtained from the experiments, but it shows the same trend. The absolute divergence is the lowest at pure DME with delta $\Delta a_2 = 8$ [1/s] and up to $\Delta a_2 = 46$ [1/s] for pure ethanol.

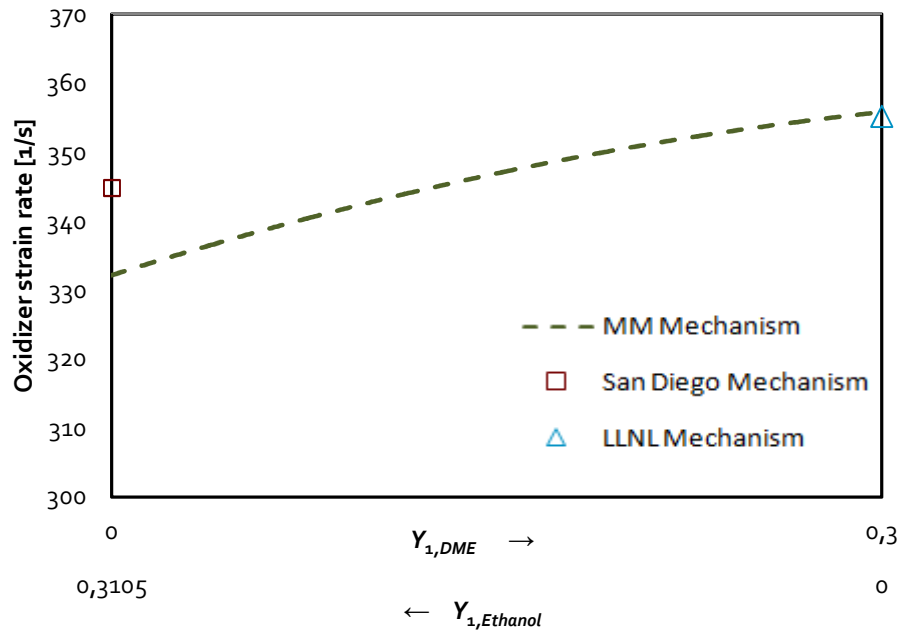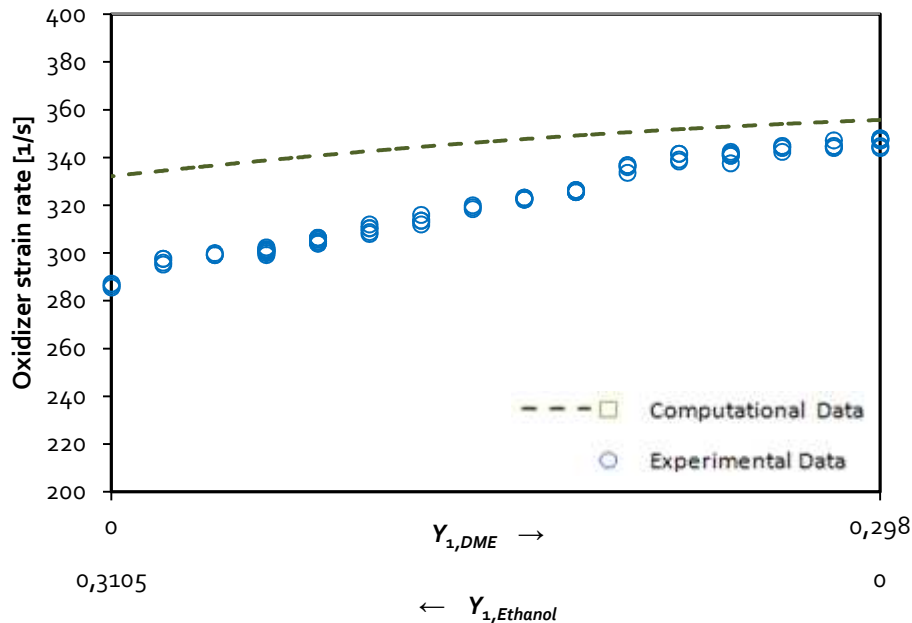Figure 5.7: Oxidizer extinction strain rates as a function of the composition of the DME/ ethanol blend. The measured mass fraction are according to table 3.1 for a constant stoichiometric mixture fraction Z_{st}=0,328 and constant adiabatic flame temperature T_{ad}=1900. The symbols represent the numerical and computational data. The lines are best-fit curves based on polynomials second order.

Chapter 6

Concluding Remarks

The main focus of this diploma thesis was to determine how dimethyl ether and ethanol influence each other under critical conditions of combustion and further develop a chemical kinetic mechanism for numeric simulations. The experimental studies of the critical conditions of autoignition and extinction show that although dimethyl ether and ethanol are isomers, they show different behaviors under the critical conditions of autoignition and extinction.

At a fixed value of the strain rate, the temperature at autoignition for DME is nearly the same as for ethanol at low strain rates. By mixing ethanol and DME, the temperature of autoignition can be increased with a peek at 20% ethanol and 80% DME. At higher strain rates, this effect is less pronounced and vanishes by further increasing the strain rate. At a low strain rate, the ignition of DME appears to be influenced by low temperature chemistry. The critical conditions of extinction are carried out with mass fractions chosen at a fixed adiabatic flame temperature and a fixed stoichiometric mixture fraction. The strain rate at extinction is found to increase with increasing amounts of DME in the combustible mixture. Thus, in mixtures of DME and ethanol, the autoignition as well as extinction is delayed with increasing amounts of DME.

By merging two short and well-tested mechanisms, a new short chemical kinetic mechanism was developed that predicts the experimental data to some extent. For both critical conditions- for autoignition as well as for extinction, the experimental and computational results show similar trends, but the computational results over predict the experimental results.

Further research is necessary to eliminate the offset between the experimental results and the computational results. The chemical-kinetic rate parameters of the mechanism are also worthy of improvement. Further research should aim at creating a detailed chemical kinetic mechanism that has a short computational time; which can predict the behavior of combustion with high accuracy. This tool would enable a better analysis of combustion outside of the limitations of experimental apparatuses and it would help improve combustion in all fields of application.

References

[1] Reinhard Seiser. 2000. *Nonpremixed Combustion of Liquid Hydrocarb on Fuels*, Graz, Austria.

[2] Stefan Humer. 2007. *Development of a Surrogate Diesel Fuel. PhD Thesis*, Vienna, Austria.

[3] Forman A. Williams. 2014. *Unexpected Discovery of Cool Flames in Experiments on the International Space Station*, Departement of Mechanical and Aerospace Engineering, University of California, San Diego.

[4] Cipolat, D. and Bhana, N. 2009. Fuelling of a compression ignition engine on ethanol with DME as ignition promoter: Effect of injector configuration. *Fuel Processing Technology* 90, 9, 1107–1113.

[5] McEnally, C. S. and Pfefferle, L. D. 2007. The effects of dimethyl ether and ethanol on benzene and soot formation in ethylene nonpremixed flames. *Proceedings of the Combustion Institute* 31, 1, 603–610.

[6] Semelsberger, T. A., Borup, R. L., and Greene, H. L. 2006. Dimethyl ether (DME) as an alternative fuel. *Journal of Power Sources* 156, 2, 497–511.

[7] National Institute of Standards and Technology. 2005. *NIST Chemistry WebBook Standard Reference Database Number 69*. http://webbook.nist.gov/chemistry/. Accessed 25 August 2014.

[8] Takashi Ogawa, Norio Inoue, Tutomu Shikada, Yotaro Ohno. 2003. *Direct Dimethyl Ether Synthesis*, DME Development Co., Ltd, Shoro-koku Shiranuka-ch, Hokkaido, 088-0563 Japan.

[9] HulyaErdener, Ayca Arinan, Sultan Orman. 2011. *Future Fossil Fuel Alternative; Dimethyl Ether (DME) A review*, Tupras, Turkish Petroleum Refineries Corporation, Korfez 41790/ TURKEY.

[10] Hahn-Hägerdal, B., Galbe, M., Gorwa-Grauslund, M. F., Lidén, G., and Zacchi, G. 2006. Bio-ethanol--the fuel of tomorrow from the residues of today. *Trends Biotechnol.* 24, 12, 549–556.

[11] Balat, M., Balat, H., and Öz, C. 2008. Progress in bioethanol processing. *Progress in Energy and Combustion Science* 34, 5, 551–573.

[12] Sarathy, S. M., Oßwald, P., Hansen, N., and Kohse-Höinghaus, K. 2014. Alcohol combustion chemistry. *Progress in Energy and Combustion Science* 44, 40–102.

[13] Tsuji, H. 1982. Counterflow diffusion flames. *Progress in Energy and Combustion Science* 8, 2, 93–119.

[14] Norbert Peters. *Technische Verbrennung I,* RWTH Aachen.

[15] Connors, K. A. ©1990. *Chemical kinetics. The study of reaction rates in solution*. VCH, New York, N.Y.

[16] Seshadri, K. and Williams, F. A. 1978. Laminar flow between parallel plates with injection of a reactant at high reynolds number. *International Journal of Heat and Mass Transfer* 21, 2, 251–253.

[17] OMEGA Engineering, I. *Thermocouple Reference tables*. http://www.omega.com/thermocouples.html. Accessed 6 October 2014.

[18] Shaddix Christopher R. 1999. Correcting thermocouple measurements for radiation loss-A critical review. *33rd National Heat Transfer Conference* (1999).

[19] Incropera, F. P. 2013. *Principles of heat and mass transfer*. John Wiley, Hoboken, NJ.

[20] Mills, A. F. 1999. *Heat transfer*. Prentice Hall, Upper Saddle River, N.J.

[21] Bradley, D. and Entwistle, A. G. 1961. Determination of the emissivity, for total radiation, of small diameter platinum-10% rhodium wires in the temperature range 600-1450 C. *Br. J. Appl. Phys.* 12, 12, 708–711.

[22] Norbert Peters. 2010. *Combustion Theory. CEFRC Summer School,* Princeton.

[23] Turns, S. R. 2000. *An introduction to combustion. Concepts and applications*. McGraw-Hill series in mechanical engineering. WCB/McGraw-Hill, Boston.

[24] Ranzi, E., Dente, M., Goldaniga, A., Bozzano, G., and Faravelli, T. 2001. Lumping procedures in detailed kinetic modeling of gasification, pyrolysis, partial oxidation and combustion of hydrocarbon mixtures. *Progress in Energy and Combustion Science* 27, 1, 99–139.

[25] CHEMKIN. 2013. *Getting Started Manual 10131, Reaction Design*, San Diego.

[26] CHEMKIN. 2013. *Input Manual 10131, Reaction Design*, San Diego.

[27] CHEMKIN. 2013. *Theory Manual 10131, Reaction Design*, San Diego.

[28] Fischer, S. L., F. L. Dryer, and H. J. Curran, Kaiser, E. W., T. J. Wallington, M. D. Hurley, J. Platz, H. J. Curran, W. J. Pitz, and C. K. Westbrook. 2000. *Dimethyl Ether 2000 Mechanism*, Livermore, CA.

[29] Mechanical and Aerospace Engineering. *Chemical-Kinetic Mechanisms for Combustion Applications*, University of California at San Diego.

List of Figures

List of Tables

fuel composition	a_2 [1/s]	a_1 [1/s]	ρ_2 [kg/m3]	ρ_1 [kg/m3}	V_2 [m/s]	V_1 [m/s]	T_2 [K]	T_1[K]	$Y_{O2,2}$	$Y_{N2,2}$	$Y_{DME,1}$	$Y_{Eth,1}$	$Y_{N2,1}$
100% DME	82,76	56,06	0,32912	1,04707	0,30	0,168	1071,7	386,3	0,233	0,767	0,40	0,00	0,6
0% Ethanol	124,14	85,28	0,31969	0,98896	0,45	0,256	1103,3	409,0	0,233	0,767	0,40	0,00	0,6
	165,52	111,20	0,31098	1,00593	0,60	0,334	1134,2	402,1	0,233	0,767	0,40	0,00	0,6
	206,90	137,61	0,30449	1,00493	0,75	0,413	1158,4	402,5	0,233	0,767	0,40	0,00	0,6
	248,28	163,83	0,29858	1,00120	0,90	0,491	1181,3	404,0	0,233	0,767	0,40	0,00	0,6
80% DME	82,76	56,14	0,32404	1,02818	0,30	0,168	1088,5	393,4	0,233	0,767	0,32	0,08	0,6
20% Ethanol	124,14	83,28	0,31510	1,02220	0,45	0,250	1119,4	395,7	0,233	0,767	0,32	0,08	0,6
	165,52	110,12	0,30816	1,01655	0,60	0,330	1144,6	397,9	0,233	0,767	0,32	0,08	0,6
	206,90	136,49	0,30294	1,01629	0,75	0,409	1164,3	398,0	0,233	0,767	0,32	0,08	0,6
	248,28	162,64	0,29831	1,01502	0,90	0,488	1182,4	398,5	0,233	0,767	0,32	0,08	0,6
60% DME	82,76	56,38	0,32566	1,02453	0,30	0,169	1083,1	394,8	0,233	0,767	0,24	0,16	0,6
40% Ethanol	124,14	82,95	0,31685	1,03608	0,45	0,249	1113,2	390,4	0,233	0,767	0,24	0,16	0,6
	165,52	110,99	0,31044	1,00793	0,60	0,333	1136,2	401,3	0,233	0,767	0,24	0,16	0,6
	206,90	138,34	0,30425	0,99357	0,75	0,415	1159,3	407,1	0,233	0,767	0,24	0,16	0,6
	248,28	164,37	0,29899	0,99602	0,90	0,493	1179,7	406,1	0,233	0,767	0,24	0,16	0,6
50% DME	82,76	56,84	0,32747	1,01374	0,30	0,171	1077,1	399,0	0,233	0,767	0,20	0,20	0,6
50% Ethanol	124,14	83,56	0,31842	1,02609	0,45	0,251	1107,7	394,2	0,233	0,767	0,20	0,20	0,6
	165,52	109,82	0,31093	1,03132	0,60	0,329	1134,4	392,2	0,233	0,767	0,20	0,20	0,6
	206,90	137,10	0,30520	1,01476	0,75	0,411	1155,7	398,6	0,233	0,767	0,20	0,20	0,6
	248,28	163,12	0,29993	1,01451	0,90	0,489	1176,0	398,7	0,233	0,767	0,20	0,20	0,6
	289,66	189,58	0,29566	1,00768	1,05	0,569	1193,0	401,4	0,233	0,767	0,20	0,20	0,6

fuel composition	a_2 [1/s]	a_1 [1/s]	ρ_2 [kg/m3]	ρ_1 [kg/m3}	V_2 [m/s]	V_1 [m/s]	T_2 [K]	T_1 [K]	$Y_{O2,2}$	$Y_{N2,2}$	$Y_{DME,1}$	$Y_{Eth,1}$	$Y_{N2,1}$
40% DME	82,76	56,64	0,32848	1,02375	0,30	0,170	1073,8	395,1	0,233	0,767	0,16	0,24	0,6
60% Ethanol	124,14	84,11	0,31964	1,01655	0,45	0,252	1103,5	397,9	0,233	0,767	0,16	0,24	0,6
	165,52	111,68	0,31250	1,00219	0,60	0,335	1128,7	403,6	0,233	0,767	0,16	0,24	0,6
	206,90	138,61	0,30650	0,99700	0,75	0,416	1150,8	405,7	0,233	0,767	0,16	0,24	0,6
	248,28	164,75	0,30129	0,99897	0,90	0,494	1170,7	404,9	0,233	0,767	0,16	0,24	0,6
	289,66	190,40	0,29760	1,00568	1,05	0,571	1185,2	402,2	0,233	0,767	0,16	0,24	0,6
20% DME	82,76	56,61	0,32934	1,02765	0,30	0,170	1071,0	393,6	0,233	0,767	0,08	0,32	0,6
80% Ethanol	124,14	83,79	0,32124	1,02948	0,45	0,251	1098,0	392,9	0,233	0,767	0,08	0,32	0,6
	165,52	110,86	0,31439	1,02323	0,60	0,333	1121,9	395,3	0,233	0,767	0,08	0,32	0,6
	206,90	137,85	0,30792	1,01273	0,75	0,414	1145,5	399,4	0,233	0,767	0,08	0,32	0,6
	248,28	164,13	0,30274	1,01146	0,90	0,492	1165,1	399,9	0,233	0,767	0,08	0,32	0,6
	289,66	190,73	0,29871	1,00593	1,05	0,572	1180,8	402,1	0,233	0,767	0,08	0,32	0,6
0% DME	82,76	56,33	0,33023	1,04061	0,30	0,169	1068,1	388,7	0,233	0,767	0,00	0,40	0,6
100% Ethanol	124,14	84,50	0,32241	1,01604	0,45	0,253	1094,0	398,1	0,233	0,767	0,00	0,40	0,6
	165,52	113,31	0,31603	0,98463	0,60	0,340	1116,1	410,8	0,233	0,767	0,00	0,40	0,6
	206,90	140,02	0,30978	0,98751	0,75	0,420	1138,6	409,6	0,233	0,767	0,00	0,40	0,6
	248,28	165,85	0,30404	0,99480	0,90	0,498	1160,1	406,6	0,233	0,767	0,00	0,40	0,6
	289,66	191,99	0,29993	0,99676	1,05	0,576	1176,0	405,8	0,233	0,767	0,00	0,40	0,6

a_2 [1/s]	a_1 [1/s]	ρ_2 [kg/m^3]	ρ_1 [kg/m^3]	V_2 [m/s]	V_1 [m/s]	T_2 [K]	T_1 [K]	$Y_{O2,2}$	$Y_{N2,2}$	$Y_{DME,1}$	$Y_{Eth,1}$	$Y_{N2,1}$
287	387	1,19161	1,02712	0,898	0,967	296	379	0,2330	0,767	0,00	0,3105	0,6895
286	387	1,19161	1,01491	0,893	0,967	296	382	0,2330	0,767	0,00	0,3105	0,6895
286	389	1,19161	1,00815	0,895	0,973	296	385	0,2330	0,767	0,00	0,3105	0,6895
295	394	1,19153	1,04453	0,923	0,985	296	372	0,2325	0,768	0,02	0,2897	0,6903
296	400	1,19153	1,02173	0,925	0,999	296	380	0,2325	0,768	0,02	0,2897	0,6903
298	405	1,19153	1,00733	0,930	1,011	296	386	0,2325	0,768	0,02	0,2897	0,6903
298	406	1,19153	1,00021	0,930	1,015	296	388	0,2325	0,768	0,02	0,2897	0,6903
299	405	1,19142	1,01764	0,935	1,012	296	382	0,2319	0,768	0,04	0,2689	0,6911
299	406	1,19142	1,01263	0,935	1,014	296	383	0,2319	0,768	0,04	0,2689	0,6911
300	407	1,19142	1,01343	0,938	1,016	296	383	0,2319	0,768	0,04	0,2689	0,6911
300	412	1,19132	0,98653	0,938	1,030	296	394	0,2313	0,769	0,06	0,2481	0,6919
302	418	1,19132	0,97554	0,945	1,044	296	398	0,2313	0,769	0,06	0,2481	0,6919
302	417	1,19132	0,97166	0,943	1,044	296	399	0,2313	0,769	0,06	0,2481	0,6919
301	416	1,19132	0,97226	0,940	1,041	296	399	0,2313	0,769	0,06	0,2481	0,6919
302	417	1,19132	0,97553	0,943	1,042	296	398	0,2313	0,769	0,06	0,2481	0,6919
301	405	1,19132	1,02935	0,940	1,011	296	377	0,2313	0,769	0,06	0,2481	0,6919
301	405	1,19132	1,02935	0,940	1,011	296	377	0,2313	0,769	0,06	0,2481	0,6919
299	400	1,19132	1,04042	0,935	1,001	296	372	0,2313	0,769	0,06	0,2481	0,6919
306	423	1,19121	0,97637	0,958	1,058	296	397	0,2307	0,769	0,08	0,2273	0,6927
306	423	1,19121	0,97842	0,958	1,057	296	396	0,2307	0,769	0,08	0,2273	0,6927
305	419	1,19121	0,98299	0,953	1,049	296	394	0,2307	0,769	0,08	0,2273	0,6927
305	419	1,19121	0,98592	0,953	1,047	296	393	0,2307	0,769	0,08	0,2273	0,6927
304	405	1,19121	1,05091	0,950	1,011	296	369	0,2307	0,769	0,08	0,2273	0,6927
306	407	1,19121	1,05409	0,958	1,018	296	368	0,2307	0,769	0,08	0,2273	0,6927
306	405	1,19121	1,05912	0,955	1,013	296	366	0,2307	0,769	0,08	0,2273	0,6927
304	403	1,19121	1,06175	0,950	1,006	296	365	0,2307	0,769	0,08	0,2273	0,6927

a$_2$ [1/s]	a$_1$ [1/s]	ρ$_2$ [kg/m^3]	ρ$_1$ [kg/m^3]	V$_2$ [m/s]	V$_1$ [m/s]	T$_2$ [K]	T$_1$ [K]	Y$_{O2,2}$	Y$_{N2,2}$	Y$_{DME,1}$	Y$_{Eth,1}$	Y$_{N2,1}$
308	414	1,19111	1,03090	0,963	1,035	296	377	0,2301	0,770	0,10	0,2065	0,6935
312	425	1,19111	1,00961	0,978	1,062	296	384	0,2301	0,770	0,10	0,2065	0,6935
310	423	1,19111	1,00247	0,970	1,057	296	387	0,2301	0,770	0,10	0,2065	0,6935
310	422	1,19111	1,00587	0,970	1,056	296	385	0,2301	0,770	0,10	0,2065	0,6935
309	424	1,19111	0,98564	0,965	1,061	296	393	0,2301	0,770	0,10	0,2065	0,6935
312	425	1,19102	1,00253	0,975	1,063	296	387	0,2296	0,770	0,12	0,1858	0,6942
316	435	1,19102	0,98404	0,988	1,086	296	394	0,2296	0,770	0,12	0,1858	0,6942
314	432	1,19102	0,97957	0,980	1,081	296	396	0,2296	0,770	0,12	0,1858	0,6942
314	433	1,19102	0,97711	0,980	1,082	296	397	0,2296	0,770	0,12	0,1858	0,6942
319	431	1,19092	1,21915	0,998	1,077	296	380	0,2290	0,771	0,14	0,1650	0,6950
318	433	1,19092	1,00732	0,995	1,082	296	385	0,2290	0,771	0,14	0,1650	0,6950
320	437	1,19092	0,99819	1,000	1,092	296	388	0,2290	0,771	0,14	0,1650	0,6950
322	443	1,19081	0,98760	1,008	1,106	296	392	0,2284	0,772	0,16	0,1442	0,6958
323	444	1,19081	0,98372	1,010	1,111	296	394	0,2284	0,772	0,16	0,1442	0,6958
322	443	1,19081	0,98351	1,008	1,109	296	394	0,2284	0,772	0,16	0,1442	0,6958
323	444	1,19081	0,98485	1,010	1,111	296	393	0,2284	0,772	0,16	0,1442	0,6958
326	453	1,19071	0,96293	1,018	1,131	296	402	0,2278	0,772	0,18	0,1234	0,6966
326	452	1,19071	0,96906	1,020	1,131	296	400	0,2278	0,772	0,18	0,1234	0,6966
326	453	1,19071	0,95934	1,018	1,134	296	404	0,2278	0,772	0,18	0,1234	0,6966
326	455	1,19071	0,95906	1,020	1,137	296	404	0,2278	0,772	0,18	0,1234	0,6966
326	448	1,19071	0,98903	1,020	1,119	296	391	0,2278	0,772	0,18	0,1234	0,6966
326	444	1,19071	0,99946	1,018	1,111	296	387	0,2278	0,772	0,18	0,1234	0,6966
326	444	1,19071	0,99946	1,018	1,111	296	387	0,2278	0,772	0,18	0,1234	0,6966
334	461	1,19060	0,97299	1,043	1,153	296	398	0,2272	0,773	0,20	0,1026	0,6974
336	469	1,19060	0,95379	1,050	1,173	296	405	0,2272	0,773	0,20	0,1026	0,6974
337	473	1,19060	0,94420	1,053	1,182	296	410	0,2272	0,773	0,20	0,1026	0,6974
337	473	1,19060	0,94403	1,053	1,182	296	410	0,2272	0,773	0,20	0,1026	0,6974

a_2 [1/s]	a_1 [1/s]	ρ_2 [kg/m^3]	ρ_1 [kg/m^3]	V_2 [m/s]	V_1 [m/s]	T_2 [K]	T_1 [K]	$Y_{O2,2}$	$Y_{N2,2}$	$Y_{DME,1}$	$Y_{Eth,1}$	$Y_{N2,1}$
342	472	1,19050	0,97480	1,068	1,180	296	397	0,2266	0,773	0,22	0,0818	0,6982
339	470	1,19050	0,96709	1,060	1,176	296	400	0,2266	0,773	0,22	0,0818	0,6982
338	470	1,19050	0,96248	1,058	1,176	296	402	0,2266	0,773	0,22	0,0818	0,6982
342	475	1,19050	0,96190	1,068	1,188	296	402	0,2266	0,773	0,22	0,0818	0,6982
338	464	1,19039	0,98494	1,055	1,160	296	393	0,2260	0,774	0,24	0,0610	0,6990
342	471	1,19039	0,98029	1,068	1,176	296	395	0,2260	0,774	0,24	0,0610	0,6990
342	472	1,19039	0,97907	1,070	1,180	296	395	0,2260	0,774	0,24	0,0610	0,6990
341	469	1,19039	0,98079	1,065	1,173	296	394	0,2260	0,774	0,24	0,0610	0,6990
342	472	1,19039	0,97576	1,068	1,179	296	396	0,2260	0,774	0,24	0,0610	0,6990
341	470	1,19039	0,97634	1,065	1,176	296	396	0,2260	0,774	0,24	0,0610	0,6990
342	474	1,19031	0,97172	1,070	1,184	296	398	0,2255	0,775	0,26	0,0403	0,6997
344	479	1,19031	0,95924	1,075	1,197	296	403	0,2255	0,775	0,26	0,0403	0,6997
345	481	1,19031	0,95563	1,078	1,203	296	404	0,2255	0,775	0,26	0,0403	0,6997
345	480	1,19031	0,95811	1,078	1,201	296	403	0,2255	0,775	0,26	0,0403	0,6997
345	470	1,19020	1,00157	1,078	1,175	296	386	0,2249	0,775	0,28	0,0195	0,7005
347	474	1,19020	0,99595	1,085	1,186	296	388	0,2249	0,775	0,28	0,0195	0,7005
344	470	1,19020	0,99568	1,075	1,175	296	388	0,2249	0,775	0,28	0,0195	0,7005
345	471	1,19020	0,99695	1,078	1,177	296	388	0,2249	0,775	0,28	0,0195	0,7005
345	473	1,19010	0,98901	1,078	1,182	296	391	0,2243	0,776	0,30	0,0000	0,7020
347	480	1,19010	0,97223	1,085	1,200	296	398	0,2243	0,776	0,30	0,0000	0,7020
348	483	1,19010	0,96537	1,088	1,207	296	400	0,2243	0,776	0,30	0,0000	0,7020
348	483	1,19010	0,96471	1,088	1,208	296	400	0,2243	0,776	0,30	0,0000	0,7020
344	478	1,19010	0,96492	1,075	1,194	296	400	0,2243	0,776	0,30	0,0000	0,7020
347	482	1,19010	0,96611	1,085	1,204	296	400	0,2243	0,776	0,30	0,0000	0,7020

x

Appendix B

Professor K. Seshadri (2014) developed following asymptotic formulation for extinction and autoignition of Ethanol/ Dimethylether in non-uniform flows under non-premixed Conditions.

Chemical Reaction

The overall chemical reaction between ethanol (C_2H_5OH) and O_2 is

$$C_2H_5OH + 3O_2 \rightarrow 2CO_2 + 3H_2O$$
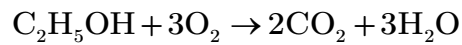
The reaction rate, w eth with units of $1/(m^3 \cdot s)$. The overall chemical reaction between dimethylether (CH_3OCH_3) and O_2 is

$$CH_3OCH_3 + 3O_2 \rightarrow 2CO_2 + 3H_2O$$
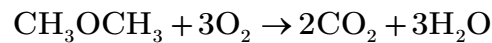
The reaction rate, ω_{dme} with units of $1/(m^3 \cdot s)$.

Formulation

Consider two counter-flowing streams flowing toward a stagnation plane. On stream called fuel stream is made up of C_2H_5OH, CH_3OCH_3 and N_2 and the other stream, called the oxidizer stream, is made up of O_2, and N_2. The mass fractions of ethanol, dimethylether, and oxygen are represented by Y_{dme}, Y_{eth} and Y_{O_2}, respectively. The mass fraction of C_2H_5OH and CH_3OCH_3 in the fuel stream respectively are $Y_{eth,1}$ and $Y_{dme,1}$ and that of O_2 in the oxidizer stream is $Y_{O_2,2}$.

The species balance equations are

$$\rho a \hat{x} \frac{dY_{eth}}{d\hat{x}} + \rho D_{eth} \frac{d^2 Y_{eth}}{d\hat{x}^2} = W_{eth} \omega_{eth}$$

$$\rho a \hat{x} \frac{dY_{dme}}{d\hat{x}} + \rho D_{dme} \frac{d^2 Y_{dme}}{d\hat{x}^2} = W_{dme} \omega_{dme} \qquad (1)$$

$$\rho a \hat{x} \frac{dY_{O_2}}{d\hat{x}} + \rho D_{O_2} \frac{d^2 Y_{O_2}}{d\hat{x}^2} = 3 W_{O_2} \omega_{eth} + 3 W_{O_2} \omega_{dme}$$

Here D_{eth}, D_{dme}, and D_{O_2} are respectively the coefficient of diffusion of C_2H_5OH, CH_3OCH_3 and O_2. The energy conservation equation is

$$\rho c_p a \hat{x} \frac{dT}{d\hat{x}} + \lambda \frac{d^2 T}{d\hat{x}^2} + \sum_{i=1}^{n} \rho D_i c_{p,i} \frac{dY_i}{d\hat{x}} \frac{dT}{d\hat{x}} = -Q_{eth} \omega_{eth} - Q_{dme} \omega_{dme} \qquad (2)$$

Here λ is the coefficient of thermal conductivity, c_p is the heat capacity of the mixture, $c_{p,i}$ is the heat capacity of species I, D_i is the coefficient of diffusion of species I, Q_{eth} is the heat released per mole of C_2H_5OH consumed and Q_{dme} is the heat released per mole of CH_3OCH_3 consumed.

Define the independent variable

$$x = \hat{x} \left(\rho c_p a / \lambda \right)^{1/2} \qquad (3)$$

For convenience, the definitions

$$X_i \equiv Y_i W_{N_2} / W_i$$
$$\tau \equiv (T - T_{ref}) / \Delta T_{ref}$$
$$M_{eth} \equiv W_{N_2} \omega_{eth} / (\rho a)$$
$$M_{dme} \equiv W_{N_2} \omega_{dme} / (\rho a) \qquad (4)$$
$$G_{eth} \equiv Q_{eth} / \left(W_{N_2} c_p \Delta T_{ref} \right)$$
$$G_{dme} \equiv Q_{dme} / \left(W_{N_2} c_p \Delta T_{ref} \right)$$

are introduced. Here W_i is the molecular weight of species i, W_{N_2}, is the molecular weight of nitrogen, T_{ref} is a reference temperature and ΔT_{ref} is a reference temperature difference. Introducing Equations (3) and (4) into Eq. (1), the following equations are obtained

$$x\frac{dX_{eth}}{dx} + \frac{1}{Le_{eth}}\frac{d^2 X_{eth}}{dx^2} = M_{eth}$$

$$x\frac{dX_{dme}}{dx} + \frac{1}{Le_{dme}}\frac{d^2 X_{dme}}{dx^2} = M_{dme} \tag{5}$$

$$x\frac{dX_{O_2}}{dx} + \frac{1}{Le_{O_2}}\frac{d^2 X_{O_2}}{dx^2} = 3M_{eth} + 3M_{dme}$$

Introducing Equations (3) and (4) into Equation (2), the following equation is obtained

$$x\frac{d\tau}{dx} + \frac{d^2\tau}{dx^2} + \sum_{i=1}^{n}\frac{1}{Le_i}\frac{W_i}{W_{N_2\ i}}\frac{c_{p,i}}{c_p}\frac{dX_i}{dx}\frac{d\tau}{dx} = -G_{eth}M_{eth} - G_{dme}M_{dme} \tag{6}$$

The conserved scalar quantities Z, Z_{eth}, and Z_{dme} are defined by the equations

$$x\frac{dZ}{dx} + \frac{d^2 Z}{dx^2} = 0,$$

$$x\frac{dZ_{eth}}{dx} + \frac{1}{Le_{eth}}\frac{d^2 Z_{eth}}{dx^2} = 0, \tag{7}$$

$$x\frac{dZ_{dme}}{dx} + \frac{1}{Le_{dme}}\frac{d^2 Z_{dme}}{dx^2} = 0,$$

Eq. (7) is constrained to satisfy the conditions

$$\begin{aligned} Z = Z_{eth} = Z_{dme} = 0; & \qquad x = \infty \\ Z = Z_{eth} = Z_{dme} = 1; & \qquad x = -\infty \end{aligned} \tag{8}$$

Integration of Eq. (7) together with Eq. (8) gives

$$Z = \frac{1}{2}erfc\left(x\sqrt{\frac{1}{2}}\right)$$

$$Z_{eth} = \frac{1}{2}erfc\left(x\sqrt{\frac{Le_{eth}}{2}}\right) \tag{9}$$

$$Z_{dme} = \frac{1}{2}erfc\left(x\sqrt{\frac{Le_{dme}}{2}}\right)$$

Differentiation of Eq. (9) gives

$$\frac{dZ}{dx} = -\left(\sqrt{\frac{1}{2\pi}}\right)exp\left(-\frac{x^2}{2}\right)$$

$$\frac{dZ_{eth}}{dx} = -\left(\sqrt{\frac{Le_{eth}}{2\pi}}\right)exp\left(-\frac{x^2 Le_{eth}}{2}\right) \tag{10}$$

$$\frac{dZ_{dme}}{dx} = -\left(\sqrt{\frac{Le_{dme}}{2\pi}}\right)exp\left(-\frac{x^2 Le_{dme}}{2}\right)$$

It follows from Eq. (10)

$$\frac{dZ_{eth}}{dx} = \left(\sqrt{Le_{eth}}\right)\frac{dZ}{dx}\left\{exp\left[\frac{x^2(1-Le_{eth})}{2}\right]\right\},$$

$$\frac{dZ_{dme}}{dx} = \left(\sqrt{Le_{dme}}\right)\frac{dZ}{dx}\left\{exp\left[\frac{x^2(1-Le_{dme})}{2}\right]\right\}, \tag{11}$$

Coupling Relations at x_{st}

Let the flame sheet be located at $x = x_{st}$. At the flame sheet, $Z = Z_{st}$, $Z_{eth} = Z_{eth,st}$, $Z_{dme} = Z_{dme,st}$. At x_{st} there is complete consumption of C_2H_5OH, CH_3OCH_3, and O_2. At x_{st+} the gradients are

$$\frac{1}{Le_{eth}}\frac{dX_{eth}}{dx} = \frac{1}{Le_{eth}}\frac{dX_{eth}}{dZ_{eth}}\frac{dZ_{eth}}{dx} = \frac{1}{Le_{eth}}\frac{X_{eth,1}}{1-Z_{eth,st}}\frac{dZ_{eth}}{dx}$$

$$\frac{1}{Le_{dme}}\frac{dX_{dme}}{dx} = \frac{1}{Le_{dme}}\frac{dX_{dme}}{dZ_{dme}}\frac{dZ_{dme}}{dx} = \frac{1}{Le_{dme}}\frac{X_{dme,1}}{1-Z_{dme,st}}\frac{dZ_{dme}}{dx}$$

$$\frac{dX_{O_2}}{dx} = 0$$

$$\frac{dX_{CO_2}}{dx} = \frac{dX_{CO_2}}{dZ}\frac{dZ}{dx} = -\frac{X_{CO_2,st}}{1-Z_{st}}\frac{dZ}{dx} \tag{12}$$

$$\frac{dX_{H_2O}}{dx} = \frac{dX_{H_2O}}{dZ}\frac{dZ}{dx} = -\frac{X_{H_2O,st}}{1-Z_{st}}\frac{dZ}{dx}$$

$$\frac{d\tau}{dx} = \frac{d\tau}{dZ}\frac{dZ}{dx} = -\frac{\tau_{st}}{1-Z_{st}}\frac{dZ}{dx}$$

At x_{st-} the gradients are

$$\frac{dX_{eth}}{dx} = \frac{dX_{dme}}{dx} = 0$$

$$\frac{dX_{O_2}}{dx} = \frac{dX_{O_2}}{dZ}\frac{dZ}{dx} = -\frac{X_{O_2,2}}{Z_{st}}\frac{dZ}{dx}$$

$$\frac{dX_{CO_2}}{dx} = \frac{dX_{CO_2}}{dZ}\frac{dZ}{dx} = -\frac{X_{CO_2,st}}{Z_{st}}\frac{dZ}{dx} \qquad (13)$$

$$\frac{dX_{H_2O}}{dx} = \frac{dX_{H_2O}}{dZ}\frac{dZ}{dx} = -\frac{X_{H_2O,st}}{Z_{st}}\frac{dZ}{dx}$$

$$\frac{d\tau}{dx} = \frac{d\tau}{dZ}\frac{dZ}{dx} = \frac{\tau_{st}}{Z_{st}}\frac{dZ}{dx}$$

The gradients at Z_{st+} are

$$\frac{1}{Le_{eth}}\frac{dX_{eth}}{dZ} = \frac{1}{\sqrt{Le_{eth}}}\frac{X_{eth,1}}{1-Z_{eth,st}}\left\{exp\left[\frac{x_{st}^2\left(1-Le_{eth}\right)}{2}\right]\right\} = g$$

$$\frac{1}{Le_{dme}}\frac{dX_{dme}}{dZ} = \frac{1}{\sqrt{Le_{dme}}}\frac{X_{dme,1}}{1-Z_{dme,st}}\left\{exp\left[\frac{x_{st}^2\left(1-Le_{dme}\right)}{2}\right]\right\} = m$$

$$\frac{dX_{O_2}}{dZ} = 0 \qquad (14)$$

$$\frac{dX_{CO_2}}{dx} = -\frac{X_{CO_2,st}}{1-Z_{st}}$$

$$\frac{dX_{H_2O}}{dx} = -\frac{X_{H_2O,st}}{1-Z_{st}}$$

$$\frac{d\tau}{dx} = -\frac{\tau_{st}}{1-Z_{st}} = -p$$

At Z_{st-} the gradients are

$$\frac{dX_{eth}}{dZ} = \frac{dX_{dme}}{dZ} = 0$$

$$\frac{dX_{O_2}}{dZ} = -\frac{X_{O_2,2}}{Z_{st}} = -c$$

$$\frac{dX_{CO_2}}{dZ} = \frac{X_{CO_2,st}}{Z_{st}} \tag{15}$$

$$\frac{dX_{H_2O}}{dZ} = \frac{X_{H_2O,st}}{Z_{st}}$$

$$\frac{d\tau}{dZ} = \frac{\tau_{st}}{Z_{st}} = s$$

Balance equation for carbon across the reaction zone at $x = x_{st}$ is

$$\left(\frac{2}{Le_{eth}} \frac{dX_{eth}}{dx} + \frac{2}{Le_{dme}} \frac{dX_{dme}}{dx} + \frac{dX_{CO_2}}{dx} \right)_\pm = 0 \tag{16}$$

Balance equation for oxygen across the reaction zone at $x = x_{st}$ is

$$\left(\frac{1}{Le_{eth}} \frac{dX_{eth}}{dx} + \frac{1}{Le_{dme}} \frac{dX_{dme}}{dx} + 2\frac{dX_{O_2}}{dx} + 2\frac{dX_{CO_2}}{dx} + \frac{dX_{H_2O}}{dx} \right)_\pm = 0 \tag{17}$$

Balance equation for hydrogen across the reaction zone at $x = x_{st}$ is

$$\left(\frac{3}{Le_{eth}} \frac{dX_{eth}}{dx} + \frac{3}{Le_{dme}} \frac{dX_{dme}}{dx} + \frac{dX_{H_2O}}{dx} \right)_\pm = 0 \tag{18}$$

It follows from Eqs. (16), (17), and (18)

$$\left(\frac{3}{Le_{eth}} \frac{dX_{eth}}{dx} + \frac{3}{Le_{dme}} \frac{dX_{dme}}{dx} - \frac{dX_{O_2}}{dx} \right)_\pm = 0 \tag{19}$$

Use of Eqs. (14), and (15), into Eq. (19) gives

$$3g + 3m = c \tag{20}$$

Coupling relations for temperature gives

$$\left(\frac{d\tau}{dx} + \frac{G_{hep}}{Le_{eth}} \frac{dX_{eth}}{dx} + \frac{G_{dme}}{Le_{dme}} \frac{dX_{dme}}{dx} \right)_{\pm} = 0 \qquad (21)$$

This gives

$$\tau_{st} = \left(G_{eth}g + G_{dme}m \right) Z_{st} \left(1 - Z_{st} \right) \qquad (22)$$

The adiabatic flame temperature T_{st} is

$$T_{st} = T_u + \frac{1}{c_p W_{N_2}} \left(Q_{eth}g + Q_{dme}m \right) Z_{st} \left(1 - Z_{st} \right) \qquad (23)$$

Appendix C

```
elements
h c o n ar he
end

species
h            h2           o            o2           oh
h2o          n2           co           hco          co2
ch3          ch4          ho2          h2o2         ch2o
ch3o         c2h6         c2h4         c2h5         ch2
ch           c2h          c2h2         c2h3         ch3oh
ch2oh        ch2co        hcco         c2h5oh       pc2h4oh
sc2h4oh      ch3co        ch2cho       ch3cho
ch3coch3     ch3coch2     c2h5cho      c2h5co
c2h5o        ch3o2        c2h5o2       ch3o2h       c2h5o2h
c2h3o1-2     ch3co2       c2h4o1-2     c2h4o2h
o2c2h4oh     ch3co3       ch3co3h      c2h3co       c2h3cho
ch3coch2o2   ch3coch2o2h  ch3coch2o    hco3h        hco3
hco2         o2c2h4o2h    ch2(s)       ch3och3      ch3och2
ch3och2o2    ch2och2o2h   ch3och2o2h   ch3och2o     o2ch2och2o2h
ho2ch2ocho   och2ocho     hoch2oco     hoch2o       hco2h
ch3ocho      ch3oco       ch2ocho      ch3och2oh    hoch2o2h
och2o2h      hoch2o2
!SanDiego
ar           he           t-ch2
c2h4ooh      oc2h3ooh     c2h4o        ch2ch2oh     oc3h5ooh
ch3choh      ch3ch2o      c3h4         c3h3         c3h5
c3h6         c3h8         i-c3h7       n-c3h7       c3h6ooh
end

reactions        cal/mole
  ch3+h(+m) = ch4(+m) 2.140e+15  -0.40  0.000E+00
    low/3.31e+30 -4.0 2108./
    troe/0.0  1.e-15  1.e-15  40./
    h2/2/ h2o/5/ co/2/ co2/3/
  ch4+h = ch3+h2  1.727E+04   3.00  8.224E+03
    rev /  6.610E+02   3.00  7.744E+03 /
  ch4+oh = ch3+h2o  1.930E+05   2.40  2.106E+03
    rev /  4.820E+02   2.90  1.486E+04 /
  ch4+o = ch3+oh  2.130E+06   2.21  6.480E+03
    rev /  3.557E+04   2.21  3.920E+03 /
  c2h6+ch3 = c2h5+ch4  1.510E-07   6.00  6.047E+03
    rev /  9.649E-10   6.56  1.022E+04 /
  hco+oh = co+h2o  1.020E+14   0.00  0.000E+00
    rev /  2.896E+15   0.00  1.052E+05 /
  co+oh = co2+h  1.400E+05   1.95 -1.347E+03
    rev /  1.568E+07   1.95  2.099E+04 /
  h+o2 = o+oh  1.970E+14   0.00  1.654E+04
    rev /  1.555E+13   0.00  4.250E+02 /
  o+h2 = h+oh  5.080E+04   2.67  6.292E+03
    rev /  2.231E+04   2.67  4.197E+03 /
  o+h2o = oh+oh  2.970E+06   2.02  1.340E+04
    rev /  3.013E+05   2.02 -3.850E+03 /
  oh+h2 = h+h2o  2.160E+08   1.51  3.430E+03
    rev /  9.352E+08   1.51  1.858E+04 /
  hco+m = h+co+m  1.860E+17  -1.00  1.700E+04
    rev /  6.467E+13   0.00 -4.420E+02 /
    h2/2.5/ h2o/12/ co/1.9/ co2/3.8/
  h2o2+oh = h2o+ho2  1.000E+12   0.00  0.000E+00
    rev /  1.685E+11   0.33  3.146E+04 /
  DUPLICATE
  c2h4+o = ch3+hco  1.020E+07   1.88  1.790E+02
    rev /  2.851E+08   1.05  3.177E+04 /
```

```
h+c2h4(+m) = c2h5(+m) 1.081E+12   0.45  1.822E+03
  low/1.112E+34 -5.000E+00  4.448E+03/
  troe/1.0  1.000E-15  9.500E+01  2.000E+02/
  h2/2/ h2o/5/ co/2/ co2/3/
ch3oh(+m) = ch3+oh(+m) 1.900E+16   0.00  9.173E+04
  low / 2.95E+44 -7.35  9.546E+04/
  troe/0.414  279.  5459./
  h2/2/ h2o/16/ co/2/ co2/3/
c2h6+h = c2h5+h2 5.540E+02   3.50  5.167E+03
  rev / 1.355E-01   4.06  8.857E+03 /
ch3oh+ho2 = ch2oh+h2o2 3.980E+13   0.00  1.940E+04
  rev / 3.130E+15  -0.90  1.075E+04 /
c2h5+o2 = c2h4+ho2 1.220E+30  -5.76  1.010E+04
  rev / 1.259E+30  -5.63  2.231E+04 /
c2h6+oh = c2h5+h2o 5.125E+06   2.06  8.550E+02
  rev / 1.010E+07   2.06  2.298E+04 /
c2h6+o = c2h5+oh 1.130E+14   0.00  7.850E+03
  rev / 2.080E+13   0.00  1.272E+04 /
ch3+ho2 = ch3o+oh 1.100E+13   0.00  0.000E+00
  rev / 4.780E+14  -0.35  2.455E+04 /
co+ho2 = co2+oh 3.010E+13   0.00  2.300E+04
  rev / 6.435E+15  -0.33  8.461E+04 /
ch3+ch3(+m) = c2h6(+m) 9.214E+16  -1.17  6.358E+02
  low/1.135E+36 -5.246  1.705E+03/
  troe/0.405 1120. 69.6 1.e+15/
  h2/2/ h2o/5/ co/2/ co2/3/
h2o+m = h+oh+m 1.837E+27 -3.00  1.226E+05
  rev/ 2.250E+22 -2.00  0.000E+00 /
  h2/2.5/ h2o/12/ co/1.9/ co2/3.8/ ar/0.38/ he/0.38/
h+o2(+m) = ho2(+m) 1.475E+12 0.60  0.000E+00
  low/3.500e+16 -4.10E-01 -1.1160E+03 /
  troe/5.0000E-01  1.0000E-30  1.0000E+30/
  h2/2.5/ h2o/12/ co/1.9/ co2/3.8/
co+o(+m) = co2(+m) 1.800E+10 0.00  2.384E+03
  low/1.350E+24 -2.788  4191./
  h2/2.5/ h2o/12/ co/1.9/ co2/3.8/
co+o2 = co2+o 1.068E-15   7.13  1.332E+04
  rev / 9.444E-15   7.13  1.954E+04 /
hco+h = co+h2 7.340E+13   0.00  0.000E+00
  rev / 4.813E+14   0.00  9.000E+04 /
hco+o = co+oh 3.020E+13   0.00  0.000E+00
  rev / 8.697E+13   0.00  8.790E+04 /
ch2o+m = hco+h+m  6.283E+29  -3.57  9.320E+04
  rev / 2.660E+24  -2.57  4.270E+02 /
ch2o+oh = hco+h2o 3.430E+09   1.18 -4.470E+02
  rev / 1.186E+09   1.18  2.938E+04 /
ch2o+h = hco+h2 9.334E+08   1.50  2.976E+03
  rev / 7.453E+07   1.50  1.765E+04 /
ch2o+o = hco+oh 6.260E+09   1.15  2.260E+03
  rev / 2.195E+08   1.15  1.484E+04 /
ch3+oh = ch2o+h2 2.250E+13   0.00  4.300E+03
  rev / 6.756E+14   0.00  7.603E+04 /
ch3+o = ch2o+h  8.000E+13   0.00  0.000E+00
  rev / 1.055E+15   0.00  6.963E+04 /
ch3+o2 = ch3o+o 1.995E+18  -1.57  2.923E+04
  rev / 3.585E+18  -1.59 -1.610E+03 /
ch2o+ch3 = hco+ch4 3.636E-06   5.42  9.980E+02
  rev / 7.584E-06   5.42  1.615E+04 /
hco+ch3 = ch4+co 1.210E+14   0.00  0.000E+00
  rev / 2.073E+16   0.00  9.048E+04 /
ch3o(+m) = ch2o+h(+m)  5.450E+13   0.00  1.350E+04
  low /2.344E+25 -2.7  3.060E+04/
c2h4(+m) = c2h2+h2(+m) 1.800E+13   0.00  7.600E+04
  low /1.500E+15 0.0  5.5443E+04/
ho2+o = oh+o2 3.250E+13   0.00  0.000E+00
  rev / 7.857E+14  -0.33  5.539E+04 /
hco+ho2 = ch2o+o2 2.974E+10   0.33 -3.861E+03
  rev / 2.050E+13   0.00  3.895E+04 /
ch3o+o2 = ch2o+ho2 5.500E+10   0.00  2.424E+03
  rev / 1.318E+09   0.35  3.139E+04 /
```

```
ch3+ho2 = ch4+o2  3.000E+12   0.00  0.000E+00
  rev / 4.314E+15  -0.33  5.796E+04 /
hco+o2 = co+ho2  7.580E+12   0.00  4.100E+02
  rev / 9.029E+11   0.33  3.293E+04 /
ho2+h = oh+oh  7.080E+13   0.00  3.000E+02
  rev / 1.352E+14  -0.33  3.957E+04 /
ho2+h = h2+o2  1.660E+13   0.00  8.200E+02
  rev / 9.138E+14  -0.33  5.830E+04 /
ho2+oh = h2o+o2 2.890E+13   0.00 -5.000E+02
  rev/ 6.888E+15 -0.33  7.214E+04 /
h2o2+o2 = ho2+ho2 5.942E+17 -0.66  5.315E+04
  rev/ 4.200E+14 0.00  1.198E+04 /
DUPLICATE
oh+oh(+m) = h2o2(+m) 1.236E+14   -.37  0.000E+00
  low /3.041E+30 -4.63 2049./
  troe /0.47 100. 2000. 1.0e+15/
  h2/2.5/ h2o/12/ co/1.9/ co2/3.8/
h2o2+h = h2o+oh  2.410E+13   0.00  3.970E+03
  rev / 7.750E+12   0.00  7.471E+04 /
ch4+ho2 = ch3+h2o2  3.420E+11   0.00  1.929E+04
  rev / 3.365E+11  -0.33  2.502E+03 /
ch2o+ho2 = hco+h2o2  5.820E-03   4.53  6.557E+03
  rev / 1.194E-02   4.20  4.921E+03 /
oh+m = o+h+m  3.909E+22  -2.00  1.053E+05
  rev / 4.720E+18  -1.00  0.000E+00 /
  h2/2.5/ h2o/12/ co/1.9/ co2/3.8/ ar/0.75/ he/0.75/
o2+m = o+o+m 6.473E+20 -1.50  1.215E+05
  rev/ 6.170E+15 -0.50  0.000E+00 /
  h2/2.5/ h2o/12/ co/1.9/ co2/3.8/ ar/0.20/ he/0.20/
h2+m = h+h+m 4.570E+19 -1.40  1.044E+05
  rev/ 2.423E+15 -0.40 -3.040E+03 /
  h2/2.5/ h2o/12/ co/1.9/ co2/3.8/ ar/0.50/ he/0.50/
c2h3+h(+m) = c2h4(+m) 6.100E+12 0.27  2.800E+02
  low /9.800E+29 -3.86  3.320E+03/
  troe /0.782 208. 2663. 6095./
  h2/2.5/ h2o/12/ co/1.9/ co2/3.8/
c2h5+c2h3 = c2h4+c2h4 3.000E+12 0.00  0.000E+00
  rev/ 4.820E+14 0.00  7.153E+04 /
c2h2+h(+m) = c2h3(+m) 3.110E+11   0.58  2.589E+03
  low/2.254e40  -7.269  6577./
  troe/ 1.0 1.e-15 675. 1.e+15/
  h2/2/ h2o/5/ co/2/ co2/3/
c2h4+h = c2h3+h2  8.420E-03   4.62  2.583E+03
  rev / 5.723E-01   3.79  3.233E+03 /
c2h4+oh = c2h3+h2o  2.050E+13   0.00  5.955E+03
  rev / 1.200E+12   0.00  1.400E+04 /
c2h3+o2 = c2h2+ho2  5.190E-15  -1.26  3.310E+03
  rev / 2.727E-16  -0.93  1.140E+04 /
DUPLICATE
c2h2+m = c2h+h+m  4.200E+16   0.00  1.070E+05
  rev / 7.130E+07   2.08 -2.891E+04 /
c2h2+o2 = hcco+oh  2.000E+08   1.50  3.010E+04
  rev / 2.232E+05   1.50  2.540E+04 /
ch2+o2 = co+h2o  7.280E+19  -2.54  1.809E+03
  rev / 8.508E+20  -2.54  1.798E+05 /
c2h2+oh = c2h+h2o  3.370E+07   2.00  1.400E+04
  rev / 4.671E+03   3.08  6.850E+02 /
o+c2h2 = c2h+oh  3.160E+15  -0.60  1.500E+04
  rev / 4.443E+10   0.48 -1.557E+04 /
c2h2+o = ch2+co  6.120E+06   2.00  1.900E+03
  rev / 1.152E+06   2.00  5.257E+04 /
c2h+o2 = hco+co  2.410E+12   0.00  0.000E+00
  rev / 1.328E+16  -1.08  1.541E+05 /
c2h+o = co+ch  1.810E+13   0.00  0.000E+00
  rev / 7.478E+16  -1.08  8.213E+04 /
ch2+o2 = hco+oh  1.290E+20  -3.30  2.840E+02
  rev / 5.310E+19  -3.30  7.317E+04 /
ch2+o = co+h+h  5.000E+13   0.00  0.000E+00
  rev / 0.000E+00   0.00  0.000E+00 /
ch2+h = ch+h2  1.000E+18  -1.56  0.000E+00
```

```
  rev / 7.026E+17  -1.56  2.990E+03 /
ch2+oh = ch+h2o  1.130E+07   2.00  3.000E+03
  rev / 3.437E+07   2.00  2.115E+04 /
ch2+o2 = co2+h+h  3.290E+21  -3.30  2.868E+03
  rev / 0.000E+00   0.00  0.000E+00 /
ch+o2 = hco+o  3.300E+13   0.00  0.000E+00
  rev / 4.402E+13   0.00  7.199E+04 /
ch3oh+oh = ch2oh+h2o  7.100E+06   1.80 -5.960E+02
  rev / 3.293E+01   3.46  2.272E+04 /
ch3oh+h = ch3o+h2  3.600E+12   0.00  6.095E+03
  rev / 7.467E+12  -0.02  7.825E+03 /
ch3oh+h = ch2oh+h2  1.440E+13   0.00  6.095E+03
  rev / 1.543E+07   1.66  1.425E+04 /
ch3oh+ch3 = ch2oh+ch4  3.190E+01   3.17  7.172E+03
  rev / 8.927E-04   4.83  1.581E+04 /
ch3oh+o = ch2oh+oh  3.880E+05   2.50  3.080E+03
  rev / 4.960E+03   2.50  8.781E+03 /
ch2oh+o2 = ch2o+ho2  3.810E+06   2.00  1.641E+03
  rev / 1.768E+11   0.67  2.418E+04 /
ch2oh(+m) = ch2o+h(+m) 2.800E+14  -0.73  3.282E+04
  low/6.01E+33 -5.39 3.62E+04/
  troe/ 0.96 67.6 1855. 7543./
c2h3+o2 = c2h2+ho2  2.120E-06   6.00  9.484E+03
  rev / 1.114E-07   6.33  1.757E+04 /
DUPLICATE
h2o2+o = oh+ho2  9.550E+06   2.00  3.970E+03
  rev / 2.541E+07   1.68  1.985E+04 /
c2h2+o = hcco+h  1.430E+07   2.00  1.900E+03
  rev / 2.021E+05   2.00  1.331E+04 /
c2h2+oh = ch2co+h  3.236E+13   0.00  1.200E+04
  rev / 3.194E+14   0.00  3.267E+04 /
ch2co+h = ch3+co  1.100E+13   0.00  3.400E+03
  rev / 2.400E+12   0.00  4.020E+04 /
ch2co+o = ch2+co2  1.750E+12   0.00  1.350E+03
  rev / 3.739E+12   0.00  5.369E+04 /
ch2+o2 = ch2o+o  3.290E+21  -3.30  2.868E+03
  rev / 3.862E+22  -3.30  6.318E+04 /
ch2co(+m) = ch2+co(+m) 3.000E+14   0.00  7.098E+04
  low/3.6000E+15  0.00  5.9270E+04/
ch2co+o = hcco+oh  1.000E+13   0.00  8.000E+03
  rev / 1.432E+10   0.00 -1.255E+03 /
ch2co+oh = hcco+h2o  1.000E+13   0.00  2.000E+03
  rev / 1.412E+11   0.00  9.995E+03 /
ch2co+h = hcco+h2  2.000E+14   0.00  8.000E+03
  rev / 6.522E+11   0.00  8.400E+02 /
hcco+oh = hco+hco  1.000E+13   0.00  0.000E+00
  rev / 4.820E+13   0.00  4.036E+04 /
hcco+h = ch2(s)+co  1.100E+14   0.00  0.000E+00
  rev / 6.660E+13   0.00  3.926E+04 /
hcco+o = h+co+co  8.000E+13   0.00  0.000E+00
  rev / 0.000E+00   0.00  0.000E+00 /
c2h6+o2 = c2h5+ho2  4.000E+13   0.00  5.090E+04
  rev / 3.000E+11   0.00  0.000E+00 /
c2h6+ho2 = c2h5+h2o2  1.700E+13   0.00  2.046E+04
  rev / 2.500E+11   0.00  6.500E+03 /
ch2+o2 = co2+h2  1.010E+21  -3.30  1.508E+03
  rev / 3.054E+23  -3.30  1.867E+05 /
ch3+c2h3 = ch4+c2h2  3.920E+11   0.00  0.000E+00
  rev / 2.962E+13   0.00  6.605E+04 /
ch3+c2h5 = ch4+c2h4  1.950E+13  -0.50  0.000E+00
  rev / 2.895E+16  -0.70  7.017E+04 /
ch3oh+ch2o = ch3o+ch3o  3.835E+13   0.05  8.472E+04
  rev / 6.030E+13   0.00  0.000E+00 /
ch2o+ch3o = ch3oh+hco  1.150E+11   0.00  1.280E+03
  rev / 3.020E+11   0.00  1.816E+04 /
ch4+ch3o = ch3+ch3oh  1.570E+11   0.00  8.842E+03
  rev / 1.046E+09   0.00  5.000E+04 /
c2h6+ch3o = c2h5+ch3oh  3.000E+11   0.00  7.000E+03
  rev / 1.714E+10   0.00  5.000E+04 /
c2h3+h = c2h2+h2  2.000E+13   0.00  2.500E+03
```

```
  rev /  1.331E+13    0.00   6.808E+04 /
ch3o+ch3oh = ch2oh+ch3oh  3.000E+11   0.00   4.074E+03
  rev /  1.549E+05    1.68   1.050E+04 /
ch3oh+oh = ch3o+h2o  1.000E+06   2.10   4.967E+02
  rev /  8.981E+06    2.08   1.738E+04 /
c2h5+h = ch3+ch3  3.610E+13   0.00   0.000E+00
  rev /  5.446E+16   -1.03   1.698E+04 /
c2h3+o2 = ch2o+hco  1.700E+29   -5.31   6.500E+03
  rev /  1.657E+29   -5.31   9.305E+04 /
c2h6 = c2h5+h  2.783E+21   -1.56   1.038E+05
  rev /  3.610E+13    0.00   0.000E+00 /
c2h5oh(+m) = ch2oh+ch3(+m)  5.710E+23   -1.68   9.441E+04
  low/3.110E+85 -18.84   1.1310E+05/
  troe/ 0.5   550.  825.  6100./
  h2/2/ h2o/5/ co/2/ co2/3/
c2h5oh(+m) = c2h5+oh(+m)  2.400E+23   -1.62   9.954E+04
  low/5.110E+85 -18.80   1.1877E+05/
  troe/ 0.5   650.  800.  1.0E+15/
  h2/2/ h2o/5/ co/2/ co2/3/
c2h5oh(+m) = c2h4+h2o(+m)  2.790E+13   0.09   6.614E+04
  low/2.570E+83 -18.85   8.6453E+04/
  troe/ 0.7   350.  800.  3800./
  h2o/5/
c2h5oh(+m) = ch3cho+h2(+m) 7.240E+11   0.10   9.101E+04
  low/4.460E+87 -19.42   1.1559E+05/
  troe/ 0.9   900.  1100.  3500./
  h2o/5/
c2h5oh+o2 = pc2h4oh+ho2  2.000E+13   0.00   5.280E+04
  rev /  3.470E+08    0.32  -1.105E+03 /
c2h5oh+o2 = sc2h4oh+ho2  1.500E+13   0.00   5.015E+04
  rev /  1.079E+09    0.63  -5.040E+02 /
c2h5oh+oh = pc2h4oh+h2o  1.740E+11   0.27   6.000E+02
  rev /  7.196E+08    0.26   1.933E+04 /
c2h5oh+oh = sc2h4oh+h2o  4.640E+11   0.15   0.000E+00
  rev /  7.957E+09    0.45   2.199E+04 /
c2h5oh+h = pc2h4oh+h2  1.230E+07   1.80   5.098E+03
  rev /  1.175E+04    1.79   8.677E+03 /
c2h5oh+h = sc2h4oh+h2  2.580E+07   1.65   2.827E+03
  rev /  1.022E+05    1.95   9.657E+03 /
c2h5oh+ho2 = pc2h4oh+h2o2  1.230E+04   2.55   1.575E+04
  rev /  3.019E+02    2.21   3.021E+03 /
c2h5oh+ho2 = sc2h4oh+h2o2  8.200E+03   2.55   1.075E+04
  rev /  8.348E+02    2.53   1.272E+03 /
c2h5oh+ho2 = c2h5o+h2o2  2.500E+12   0.00   2.400E+04
  rev /  1.514E+14   -1.80   3.800E+04 /
c2h5oh+o = pc2h4oh+oh  9.410E+07   1.70   5.459E+03
  rev /  3.947E+04    1.69   6.943E+03 /
c2h5oh+o = sc2h4oh+oh  1.880E+07   1.85   1.824E+03
  rev /  3.270E+04    2.15   6.559E+03 /
c2h5oh+ch3 = pc2h4oh+ch4  1.330E+02   3.18   9.362E+03
  rev /  3.319E+00    3.17   1.342E+04 /
c2h5oh+ch3 = sc2h4oh+ch4  4.440E+02   2.90   7.690E+03
  rev /  4.594E+01    3.20   1.500E+04 /
c2h5oh+c2h5 = pc2h4oh+c2h6  5.000E+10   0.00   1.340E+04
  rev /  6.995E+10    0.00   2.699E+04 /
c2h5oh+c2h5 = sc2h4oh+c2h6  5.000E+10   0.00   1.040E+04
  rev /  6.995E+10    0.00   2.399E+00 /
pc2h4oh = c2h4+oh  1.293E+12   -0.37   2.685E+04
  rev /  9.930E+11    0.00  -9.600E+02 /
sc2h4oh+m = ch3cho+h+m  1.000E+14   0.00   2.500E+04
  rev /  8.166E+12    0.37   7.300E+02 /
c2h4+ch3 = c2h3+ch4  6.620E+00   3.70   9.500E+03
  rev /  1.440E+00    4.02   5.472E+03 /
ch3co(+m) = ch3+co(+m)  3.000E+12   0.00   1.672E+04
  low/1.20E+15  0.00   1.2518E+04/
ch3cho = ch3+hco  2.614E+15   0.15   8.055E+04
  rev /  2.000E+13    0.00   0.000E+00 /
ch3cho+o2 = ch3co+ho2  3.010E+13   0.00   3.915E+04
  rev /  8.552E+10    0.32  -1.940E+03 /
ch3cho+oh = ch3co+h2o  2.000E+06   1.80   1.300E+03
```

```
   rev /  1.354E+06   1.79  3.285E+04 /
ch3cho+h = ch3co+h2  1.340E+13   0.00  3.300E+03
   rev /  2.096E+12  -0.01  1.969E+04 /
ch3cho+o = ch3co+oh  5.940E+12   0.00  1.868E+03
   rev /  4.080E+11  -0.01  1.617E+04 /
ch3cho+ho2 = ch3co+h2o2  3.010E+12   0.00  1.193E+04
   rev /  1.210E+13  -0.34  1.201E+04 /
ch3cho+ch3 = ch3co+ch4  2.608E+06   1.78  5.911E+03
   rev /  1.066E+07   1.77  2.279E+04 /
c2h4+o2 = c2h3+ho2  4.000E+13   0.00  5.820E+04
   rev /  4.939E+13  -0.50  1.368E+03 /
ch2o+m = co+h2+m  1.826E+32  -4.42  8.712E+04
   rev /  5.070E+27  -3.42  8.435E+04 /
c2h4+ch3o = c2h3+ch3oh  1.200E+11   0.00  6.750E+03
   rev /  1.000E+10   0.00  9.000E+03 /
ch3coch3 = ch3co+ch3  1.219E+23  -1.99  8.395E+04
   rev /  1.000E+13   0.00  0.000E+00 /
ch3coch3+oh = ch3coch2+h2o  1.054E+10   0.97  1.586E+03
   rev /  6.931E+09   0.97  2.325E+04 /
ch3coch3+h = ch3coch2+h2  5.628E+07   2.00  7.700E+03
   rev /  9.000E+12   0.00  1.450E+05 /
ch3coch3+o = ch3coch2+oh  1.130E+14   0.00  7.850E+03
   rev /  7.500E+12   0.00  1.230E+04 /
ch3coch3+ch3 = ch3coch2+ch4  3.960E+11   0.00  9.784E+03
   rev /  5.378E+08   0.86  1.754E+04 /
ch3coch3+ch3o = ch3coch2+ch3oh  1.000E+11   0.00  7.000E+03
   rev /  1.000E+10   0.00  9.000E+03 /
ch3coch2 = ch2co+ch3  1.000E+14   0.00  3.100E+04
   rev /  1.000E+11   0.00  6.000E+03 /
ch3coch3+o2 = ch3coch2+ho2  1.200E+14   0.00  4.600E+04
   rev /  2.000E+12   0.00  2.000E+03 /
ch3coch3+ho2 = ch3coch2+h2o2  1.700E+13   0.00  2.046E+04
   rev /  1.000E+11   0.00  8.000E+03 /
c2h5co = c2h5+co  1.834E+15  -0.73  1.291E+04
   rev /  1.510E+11   0.00  4.810E+03 /
c2h5cho+h = c2h5co+h2  3.980E+13   0.00  4.200E+03
   rev /  1.778E+13   0.00  2.367E+04 /
c2h5cho+o = c2h5co+oh  5.010E+12   0.00  1.790E+03
   rev /  1.000E+12   0.00  1.916E+04 /
c2h5cho+oh = c2h5co+h2o  9.240E+06   1.50 -9.620E+02
   rev /  5.855E+06   1.50  3.058E+04 /
c2h5cho+ch3 = c2h5co+ch4  2.608E+06   1.78  5.911E+03
   rev /  9.972E+06   1.78  2.278E+04 /
c2h5cho+ho2 = c2h5co+h2o2  1.000E+12   0.00  1.100E+04
   rev /  1.000E+12   0.00  1.400E+04 /
c2h5cho+ch3o = c2h5co+ch3oh  1.000E+12   0.00  3.300E+03
   rev /  3.160E+11   0.00  1.800E+04 /
c2h5cho+c2h5 = c2h5co+c2h6  1.000E+12   0.00  8.000E+03
   rev /  1.585E+13   0.00  2.800E+04 /
c2h5cho = c2h5+hco  9.850E+18  -0.73  8.171E+04
   rev /  1.810E+13   0.00  0.000E+00 /
c2h5cho+o2 = c2h5co+ho2  2.000E+13   0.50  4.220E+04
   rev /  1.909E+14   0.50  3.090E+03 /
c2h5cho+c2h3 = c2h5co+c2h4  1.700E+12   0.00  8.440E+03
   rev /  2.488E+14   0.00  2.619E+04 /
h2o2+h = h2+ho2  4.820E+13   0.00  7.950E+03
   rev /  1.875E+12   0.33  2.426E+04 /
hco+o = co2+h  3.000E+13   0.00  0.000E+00
   rev /  9.677E+15   0.00  1.102E+05 /
ch3+m = ch2+h+m  1.968E+16   0.00  9.252E+04
   rev /  2.107E+11   1.00 -1.962E+04 /
ch3+h = ch2+h2  9.000E+13   0.00  1.510E+04
   rev /  1.818E+13   0.00  1.040E+04 /
ch3+oh = ch2+h2o  3.000E+06   2.00  2.500E+03
   rev /  2.623E+06   2.00  1.296E+04 /
ch+ch4 = c2h4+h  6.000E+13   0.00  0.000E+00
   rev /  3.573E+14   0.00  5.548E+04 /
ch3oh(+m) = ch2oh+h(+m)  2.690E+16  -0.08  9.894E+04
   low /  2.34E+40 -6.33  1.031E+05/
   troe/  0.773  693.  5333./
```

```
ch3co+h = ch2co+h2   2.000E+13   0.00   1.000E-10
  rev /  7.270E+09   0.00   8.304E+04 /
ch3co+o = ch2co+oh   2.000E+13   0.00   1.000E-10
  rev /  7.270E+09   0.00   8.304E+04 /
ch3co+ch3 = ch2co+ch4  5.000E+13   0.00   1.000E-10
  rev /  7.270E+09   0.00   8.304E+04 /
c2h4+o = ch2cho+h   3.390E+06   1.88   1.790E+02
  rev /  9.481E+06   1.79   1.605E+04 /
c2h5+o = ch3cho+h   5.000E+13   0.00   0.000E+00
  rev /  9.000E+13   0.00   7.268E+04 /
c2h6+ch = c2h5+ch2   1.100E+14   0.00  -2.600E+02
  rev /  3.829E+10   0.56   4.400E+02 /
ch2oh+ch2o=ch3oh+hco   1.292E-01   4.56   6.596E+03
  rev /  9.630E+03   2.90   1.311E+04 /
c2h5oh+oh = c2h5o+h2o   7.460E+11   0.30   1.634E+03
  rev /  3.956E+13  -0.14   1.852E+04 /
c2h5oh+h = c2h5o+h2   1.500E+07   1.60   3.038E+03
  rev /  1.837E+08   1.17   4.772E+03 /
c2h5oh+o = c2h5o+oh   1.580E+07   2.00   4.448E+03
  rev /  8.500E+07   1.56   4.087E+03 /
c2h5oh+ch3 = c2h5o+ch4   1.340E+02   2.92   7.452E+03
  rev /  4.288E+04   2.48   9.666E+03 /
sc2h4oh+o2 = ch3cho+ho2   3.810E+06   2.00   1.641E+03
  rev /  1.066E+08   1.70   2.733E+04 /
c2h5o+o2 = ch3cho+ho2   4.280E+10   0.00   1.097E+03
  rev /  3.872E+08   0.44   3.188E+04 /
h2o2+o2 = ho2+ho2   1.839E+14  -0.66   3.955E+04
  rev /  1.300E+11   0.00  -1.629E+03 /
DUPLICATE
h2o2+oh = h2o+ho2   5.800E+14   0.00   9.560E+03
  rev /  9.771E+13   0.33   4.102E+04 /
DUPLICATE
c2h5o2 = c2h5+o2   4.930E+50 -11.50   4.225E+04
  rev /  1.090E+48 -11.54   1.022E+04 /
ch3o2+m = ch3+o2+m   4.343E+27  -3.42   3.047E+04
  rev /  5.440E+25  -3.30   0.000E+00 /
ch3o2h = ch3o+oh   6.310E+14   0.00   4.230E+04
  rev /  1.166E+11   0.60  -1.771E+03 /
c2h5o2h = c2h5o+oh   6.310E+14   0.00   4.230E+04
  rev /  1.012E+08   1.48  -3.887E+03 /
c2h5o+m = ch3+ch2o+m   1.350E+38  -6.96   2.380E+04
  rev /  6.442E+36  -6.99   1.685E+04 /
ch3o2+ch2o = ch3o2h+hco   1.990E+12   0.00   1.167E+04
  rev /  8.504E+12  -0.50   7.009E+03 /
c2h5o2+ch2o = c2h5o2h+hco   1.990E+12   0.00   1.167E+04
  rev /  6.411E+12  -0.47   6.967E+03 /
c2h4+ch3o2 = c2h3+ch3o2h   1.130E+13   0.00   3.043E+04
  rev /  3.000E+12   0.00   1.150E+04 /
c2h4+c2h5o2 = c2h3+c2h5o2h   1.130E+13   0.00   3.043E+04
  rev /  3.000E+12   0.00   1.150E+04 /
ch4+ch3o2 = ch3+ch3o2h   1.810E+11   0.00   1.848E+04
  rev /  3.708E+11  -0.50  -1.327E+03 /
ch4+c2h5o2 = ch3+c2h5o2h   1.810E+11   0.00   1.848E+04
  rev /  2.796E+11  -0.47  -1.369E+03 /
ch3oh+ch3o2 = ch2oh+ch3o2h   1.810E+12   0.00   1.371E+04
  rev /  1.038E+08   1.16   2.542E+03 /
ch3oh+c2h5o2 = ch2oh+c2h5o2h   1.810E+12   0.00   1.371E+04
  rev /  7.824E+07   1.19   2.500E+03 /
c2h5+ho2 = c2h5o+oh   3.200E+13   0.00   0.000E+00
  rev /  3.075E+15  -0.32   2.749E+04 /
ch3o2+ch3 = ch3o+ch3o   7.000E+12   0.00  -1.000E+03
  rev /  2.971E+16  -0.93   2.831E+04 /
ch3o2+c2h5 = ch3o+c2h5o   7.000E+12   0.00  -1.000E+03
  rev /  6.569E+16  -0.90   3.126E+04 /
ch3o2+ho2 = ch3o2h+o2   1.750E+10   0.00  -3.275E+03
  rev /  5.156E+13  -0.83   3.488E+04 /
ch3oh+o2 = ch2oh+ho2   2.050E+13   0.00   4.490E+04
  rev /  3.989E+05   1.99  -4.424E+03 /
c2h5o2+ho2 = c2h5o2h+o2   1.750E+10   0.00  -3.275E+03
  rev /  3.887E+13  -0.79   3.484E+04 /
```

```
ch3o2+ch3o2 = ch2o+ch3oh+o2  3.110E+14  -1.61 -1.051E+03
   rev /  0.000E+00   0.00  0.000E+00 /
ch3o2+ch3o2 = o2+ch3o+ch3o  1.400E+16  -1.61  1.860E+03
   rev /  0.000E+00   0.00  0.000E+00 /
c2h6+ch3o2 = c2h5+ch3o2h  1.700E+13   0.00  2.046E+04
   rev /  7.500E+11   0.00  1.280E+03 /
c2h6+c2h5o2 = c2h5+c2h5o2h  1.700E+13   0.00  2.046E+04
   rev /  7.500E+11   0.00  1.280E+03 /
o2c2h4oh = pc2h4oh+o2  3.900E+16  -1.00  3.000E+04
   rev /  1.200E+11   0.00 -1.100E+03 /
o2c2h4oh = oh+ch2o+ch2o  1.250E+10   0.00  1.890E+04
   rev /  0.000E+00   0.00  0.000E+00 /
c2h5o2 = c2h4o2h  5.640E+47 -11.44  3.732E+04
   rev /  6.990E+48 -12.22  2.585E+04 /
c2h4o2h = c2h4o1-2+oh  4.250E+22  -4.18  2.235E+04
   rev /  0.000E+00   0.00  0.000E+00 /
ch3co3 = ch3co+o2  4.732E+19  -1.93  2.590E+04
   rev /  1.200E+11   0.00 -1.100E+03 /
ch3co2+m = ch3+co2+m  4.400E+15   0.00  1.050E+04
   rev /  1.000E-10   0.00  0.000E+00 /
ch3co3h = ch3co2+oh  5.010E+14   0.00  4.015E+04
   rev /  1.738E+08   1.57  1.305E+03 /
ch3co3+ho2 = ch3co3h+o2  1.750E+10   0.00 -3.275E+03
   rev /  4.000E+12  -0.30  5.270E+04 /
c2h5o+m = ch3cho+h+m  1.160E+35  -5.89  2.527E+04
   rev /  3.063E+30  -4.78  6.100E+03 /
h2o2+ch3co3 = ho2+ch3co3h  2.410E+12   0.00  9.936E+03
   rev /  3.894E+11   0.35  2.473E+04 /
ch4+ch3co3 = ch3+ch3co3h  1.810E+11   0.00  1.848E+04
   rev /  2.877E+10   0.03  1.649E+04 /
c2h4+ch3co3 = c2h3+ch3co3h  1.130E+13   0.00  3.043E+04
   rev /  3.189E+15  -0.80  2.957E+04 /
c2h6+ch3co3 = c2h5+ch3co3h  1.700E+13   0.00  2.046E+04
   rev /  1.727E+10   0.59  2.264E+04 /
ch2o+ch3co3 = hco+ch3co3h  1.990E+12   0.00  1.167E+04
   rev /  6.598E+11   0.03  2.483E+04 /
ch3o2+ch3cho = ch3o2h+ch3co  3.010E+12   0.00  1.193E+04
   rev /  2.519E+13  -0.51  8.991E+03 /
ch3cho+ch3co3 = ch3co+ch3co3h  3.010E+12   0.00  1.193E+04
   rev /  1.955E+12   0.02  2.681E+04 /
c2h3co = c2h3+co  2.040E+14  -0.40  3.145E+04
   rev /  1.510E+11   0.00  4.810E+03 /
c2h3cho+oh = c2h3co+h2o  9.240E+06   1.50 -9.620E+02
   rev /  1.439E+07   1.53  3.645E+04 /
c2h3cho+h = c2h3co+h2  1.340E+13   0.00  3.300E+03
   rev /  4.820E+12   0.03  2.556E+04 /
c2h3cho+o = c2h3co+oh  5.940E+12   0.00  1.868E+03
   rev /  9.384E+11   0.03  2.203E+04 /
c2h3cho+ho2 = c2h3co+h2o2  3.010E+12   0.00  1.193E+04
   rev /  2.783E+13  -0.30  1.788E+04 /
c2h3cho+ch3 = c2h3co+ch4  2.608E+06   1.78  5.911E+03
   rev /  2.451E+07   1.81  2.865E+04 /
c2h3cho+ch3o2 = c2h3co+ch3o2h  3.010E+12   0.00  1.193E+04
   rev /  5.794E+13  -0.48  1.486E+04 /
c2h4o2h = c2h4+ho2  9.290E+30  -6.10  1.993E+04
   rev /  1.879E+25  -4.48  1.166E+04 /
c2h4+ch3o2 = c2h4o1-2+ch3o  2.820E+12   0.00  1.711E+04
   rev /  0.000E+00   0.00  0.000E+00 /
c2h4+c2h5o2 = c2h4o1-2+c2h5o  2.820E+12   0.00  1.711E+04
   rev /  0.000E+00   0.00  0.000E+00 /
c2h4o1-2 = ch3+hco  3.630E+13   0.00  5.720E+04
   rev /  1.482E+06   1.00  2.420E+02 /
c2h4o1-2 = ch3cho  7.407E+12   0.00  5.380E+04
   rev /  3.953E+07   1.15  7.739E+04 /
c2h4o1-2+oh = c2h3o1-2+h2o  1.780E+13   0.00  3.610E+03
   rev /  4.815E+12  -0.98  3.923E+04 /
c2h4o1-2+h = c2h3o1-2+h2  8.000E+13   0.00  9.680E+03
   rev /  4.998E+12  -0.98  3.014E+04 /
c2h4o1-2+ho2 = c2h3o1-2+h2o2  1.130E+13   0.00  3.043E+04
   rev /  1.814E+13  -1.30  3.458E+04 /
```

```
c2h4o1-2+ch3o2 = c2h3o1-2+ch3o2h  1.130E+13   0.00  3.043E+04
  rev /  3.778E+13  -1.48  3.156E+04 /
c2h4o1-2+c2h5o2 = c2h3o1-2+c2h5o2h  1.130E+13   0.00  3.043E+04
  rev /  2.849E+13  -1.44  3.152E+04 /
c2h4o1-2+ch3 = c2h3o1-2+ch4  1.070E+12   0.00  1.183E+04
  rev /  1.746E+12  -0.98  3.277E+04 /
c2h4o1-2+ch3o = c2h3o1-2+ch3oh  1.200E+11   0.00  6.750E+03
  rev /  3.614E+09  -0.95  2.548E+04 /
ch3coch2o2 = ch3coch2+o2  8.093E+15  -1.11  2.745E+04
  rev /  1.200E+11   0.00  -1.100E+03 /
ch3coch3+ch3coch2o2  = ch3coch2+ch3coch2o2h 1.000E+11   0.00  5.000E+03
  rev /  1.995E+10   0.00  1.000E+04 /
ch2o+ch3coch2o2 = hco+ch3coch2o2h  1.288E+11   0.00  9.000E+03
  rev /  2.512E+10   0.00  1.010E+04 /
ho2+ch3coch2o2 = ch3coch2o2h+o2  1.000E+12   0.00  0.000E+00
  rev /  0.000E+00   0.00  0.000E+00 /
ch3coch2o2h = ch3coch2o+oh  1.000E+16   0.00  4.300E+04
  rev /  9.732E+08   1.70  -4.175E+03 /
ch3coch2o = ch3co+ch2o  4.159E+16  -1.03  1.396E+04
  rev /  1.000E+11   0.00  1.190E+04 /
c2h5cho+ch3o2 = c2h5co+ch3o2h  3.010E+12   0.00  1.193E+04
  rev /  2.358E+13  -0.51  8.983E+03 /
c2h5cho+c2h5o = c2h5co+c2h5oh  6.026E+11   0.00  3.300E+03
  rev /  3.020E+11   0.00  1.816E+04 /
c2h5cho+c2h5o2 = c2h5co+c2h5o2h  3.010E+12   0.00  1.193E+04
  rev /  1.778E+13  -0.47  8.941E+03 /
c2h5cho+ch3co3 = c2h5co+ch3co3h  3.010E+12   0.00  1.193E+04
  rev /  1.829E+12   0.02  2.680E+04 /
ch3cho+oh = ch3 + hco2h  3.000E+15  -1.08  0.000E+00
  rev /  5.350E+19  -1.68  1.198E+05 /
c2h3o1-2 = ch3co  8.500E+14   0.00  1.400E+04
  rev /  1.136E+10   2.11  3.352E+04 /
c2h3o1-2 = ch2cho  1.000E+14   0.00  1.400E+04
  rev /  1.233E+11   1.71  2.830E+04 /
ch2cho = ch2co+h  3.094E+15  -0.26  5.082E+04
  rev /  5.000E+13   0.00  1.230E+04 /
ch2cho+o2 = ch2o+co+oh  2.000E+13   0.00  4.200E+03
  rev /  0.000E+00   0.00  0.000E+00 /
hco3 = hco+o2  7.766E+26  -3.96  4.423E+04
  rev /  1.200E+11   0.00  -1.100E+03 /
ch2o+hco3 = hco+hco3h  1.990E+12   0.00  1.167E+04
  rev /  2.331E+02   2.30  4.687E+03 /
hco3h = hco2+oh  5.010E+14   0.00  4.015E+04
  rev /  2.322E+06   2.15  6.550E+02 /
hco2+m = h+co2+m  2.443E+15  -0.50  2.650E+04
  rev /  7.500E+13   0.00  2.900E+04 /
hcco+o2 = co2+hco  2.400E+11   0.00  -8.540E+02
  rev /  1.474E+14   0.00  1.336E+05 /
ch3cho+oh = ch2cho + h2o  1.720E+05   2.40  8.150E+02
  rev /  6.181E+08   1.25  8.984E+04 /
ch2co+oh = ch2oh+co  3.730E+12   0.00  -1.013E+03
  rev /  9.430E+06   1.66  2.749E+04 /
ch3+o2 = ch2o+oh  7.470E+11   0.00  1.425E+04
  rev /  7.778E+11   0.00  6.777E+04 /
c2h4+h2 = ch3+ch3  3.767E+12   0.83  8.471E+04
  rev /  1.000E+14   0.00  3.200E+04 /
ch3+oh = ch2(s)+h2o  2.650E+13   0.00  2.186E+03
  rev /  3.236E+10   0.89  1.211E+03 /
c2h4+ho2 = c2h4o1-2+oh  2.230E+12   0.00  1.719E+04
  rev /  3.518E+17  -1.16  3.967E+04 /
ch3och3 = ch3+ch3o  4.860E+55 -11.56  1.021E+05
  rev /  1.173E+54 -11.88  2.310E+04 /
ch3och3+oh = ch3och2+h2o  9.350E+05   2.29 -7.800E+02
  rev /  1.030E+06   1.99  2.329E+04 /
ch3och3+h = ch3och2+h2  7.721E+06   2.09  3.384E+03
  rev /  1.964E+06   1.79  1.230E+04 /
ch3och3+o = ch3och2+oh  1.855E-03   5.29 -1.090E+02
  rev /  2.073E-04   5.00  6.708E+03 /
ch3och3+ho2 = ch3och2+h2o2  1.680E+13   0.00  1.769E+04
  rev /  1.098E+14  -0.62  1.029E+04 /
```

```
ch3och3+ch3o2 = ch3och2+ch3o2h  1.680E+13   0.00  1.769E+04
  rev /  2.287E+14  -0.80  7.270E+03 /
ch3och3+ch3 = ch3och2+ch4  1.445E-06   5.73  5.699E+03
  rev /  9.603E-06   5.43  1.509E+04 /
ch3och3+o2 = ch3och2+ho2  4.100E+13   0.00  4.491E+04
  rev /  1.895E+11   0.03 -3.659E+03 /
ch3och3+ch3o = ch3och2+ch3oh  6.020E+11   0.00  4.074E+03
  rev /  7.383E+10  -0.27  1.026E+04 /
ch3och2 = ch2o+ch3  1.600E+13   0.00  2.550E+04
  rev /  2.002E+12   0.00  2.400E+04 /
ch3och2+ch3o = ch3och3+ch2o  2.410E+13   0.00  0.000E+00
  rev /  1.250E+14   0.32  7.854E+04 /
ch3och2+ch2o = ch3och3+hco  5.490E+03   2.80  5.862E+03
  rev /  1.723E+03   3.10  1.162E+04 /
ch3och2+ch3cho = ch3och3+ch3co  1.260E+12   0.00  8.499E+03
  rev /  7.746E+11   0.28  1.698E+04 /
ch3och2+ho2 = ch3och2o+oh  9.000E+12   0.00  0.000E+00
  rev /  2.535E+15  -0.48  3.051E+04 /
ch3och2o2 = ch3och2+o2  4.439E+19  -1.59  3.624E+04
  rev /  2.000E+12   0.00  0.000E+00 /
ch3och3+ch3och2o2 = ch3och2+ch3och2o2h  5.000E+12   0.00  1.769E+04
  rev /  6.428E+13  -0.79  7.258E+03 /
ch3och2o2+ch2o = ch3och2o2h+hco  1.000E+12   0.00  1.167E+04
  rev /  4.035E+12  -0.50  6.997E+03 /
ch3och2o2+ch3cho = ch3och2o2h+ch3co  2.800E+12   0.00  1.360E+04
  rev /  1.000E+12   0.00  1.000E+04 /
ch3och2o2h = ch3och2o+oh  4.384E+21  -1.94  4.387E+04
  rev /  2.000E+13   0.00  0.000E+00 /
ch3och2o = ch3o+ch2o  5.180E+12  -0.13  1.937E+04
  rev /  1.000E+11   0.00  1.190E+04 /
ch3och2o2 = ch2och2o2h  6.000E+10   0.00  2.158E+04
  rev /  1.248E+12  -0.77  1.122E+04 /
ch2och2o2h = oh+ch2o+ch2o  1.500E+13   0.00  2.076E+04
  rev /  0.000E+00   0.00  0.000E+00 /
o2ch2och2o2h = ch2och2o2h+o2  1.924E+19  -1.62  3.627E+04
  rev /  7.000E+11   0.00  0.000E+00 /
o2ch2och2o2h = ho2ch2ocho+oh  4.000E+10   0.00  1.858E+04
  rev /  7.814E+03   1.49  5.881E+04 /
ho2ch2ocho = och2ocho+oh  2.000E+16   0.00  4.050E+04
  rev /  1.761E+09   1.49 -3.185E+03 /
och2ocho = ch2o+hco2  5.964E+16  -1.50  1.962E+04
  rev /  1.250E+11   0.00  1.190E+04 /
c2h5o2 = c2h4+ho2  3.370E+55 -13.42  4.467E+04
  rev /  1.290E+50 -12.28  2.130E+04 /
c2h4o2h = c2h5+o2  2.150E+37  -8.21  2.802E+04
  rev /  2.420E+35  -8.03  8.312E+03 /
ch3o+ch3 = ch2o+ch4  2.400E+13   0.00  0.000E+00
  rev /  8.270E+14   0.02  8.693E+04 /
ch3och3+hco3 = ch3och2+hco3h  4.425E+04   2.60  1.391E+04
  rev /  1.651E-05   4.61  1.172E+03 /
och2ocho = hoch2oco  1.000E+11   0.00  1.400E+04
  rev /  2.746E+08  -0.79  2.008E+04 /
hoch2oco = hoch2o+co  2.177E+16  -2.69  1.720E+04
  rev /  1.500E+11   0.00  4.800E+03 /
hoch2oco = ch2oh+co2  8.672E+17  -3.45  1.908E+04
  rev /  1.500E+11   0.00  3.520E+04 /
ch2oh+ho2 = hoch2o+oh  1.000E+13   0.00  0.000E+00
  rev /  8.515E+16  -1.09  3.309E+04 /
hoch2o = ch2o+oh  1.482E+17  -1.21  2.124E+04
  rev /  4.500E+15  -1.10  0.000E+00 /
hoch2o = hco2h+h  1.000E+14   0.00  1.490E+04
  rev /  5.904E+11   0.64  9.214E+03 /
hco2h+m = co+h2o+m  2.300E+13   0.00  5.000E+04
  rev /  1.422E+10   0.46  4.684E+04 /
hco2h+m = co2+h2+m  1.500E+16   0.00  5.700E+04
  rev /  2.399E+14   0.46  6.102E+04 /
ch3och2o2+ch3och2o2 = ch3ocho+ch3och2oh+o2 6.630E+22  -4.50  0.000E+00
  rev /  0.000E+00   0.00  0.000E+00 /
ch3och2o2+ch3och2o2 = o2+ch3och2o+ch3och2o 1.547E+23  -4.50  0.000E+00
  rev /  0.000E+00   0.00  0.000E+00 /
```

```
ch3och2o = ch3ocho+h  1.745E+16  -0.66  1.172E+04
  rev /  1.000E+13   0.00  7.838E+03 /
ch3ocho = ch3+hco2  1.392E+18  -0.99  7.914E+04
  rev /  1.000E+13   0.00  0.000E+00 /
ch3ocho+o2 = ch3oco+ho2  1.000E+13   0.00  4.970E+04
  rev /  8.437E+09  -0.96  8.000E+00 /
ch3ocho+oh = ch3oco+h2o  2.340E+07   1.61  -3.500E+01
  rev /  4.706E+06   0.32  2.291E+04 /
ch3ocho+ho2 = ch3oco+h2o2  1.220E+12   0.00  1.700E+04
  rev /  1.456E+12  -1.61  8.482E+03 /
ch3ocho+o = ch3oco+oh  2.350E+05   2.50  2.230E+03
  rev /  4.794E+03   1.21  7.925E+03 /
ch3ocho+h = ch3oco+h2  4.550E+06   2.00  5.000E+03
  rev /  2.113E+05   0.71  1.279E+04 /
ch3ocho+ch3 = ch3oco+ch4  7.550E-01   3.46  5.481E+03
  rev /  9.161E-01   2.17  1.375E+04 /
ch3ocho+ch3o = ch3oco+ch3oh  5.480E+11   0.00  5.000E+03
  rev /  1.227E+10  -1.26  1.106E+04 /
ch3ocho+ch3o2 = ch3oco+ch3o2h  1.220E+12   0.00  1.700E+04
  rev /  3.033E+12  -1.79  5.462E+03 /
ch3oco = ch3o+co  7.451E+12  -1.76  1.715E+04
  rev /  1.500E+11   0.00  3.000E+03 /
ch3oco = ch3+co2  1.514E+12  -1.78  1.382E+04
  rev /  1.500E+11   0.00  3.673E+04 /
och2o2h = ch2o+ho2  1.278E+18  -1.80  1.046E+04
  rev /  1.500E+11   0.00  1.190E+04 /
och2o2h = hoch2o2  3.000E+11   0.00  8.600E+03
  rev /  4.241E+08   0.95  2.620E+04 /
hoch2o2+ho2 = hoch2o2h+o2  3.500E+10   0.00  -3.275E+03
  rev /  1.046E+14  -0.84  3.487E+04 /
ch3och3+hco2 = ch3och2+hco2h  1.000E+13   0.00  1.769E+04
  rev /  4.884E+12  -0.26  2.508E+04 /
hco2h = hco+oh  4.593E+18  -0.46  1.083E+05
  rev /  1.000E+14   0.00  0.000E+00 /
ch2o+hco2 = hco+hco2h  5.600E+12   0.00  1.360E+04
  rev /  8.584E+11   0.04  2.675E+04 /
hco2+ho2 = hco2h+o2  3.500E+10   0.00  -3.275E+03
  rev /  3.699E+12  -0.29  5.269E+04 /
hco2+h2o2 = hco2h+ho2  2.400E+12   0.00  1.000E+04
  rev /  1.793E+11   0.36  2.479E+04 /
hco2h+oh = h2o+co2+h  2.620E+06   2.06  9.160E+02
  rev /  0.000E+00   0.00  0.000E+00 /
hco2h+oh = h2o+co+oh  1.850E+07   1.51  -9.620E+02
  rev /  0.000E+00   0.00  0.000E+00 /
hco2h+h = h2+co2+h  4.240E+06   2.10  4.868E+03
  rev /  0.000E+00   0.00  0.000E+00 /
hco2h+h = h2+co+oh  6.030E+13  -0.35  2.988E+03
  rev /  0.000E+00   0.00  0.000E+00 /
hco2h+ch3 = ch4+co+oh  3.900E-07   5.80  2.200E+03
  rev /  0.000E+00   0.00  0.000E+00 /
hco2h+ho2 = h2o2+co+oh  1.000E+12   0.00  1.192E+04
  rev /  0.000E+00   0.00  0.000E+00 /
hco2h+o = co+oh+oh  1.770E+18  -1.90  2.975E+03
  rev /  0.000E+00   0.00  0.000E+00 /
ch2(s)+m = ch2+m  1.000E+13   0.00  0.000E+00
  rev /  7.161E+15  -0.89  1.143E+04 /
ch2(s)+ch4 = ch3+ch3  4.000E+13   0.00  0.000E+00
  rev /  5.429E+15  -0.89  1.565E+04 /
ch2(s)+c2h6 = ch3+c2h5  1.200E+14   0.00  0.000E+00
  rev /  1.041E+14  -0.33  1.982E+04 /
ch2(s)+o2 = co+oh+h  7.000E+13   0.00  0.000E+00
  rev /  0.000E+00   0.00  0.000E+00 /
ch2(s)+h2 = ch3+h  7.000E+13   0.00  0.000E+00
  rev /  2.482E+17  -0.89  1.613E+04 /
ch2(s)+h = ch+h2  3.000E+13   0.00  0.000E+00
  rev /  1.509E+16  -0.89  1.442E+04 /
ch2(s)+o = co+h+h  3.000E+13   0.00  0.000E+00
  rev /  0.000E+00   0.00  0.000E+00 /
ch2(s)+oh = ch2o+h  3.000E+13   0.00  0.000E+00
  rev /  3.194E+18  -0.89  8.786E+04 /
```

```
ch2(s)+co2 = ch2o+co  3.000E+12   0.00  0.000E+00
   rev / 2.852E+15  -0.89  6.552E+04 /
ch2(s)+ch3 = c2h4+h  2.000E+13   0.00  0.000E+00
   rev / 2.671E+15  -0.06  6.884E+04 /
ch2(s)+ch2co = c2h4+co  1.600E+14   0.00  0.000E+00
   rev / 4.596E+15  -0.06  1.056E+05 /
c2h3+o2 = ch2cho+o  3.500E+14  -0.61  5.260E+03
   rev / 2.589E+12   0.12  6.459E+03 /

!SanDiego
 o+oh+m = ho2 + m  8.000E+15  0.000  0.00
   ar/0.75/ he/0.75/ h2/2.50/ h2o/12.00/ co/1.90/ co2/3.80/
   ho2+h = h2o+o  3.100E+13  0.000  1720.84
 ch3+h = t-ch2+h2  1.800E+14  0.000  15105.16
 ch3+t-ch2 = c2h4+h  4.220E+13  0.000  0.00
 ch2(s)+m = t-ch2+m  6.000E+12  0.000  0.00
   h2/2.40/ h2o/15.40/ co/1.80/ co2/3.60/
 t-ch2+h=ch+h2  6.020E+12  0.000  -1787.76
 t-ch2+oh = ch2o+h  2.500E+13  0.000  0.00
 t-ch2+oh = ch+h2o  1.130E+07  2.000  2999.52
 t-ch2+o = co+2 h  8.000E+13  0.000  0.00
 t-ch2+o = co+h2  4.000E+13  0.000  0.00
 t-ch2+o2 = co2+h2  2.630E+12  0.000  1491.40
 t-ch2+o2 = co+oh+h  6.580E+12  0.000  1491.40
 2 t-ch2 = c2h2+2 h  1.000E+14  0.000  0.00
 ch+o = co+h  4.000E+13  0.000  0.00
 ch+h2o = ch2o+h  1.170E+15  -0.750  0.00
 ch+co2 = hco+co  4.800E+01  3.220  -3226.58
 ch3o+h = ch2o+h2  2.000E+13  0.000  0.00
 ch3o+h = ch2(s)+h2o  1.600E+13  0.000  0.00
 ch3o+oh = ch2o+h2o  5.000E+12  0.000  0.00
 ch3o+o = oh+ch2o  1.000E+13  0.000  0.00
 c2h5+h = c2h4+h2  3.000E+13  0.000  0.00
 c2h5+o = c2h4+oh  3.060E+13  0.000  0.00
 c2h5+o = ch3+ch2o  4.240E+13  0.000  0.00
 c2h4ooh+o2 = oc2h3ooh+oh  7.500E+05  1.300  -5799.95
 oc2h3ooh = ch2o+hco+oh  1.000E+15  0.000  43000.00
 c2h4+ho2 = c2h4o+oh  2.230E+12  0.000  17189.29
 c2h4o+ho2 = ch3+co+h2o2  4.000E+12  0.000  17007.65
 c2h2+o = t-ch2+co  1.600E+14  0.000  9894.84
 c2h2+o2 = ch2o+co  4.600E+15  -0.540  44933.08
 ch2co+o = t-ch2+co2  2.000E+13  0.000  2294.46
 ch2co+ch3 = c2h5+co  9.000E+10  0.000  0.00
 hcco+oh = hco+co+h  2.000E+12  0.000  0.00
 hcco+o2 = 2 co+oh  2.880E+07  1.700  1001.43
 hcco+o2 = co2+co+h  1.400E+07  1.700  1001.43
 c2h+oh = hcco+h  2.000E+13  0.000  0.00
 c2h+o2 = hcco+o  6.020E+11  0.000  0.00
 c2h+o2 = ch+co2  4.500E+15  0.000  25095.60
 ch2oh+h = ch2o+h2  3.000E+13  0.000  0.00
 ch2oh+h = ch3+oh  2.500E+17  -0.930  5126.91
 ch2oh+oh = ch2o+h2o  2.400E+13  0.000  0.00
 ch3o+m = ch2oh+m  1.000E+14  0.000  19120.46
   ar/0.70/ h2/2.00/ h2o/6.00/ co/1.50/ co2/2.00/ ch4/2.00/
 ch2cho+h = ch3+hco  5.000E+13  0.000  0.00
 ch2cho+h = ch2co+h2  2.000E+13  0.000  0.00
 ch2cho+o = ch2o+hco  1.000E+14  0.000  0.00
 ch2cho+oh = ch2co+h2o  3.000E+13  0.000  0.00
 ch2cho+ch3 = c2h5+co+h  4.900E+14  -0.500  0.00
 ch2cho+ho2 = ch2o+hco+oh  7.000E+12  0.000  0.00
 ch2cho+ho2 = ch3cho+o2  3.000E+12  0.000  0.00
 ch2cho = ch3+co  1.170E+43  -9.800  43799.95
 ch3cho+o = ch2cho+oh  3.720E+13  -0.200  3559.99
 ch3cho+h = ch2cho+h2  1.850E+12  0.400  5359.94
 ch3cho+ch3 = ch2cho+ch4  2.450E+01  3.100  5729.92
 ch3cho+ho2 = ch2cho+h2o2  2.320E+11  0.400  14900.10
 c2h5oh+oh = ch2ch2oh+h2o  1.810E+11  0.400  717.02
 c2h5oh+oh = ch3choh+h2o  3.090E+10  0.500  -380.02
 c2h5oh+oh = ch3ch2o+h2o  1.050E+10  0.800  717.02
 c2h5oh+h = ch2ch2oh+h2  1.900E+07  1.800  5099.90
```

```
c2h5oh+h = ch3choh+h2  2.580E+07  1.600  2830.07
c2h5oh+h = ch3ch2o+h2  1.500E+07  1.600  3039.91
c2h5oh+o = ch2ch2oh+oh  9.410E+07  1.700  5460.09
c2h5oh+o = ch3choh+oh  1.880E+07  1.900  1820.03
c2h5oh+o = ch3ch2o+oh  1.580E+07  2.000  4450.05
c2h5oh+ch3 = ch2ch2oh+ch4  2.190E+02  3.200  9619.98
c2h5oh+ch3 = ch3choh+ch4  7.280E+02  3.000  7950.05
c2h5oh+ch3 = ch3ch2o+ch4  1.450E+02  3.000  7650.10
c2h5oh+ho2 = ch3choh+h2o2  8.200e+03  2.500  10799.95
c2h5oh+ho2 = ch2ch2oh+h2o2  2.430E+04  2.500  15799.95
c2h5oh+ho2 = ch3ch2o+h2o2  3.800E+12  0.000 24000.00
c2h4+oh = ch2ch2oh  2.410E+11  0.000  -2380.02
c2h5+ho2 = ch3ch2o+oh  4.000E+13  0.000  0.00
ch3ch2o+m = ch3cho+h+m  5.600E+34  -5.900  25299.95
   ar/0.70/ h2/2.00/ h2o/6.00/ co/1.50/ co2/2.00/ ch4/2.00/
ch3ch2o+m = ch3+ch2o+m  5.350E+37  -7.000  23799.95
   ar/0.70/ h2/2.00/ h2o/6.00/ co/1.50/ co2/2.00/ ch4/2.00/
ch3ch2o+o2 = ch3cho+ho2  4.000E+10  0.000  1099.90
ch3ch2o+co = c2h5+co2  4.680E+02  3.200  5380.02
ch3ch2o+h = ch3+ch2oh  3.000E+13  0.000  0.00
ch3ch2o+h = c2h4+h2o  3.000E+13  0.000  0.00
ch3ch2o+oh = ch3cho+h2o  1.000E+13  0.000  0.00
ch3choh+o2 = ch3cho+ho2  4.820E+13  0.000  5020.08
ch3choh+o = ch3cho+oh  1.000E+14  0.000  0.00
ch3choh+h = c2h4+h2o  3.000E+13  0.000  0.00
ch3choh+h = ch3+ch2oh  3.000E+13  0.000  0.00
ch3choh+ho2 = ch3cho+2 oh  4.000E+13  0.000  0.00
ch3choh+oh = ch3cho+h2o  5.000E+12  0.000  0.00
ch3choh+m = ch3cho+h+m  1.000E+14  0.000  25000.00
   ar/0.70/ h2/2.00/ h2o/6.00/ co/1.50/ co2/2.00/ ch4/2.00/
c3h4+o = c2h4+co  2.000E+07  1.800  1000.00
ch3+c2h2 = c3h4+h  2.560E+09  1.100  13643.88
c3h4+o = hcco+ch3  7.300E+12  0.000  2250.0
c3h3+h(+m) = c3h4(+m)  3.000E+13  0.000  0.00
   low/ 9.000E+15  1.000  0.00/
   troe/ 0.5  1E+30  1E-30/
c3h3+ho2 = c3h4+o2  2.500E+12  0.000  0.00
c3h4+oh = c3h3+h2o  5.300E+06  2.000  2000.00
c3h3+o2 = ch2co+hco  3.000E+10  0.000  2868.07
c3h4+h(+m) = c3h5(+m)  4.000E+13  0.000  0.00
   low/ 3.000E+24  -2.000  0.00/
   troe/ 0.8  1E+30  1E-30/
c3h5+h = c3h4+h2  1.800E+13  0.000  0.00
c3h5+o2 = c3h4+ho2  4.990E+15  -1.400  22428.06
c3h5+ch3 = c3h4+ch4  3.000E+12  -0.320  -130.98
c2h2+ch3(+m) = c3h5(+m)  6.000E+08  0.000  0.00
   low/ 2.000E+09  1.000  0.00/
   troe/ 0.5  1E+30  1E-30/
c3h5+oh = c3h4+h2o  6.000E+12  0.000  0.00
c3h3+hco = c3h4+co  2.500E+13  0.000  0.00
c3h3+ho2 = oh+co+c2h3  8.000E+11  0.000  0.00
c3h4+o2 = ch3+hco+co  4.000E+14  0.000  41826.00
c3h6+o = c2h5+hco  3.500E+07  1.650  -972.75
c3h6+oh = c3h5+h2o  3.100E+06  2.000  -298.28
c3h6+o = ch2co+ch3+h  1.200E+08  1.650  327.44
c3h6+h = c3h5+h2  1.700e05  2.500  2492.83
c3h5+h(+m) = c3h6(+m)  2.000E+14  0.000  0.00
   ar/0.70/ h2/2.00/ h2o/6.00/ co/1.50/ co2/2.00/ ch4/2.00/ c2h6/3.00/
   low/ 1.330E+60  -12.000  5967.97 /
   troe/ 0.02  1097  1097  6860 /
c3h5+ho2 = c3h6+o2  2.660E+12  0.000  0.00
c3h5+ho2 = oh+c2h3+ch2o  3.000E+12  0.000  0.00
c2h3+ch3(+m) = c3h6(+m)  2.500E+13  0.000  0.00
   ar/0.70/ h2/2.00/ h2o/6.00/ co/1.50/ co2/2.00/ ch4/2.00/ c2h6/3.00/
   low/ 4.270E+58  -11.940  9770.55 /
   troe/ 0.175  1341  6E+04  1.014E+04 /
c3h6+h = c2h4+ch3  1.600E+22  -2.390  11185.47
ch3+c2h3 = c3h5+h  1.500E+24  -2.830  18618.55
c3h8(+m) = ch3+c2h5(+m)  1.100E+17  0.000  84392.93
   low/ 7.830E+18  0.000  64978.01 /
```

```
  troe/ 0.76  1.9E+03  38 /
c3h8+o2 = i-c3h7+ho2  4.000E+13  0.000  47500.00
c3h8+o2 = n-c3h7+ho2  4.000E+13  0.000  50932.12
c3h8+h = i-c3h7+h2  1.300E+06  2.400  4471.08
c3h8+h = n-c3h7+h2  1.330E+06  2.540  6761.47
c3h8+o = i-c3h7+oh  4.760E+04  2.710  2107.31
c3h8+o = n-c3h7+oh  1.900E+05  2.680  3718.45
c3h8+oh = n-c3h7+h2o  1.000E+10  1.000  1599.90
c3h8+oh = i-c3h7+h2o  2.000E+07  -1.600  -99.90
c3h8+ho2 = i-c3h7+h2o2  9.640E+03  2.600  13917.30
c3h8+ho2 = n-c3h7+h2o2  4.760E+04  2.550  16491.40
i-c3h7+c3h8 = n-c3h7+c3h8  8.400E-03  4.200  8675.91
c3h6+h(+m) = i-c3h7(+m)  1.330E+13  0.000  1560.71
  ar/0.70/ h2/2.00/ h2o/6.00/ co/1.50/ co2/2.00/ ch4/2.00/ c2h6/3.00/
  low/ 8.700E+42  -7.500  4732.31 /
  troe/ 1  1000  645.4  6844 /
i-c3h7+o2 = c3h6+ho2  1.300E+11  0.000  0.00
n-c3h7(+m) = ch3+c2h4(+m)  1.230E+13  -0.100  30210.33
  low/ 5.490E+49  -10.000  35778.92 /
  troe/ -1.17  251  1E-15  1185 /
h+c3h6(+m) = n-c3h7(+m)  1.330E+13  0.000  3260.04
  ar/0.70/ h2/2.00/ h2o/6.00/ co/1.50/ co2/2.00/ ch4/2.00/ c2h6/3.00/
  low/ 6.260E+38  -6.660  7000.48 /
  troe/ 1  1000  1310  4.81E+04 /
n-c3h7+o2 = c3h6+ho2  3.500E+16  -1.600  3500.00
n-c3h7+o2 = c3h6ooh  2.000E+12  0.000  0.00
c3h6ooh = c3h6+ho2  2.500E+35  -8.300  22000.00
c3h6ooh+o2 = oc3h5ooh+oh  1.500E+08  0.000  -7000.00
oc3h5ooh = ch2cho+ch2o+oh  1.000E+15  0.000  43000.00
end
```
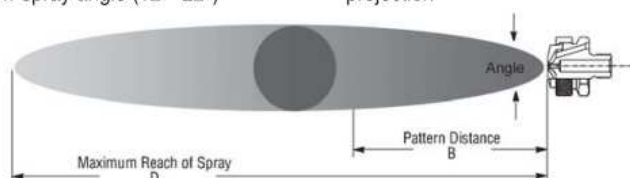
Appendix D

XA_SR

Siphon-fed Round

DESIGN FEATURES
- Lowest flow available
- Very fine atomization
- Narrow spray angle (12°- 22°)
- Full cone pattern
- Short to moderate forward spray projection

Angle
Pattern Distance B
Maximum Reach of Spray D

1/4"XA SR 200 B
XA 00 Body; B Hardware

Dimensions are approximate. Check with BETE for critical dimension applications.
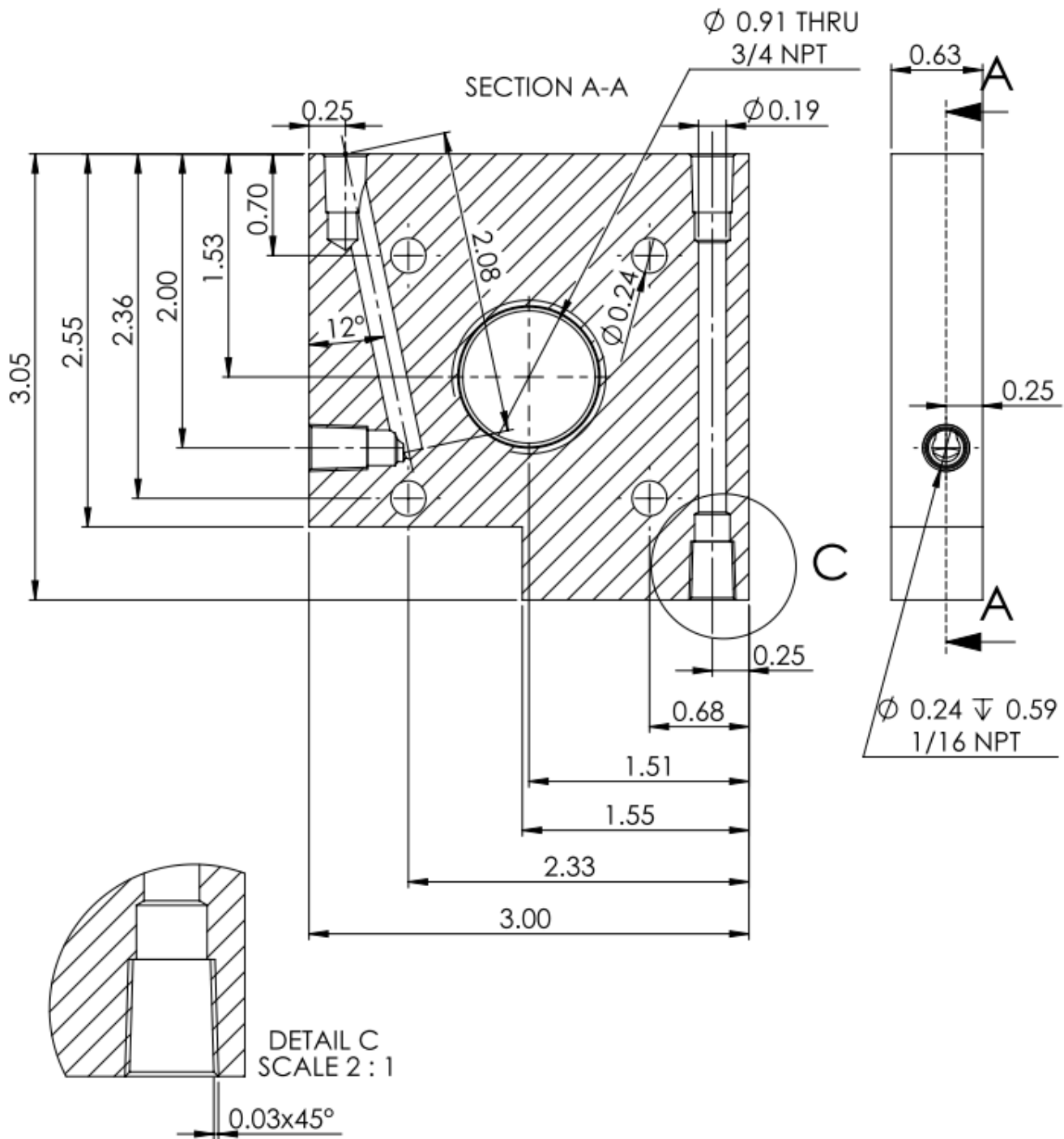
XA SR Set-up Flow Rates and Dimensions
Siphon-fed, External Mix, Round Spray Pattern, 1/8" and 1/4" Pipe Sizes

Pipe Size	Spray Set-up Number	Fluid and Air Cap Numbers	ATOMIZING AIR		Liquid Capacity in GPH (Gallons Per Hour)								Spray Dimensions at 8" Siphon Height			
			PSI air	Air Capacity SCFM	Gravity Head			Siphon Height					PSI air	Angle deg.	B in.	D feet
					18"	12"	6"	4"	8"	12"	24"	36"				
1/8 or 1/4	SR 050	Fluid Cap FC7 & Air Cap AC1201	10	0.4	0.4	0.4	0.3	0.2	0.2	0.1			10	18	11	6
			20	0.6	0.5	0.4	0.4	0.3	0.3	0.3	0.1		20	18	11	6
			40	1.0	0.5	0.5	0.5	0.4	0.4	0.4	0.3	0.2	40	18	12	7
			60	1.3	0.6	0.5	0.5	0.4	0.4	0.4	0.3	0.2	60	18	14	8
	SR 150	Fluid Cap FC4 & Air Cap AC1201	10	0.5	0.6	0.6	0.5	0.4	0.3	0.2			10	18	12	7
			20	0.7	0.7	0.7	0.6	0.5	0.5	0.4	0.2	0.1	20	18	13	8
			40	1.1	0.9	0.8	0.8	0.7	0.7	0.6	0.4	0.3	40	18	15	9
			60	1.5	1.0	0.9	0.9	0.8	0.8	0.7	0.6	0.4	60	19	17	10
	SR 200	Fluid Cap FC4 & Air Cap AC1202	10	0.8	0.7	0.6	0.5	0.4	0.4	0.3			10	18	12	8
			20	1.2	0.8	0.7	0.6	0.6	0.5	0.4	0.2		20	18	13	9
			40	1.9	0.9	0.9	0.8	0.8	0.7	0.7	0.5	0.3	40	19	15	11
			60	2.7	1.0	1.0	0.9	0.9	0.9	0.8	0.7	0.6	60	20	17	12
	SR 250	Fluid Cap FC3 & Air Cap AC1202	10	0.7	1.2	1.1	0.9	0.6	0.5	0.4			10	21	15	10
			20	1.0	1.4	1.3	1.1	0.9	0.8	0.7	0.5		20	21	16	11
			40	1.7	1.6	1.5	1.3	1.2	1.1	0.9	0.6	0.3	40	21	18	12
			60	2.4	1.5	1.4	1.3	1.1	1.0	0.9	0.7	0.5	60	22	20	14
	SR 400	Fluid Cap FC1 & Air Cap AC1204	20	1.9	5.8	5.2	4.2	3.1	2.7	1.9	0.6		20	17	18	12
			40	3.0	6.5	6.0	5.1	4.3	3.7	3.0	1.7	0.7	40	18	20	13
			60	4.1	6.8	6.4	5.6	4.9	4.2	3.5	2.2	1.3	60	18	21	15
			80	5.2	6.8	6.4	5.8	5.2	4.5	3.9	2.6	1.6	80	19	23	16
	SR 450	Fluid Cap FC5 & Air Cap AC1205	30	5.3				7.2	6.0	4.6			30	20	20	22
			40	6.5				7.8	6.8	5.3			40	20	21	23
			60	8.8		11.4	10.6	8.3	7.4	6.2	3.2		60	21	23	25
			80	11.1	11.6	11.0	10.3	8.3	7.5	6.4	3.6	2.2	80	22	25	27

Standard Materials: Nickel Plated Brass, 303 Stainless Steel and 316 Stainless Steel.

Spray angle performance varies with pressure. Contact BETE for specific data on critical applications.

SECTION A-A

Ø 0.91 THRU
3/4 NPT

Ø0.19

0.63

0.25

0.70

0.25

1.53

2.08

12°

Ø 0.24

2.00

2.36

2.55

3.05

Ø0.24

0.25

C

0.25

Ø 0.24 ⊽ 0.59
1/16 NPT

0.68

1.51

1.55

2.33

3.00

DETAIL C
SCALE 2 : 1

0.03x45°

		DIMENSIONS ARE IN INCHES		NAME	DATE	
		TOLERANCES:	DRAWN	REITER	10/2014	
		FRACTIONAL ±	CHECKED			
		ANGULAR: MACH ± BEND ±	ENG APPR.			
		TWO PLACE DECIMAL ±	MFG APPR.			
		THREE PLACE DECIMAL ±	Q.A.			
		MATERIAL	COMMENTS:			
		6061-T6				
NEXT ASSY	USED ON	FINISH				
APPLICATION		DO NOT SCALE DRAWING				

Coolingplate

SIZE **A** DWG. NO. REV.

SCALE:1:1 WEIGHT: SHEET 1 OF 1

xxxiii

Assembly

TITLE:

	NAME	DATE
DRAWN	REITER	10/2014
CHECKED		
ENG APPR.		
MFG APPR.		
Q.A.		
COMMENTS:		

UNLESS OTHERWISE SPECIFIED:
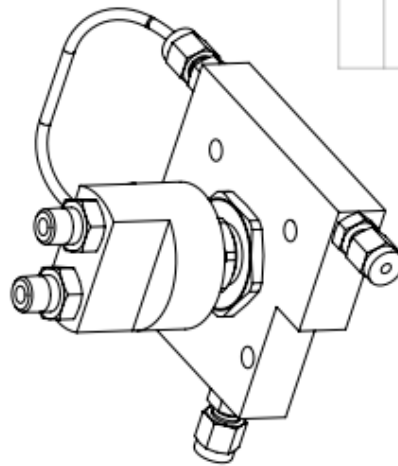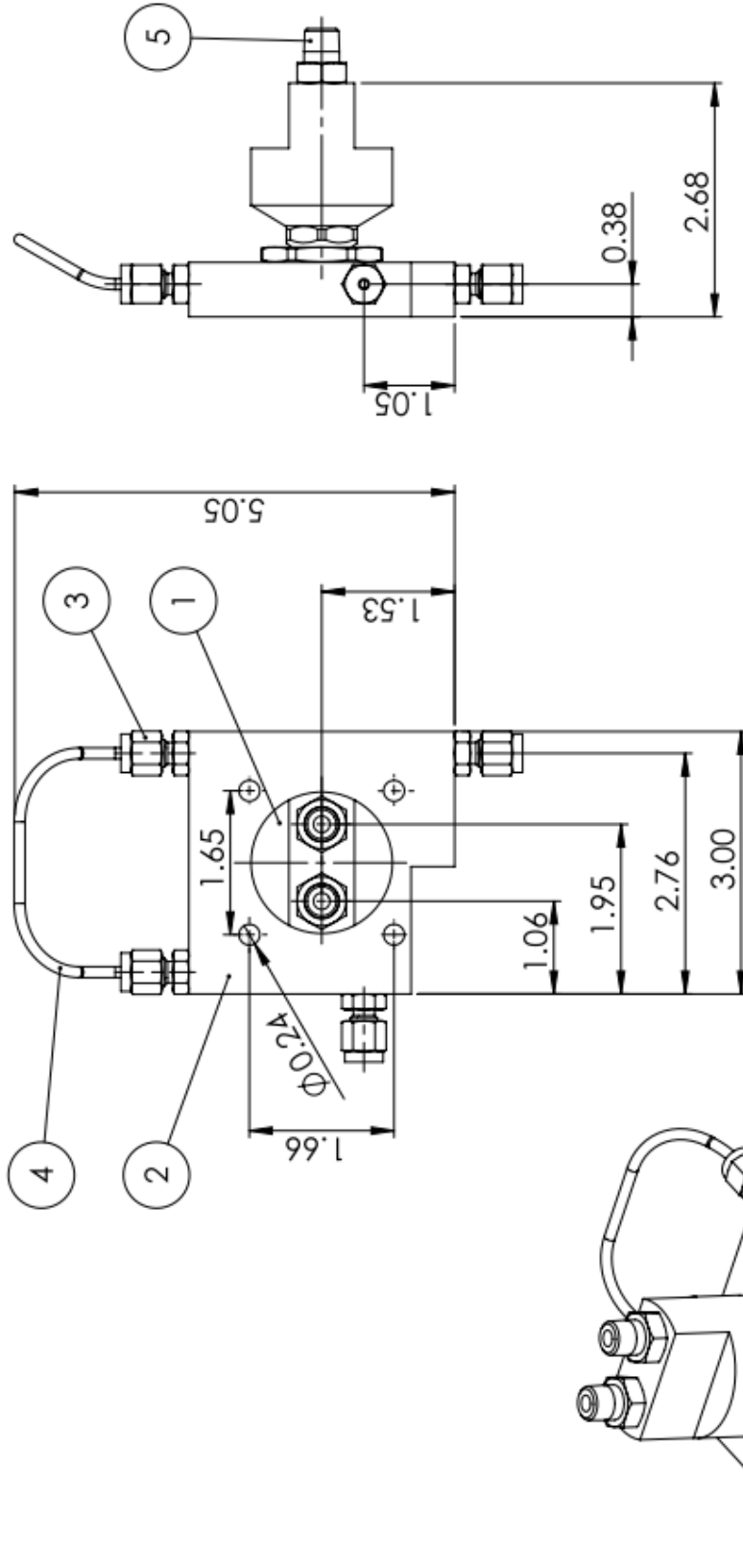
DIMENSIONS ARE IN INCHES
TOLERANCES:
FRACTIONAL±
ANGULAR: MACH± BEND ±
TWO PLACE DECIMAL ±
THREE PLACE DECIMAL ±

INTERPRET GEOMETRIC
TOLERANCING PER:

MATERIAL

FINISH

DO NOT SCALE DRAWING

SIZE | DWG. NO. | REV
A | |

SCALE: 1:1 | WEIGHT: | SHEET 1 OF 1

SolidWorks Student Edition.
For Academic Use Only.

APPLICATION | USED ON

5.05
1.53
1.65
1.06
1.95
2.76
3.00
1.66
Ø.24
2.68
0.38
1.05

Parts list					
Pos.Nr.	Designation	Nr.	Material	Dimensions [in]	Manufacturer/ Notes
1	Nozzle	1	SS		Bete
2	Cooling Plate	1	6061-T6	3.00x3.05x0.63	
3	Tube Fitting	4	SS		Swagelok SS-200-1-4
4	Tube	1	SS	1/8"x5.5	
5	Fitting	2	SS		Swagelok SS-4-HRN-2